

Characterization of Alaskan Hot-Mix Asphalt containing Reclaimed Asphalt Pavement Material



Prepared by:

Jenny Liu, Ph.D., P.E., Sheng Zhao, Ph.D., and Lin Li, Ph.D.
University of Alaska Fairbanks

June 2016

Prepared for:

Center for Environmentally Sustainable
Transportation in Cold Climates
University of Alaska Fairbanks
P.O. Box 755900
Fairbanks, AK 99775

U.S. Department of Transportation
1200 New Jersey Avenue, SE
Washington, DC 20590

INE/CESTiCC 101418



REPORT DOCUMENTATION PAGE

Form approved OMB No.

Public reporting for this collection of information is estimated to average 1 hour per response, including the time for reviewing instructions, searching existing data sources, gathering and maintaining the data needed, and completing and reviewing the collection of information. Send comments regarding this burden estimate or any other aspect of this collection of information, including suggestion for reducing this burden to Washington Headquarters Services, Directorate for Information Operations and Reports, 1215 Jefferson Davis Highway, Suite 1204, Arlington, VA 22202-4302, and to the Office of Management and Budget, Paperwork Reduction Project (0704-1833), Washington, DC 20503

1. AGENCY USE ONLY (LEAVE BLANK)		2. REPORT DATE 06/2016	3. REPORT TYPE AND DATES COVERED Final Report: 09/2014 – 06/2016	
4. TITLE AND SUBTITLE Characterization of Alaskan Hot-Mix Asphalt Containing Reclaimed Asphalt Pavement Material			5. FUNDING NUMBERS INE/CESTiCC 101418	
6. AUTHOR(S) Jenny Liu, Sheng Zhao, and Lin Li				
7. PERFORMING ORGANIZATION NAME(S) AND ADDRESS(ES) Center for Environmentally Sustainable Transportation in Cold Climates University of Alaska Fairbanks Duckering Building Room 245 P.O. Box 755900 Fairbanks, AK 99775-5900			8. PERFORMING ORGANIZATION REPORT NUMBER INE/CESTiCC 101418	
9. SPONSORING/MONITORING AGENCY NAME(S) AND ADDRESS(ES) U.S. Department of Transportation 1200 New Jersey Avenue, SE Washington, DC 20590 Alaska Department of Transportation Statewide Research Office 3132 Channel Drive Juneau, AK 99801-7898			10. SPONSORING/MONITORING AGENCY REPORT NUMBER FHWA-AK-RD-4000(137)	
11. SUPPLEMENTARY NOTES				
12a. DISTRIBUTION / AVAILABILITY STATEMENT No restrictions			12b. DISTRIBUTION CODE	
13. ABSTRACT (Maximum 200 words) In order to properly characterize Alaskan HMA materials containing RAP, this study evaluated properties of 3 asphalt binders typically used in Alaska, PG 52-28, PG 52-40, and PG 58-34, and 11 HMA mixtures containing up to 35% RAP that were either produced in the lab or collected from existing paving projects in Alaska. Various binder and mixture engineering properties were determined, including true high binder grades, complex modulus ($ G^* $), and phase angle (δ) at high performance temperatures, MSCR recovery rate and compliance, BBR stiffness and m -value, DTT failure stress and strain for binders, and dynamic modulus, flow number, IDT creep stiffness and strength for mixtures. Binder cracking temperatures were determined through Thermal Stress Analysis Routine (TSAR) software along with BBR and DTT data. Mixture cracking temperatures were determined with IDT creep stiffness and strength data. It was found that rutting may not be a concern with Alaskan RAP mix, while low-temperature cracking concerns may still exist in RAP mix in Alaska. A savings of \$13.3/ton was estimated for a 25% RAP mix, with consideration of Alaskan situations. Many recommendations for future RAP practice and research are recommended based on testing results and cost analysis.				
14- KEYWORDS : Recycled Asphalt Pavement (RAP), Dynamic Modulus, Flow Number, Low Temperature Cracking, Cracking Temperature, Thermal Stress Analysis Routine (TSAR)			15. NUMBER OF PAGES 177	
			16. PRICE CODE N/A	
17. SECURITY CLASSIFICATION OF REPORT Unclassified	18. SECURITY CLASSIFICATION OF THIS PAGE Unclassified	19. SECURITY CLASSIFICATION OF ABSTRACT Unclassified	20. LIMITATION OF ABSTRACT N/A	

**CHARACTERIZATION OF ALASKAN HOT-MIX ASPHALT
CONTAINING RECLAIMED ASPHALT PAVEMENT
MATERIAL**

FINAL REPORT

Prepared for

**Center for Environmentally Sustainable Transportation in Cold
Climates**

Author(s):

Jenny Liu, Ph.D., P.E.

Sheng Zhao, Ph.D.

Lin Li, Ph.D.

University of Alaska Fairbanks

INE/CESTiCC 101418

June 2016

DISCLAIMER

This document is disseminated under the sponsorship of the U. S. Department of Transportation in the interest of information exchange. The U.S. Government assumes no liability for the use of the information contained in this document. The U.S. Government does not endorse products or manufacturers. Trademarks or manufacturers' names appear in this report only because they are considered essential to the objective of the document.

METRIC (SI*) CONVERSION FACTORS

APPROXIMATE CONVERSIONS TO SI UNITS					APPROXIMATE CONVERSIONS FROM SI UNITS				
Symbol	When You Know	Multiply By	To Find	Symbol	Symbol	When You Know	Multiply By	To Find	Symbol
<u>LENGTH</u>					<u>LENGTH</u>				
in	inches	25.4	mm	mm	millimeters	0.039	inches	in	
ft	feet	0.3048	m	m	meters	3.28	feet	ft	
yd	yards	0.914	m	m	meters	1.09	yards	yd	
mi	Miles (statute)	1.61	km	km	kilometers	0.621	Miles (statute)	mi	
<u>AREA</u>					<u>AREA</u>				
in ²	square inches	645.2	millimeters squared	cm ²	mm ²	millimeters squared	0.0016	square inches	in ²
ft ²	square feet	0.0929	meters squared	m ²	m ²	meters squared	10.764	square feet	ft ²
yd ²	square yards	0.836	meters squared	m ²	km ²	kilometers squared	0.39	square miles	mi ²
mi ²	square miles	2.59	kilometers squared	km ²	ha	hectares (10,000 m ²)	2.471	acres	ac
ac	acres	0.4046	hectares	ha					
<u>MASS (weight)</u>					<u>MASS (weight)</u>				
oz	Ounces (avdp)	28.35	grams	g	g	grams	0.0353	Ounces (avdp)	oz
lb	Pounds (avdp)	0.454	kilograms	kg	kg	kilograms	2.205	Pounds (avdp)	lb
T	Short tons (2000 lb)	0.907	megagrams	mg	mg	megagrams (1000 kg)	1.103	short tons	T
<u>VOLUME</u>					<u>VOLUME</u>				
fl oz	fluid ounces (US)	29.57	milliliters	mL	mL	milliliters	0.034	fluid ounces (US)	fl oz
gal	Gallons (liq)	3.785	liters	liters	liters	liters	0.264	Gallons (liq)	gal
ft ³	cubic feet	0.0283	meters cubed	m ³	m ³	meters cubed	35.315	cubic feet	ft ³
yd ³	cubic yards	0.765	meters cubed	m ³	m ³	meters cubed	1.308	cubic yards	yd ³
Note: Volumes greater than 1000 L shall be shown in m ³									
<u>TEMPERATURE (exact)</u>					<u>TEMPERATURE (exact)</u>				
°F	Fahrenheit temperature	5/9 (°F-32)	Celsius temperature	°C	°C	Celsius temperature	9/5 °C+32	Fahrenheit temperature	°F
<u>ILLUMINATION</u>					<u>ILLUMINATION</u>				
fc	Foot-candles	10.76	lux	lx	lx	lux	0.0929	foot-candles	fc
fl	foot-lamberts	3.426	candela/m ²	cd/cm ²	cd/cm ²	candela/m ²	0.2919	foot-lamberts	fl
<u>FORCE and PRESSURE or STRESS</u>					<u>FORCE and PRESSURE or STRESS</u>				
lbf	pound-force	4.45	newtons	N	N	newtons	0.225	pound-force	lbf
psi	pound-force per square inch	6.89	kilopascals	kPa	kPa	kilopascals	0.145	pound-force per square inch	psi
These factors conform to the requirement of FHWA Order 5190.1A *SI is the symbol for the International System of Measurements									

ACKNOWLEDGMENTS

The authors wish to express their appreciation to the ADOT&PF personnel for their support throughout this study, as well as the Center for Environmentally Sustainable Transportation in Cold Climates (CESTiCC). The authors would also like to thank all members of the Project Technical Advisory Committee. Acknowledgment is extended to students Beaux Kemp, Paul Eckman, Gabriel Fulton, and Kannon Lee for their contributions with material collection, laboratory testing, and data analysis related to the project.

TABLE OF CONTENTS

EXECUTIVE SUMMARY	1
CHAPTER 1.0 INTRODUCTION	6
1.1 Problem Statement	6
1.2 Background	7
1.3 Objectives.....	10
1.4 Research Methodology	10
1.4.1 Task 1: Literature Review	11
1.4.2 Task 2: Development of Materials Collection Plan	11
1.4.3 Task 3: Specimens Fabrication and Performance Tests.....	12
1.4.4 Task 4: Characterization of Asphalt Binder with RAP.....	13
1.4.5 Task 5: Data Processing and Analyses	13
1.4.6 Task 6: Draft of Final Report and Recommendations	14
CHAPTER 2.0 LITERATURE REVIEW	15
2.1 Background of RAP	16
2.2 RAP Management.....	18
2.3 RAP Properties	21
2.4 Design of Mixture with RAP	23
2.5 Laboratory Evaluation of RAP Mixtures.....	25

2.5.1 Stiffness – Dynamic Modulus.....	25
2.5.2 Rutting Resistance	27
2.5.3 Fatigue Resistance	29
2.5.4 Low Temperature Cracking	31
2.5.5 Moisture Resistance	32
2.6 Field Evaluation	34
2.7 State Specifications.....	37
2.8 Economic Analysis of Using RAP.....	40
CHAPTER 3.0 EXPERIMENTAL DETAILS.....	48
3.1 Materials	48
3.2 Binder Tests	53
3.2.1 Dynamic Shear Rheometer	54
3.2.2 Bending Beam Rheometer	57
3.2.3 Direct Tension Test.....	59
3.3 Mixture Specimen Fabrication.....	61
3.4 Laboratory Mixture Performance Tests	68
3.4.1 Asphalt Mixture Performance Tests	69
3.4.2 Indirect Tension Tests.....	72
CHAPTER 4.0 RESULTS AND ANALYSIS.....	76
4.1 Binder Tests	76

4.1.1 High-Temperature Binder Grade	76
4.1.2 Viscoelastic Behavior	77
4.1.3 Master Curves	78
4.1.4 MSCR	81
4.1.5 BBR Results	82
4.1.6 DTT Results	86
4.1.7 TSAR Analysis	89
4.2 Asphalt Mixture Performance Tests	102
4.2.1 Dynamic Modulus	102
4.2.2 Flow Number (FN)	109
4.3 Indirect Tension Tests	111
4.3.1 Creep Stiffness	111
4.3.2 IDT strength	118
4.3.3 Mixture Cracking Temperature	122
4.4 Cost Analysis	130
CHAPTER 5 SUMMARIES AND CONCLUSIONS	133
REFERENCES	139
APPENDIX A JOB MIX FORMULAE	149
APPENDIX B AIR VOIDS OF SPECIMENS	155
APPENDIX C BINDER TESTING RESULTS	159

APPENDIX D MIXTURE TESTING RESULTS..... 174

LIST OF FIGURES

Figure 2.1 Estimated average percent of RAP by state (Hansen and Copeland 2015).....	39
Figure 2.2 Average estimated RAP percent (Hansen and Copeland 2015).....	39
Figure 3.1 Collected aggregates.....	51
Figure 3.2 Collected RAP	52
Figure 3.3 Binder content determination with ignition test	52
Figure 3.4 Gradation verification of RAP.....	53
Figure 3.5 DSR equipment	56
Figure 3.6 Rolling thin film oven (RTFO).....	56
Figure 3.7 DSR specimen	56
Figure 3.8 Bending beam rheometer.....	58
Figure 3.9 BBR specimen.....	58
Figure 3.10 PAV aging	59
Figure 3.11 Direct tension test	60
Figure 3.12 Asphalt mixer	62
Figure 3.13 Superpave gyratory compactor.....	62
Figure 3.14 Representative specimens for AMPT tests.....	65
Figure 3.15 Asphalt specimen core drill.....	65
Figure 3.16 Masonry saw.....	66

Figure 3.17 Gauge point fixing jig.....	66
Figure 3.18 Specimens for IDT tests	67
Figure 3.19 LVDT hardware mounting jig	67
Figure 3.20 Sample setup for AMPT test	70
Figure 3.21 Flow number samples before and after the test	72
Figure 3.22 IDT setup for creep stiffness test.....	73
Figure 4.1 $ G^* $ master curve of RTFO-aged PG 52-28	78
Figure 4.2 Phase angle master curve of RTFO-aged PG 52-28.....	79
Figure 4.3 $ G^* $ master curve of RTFO-aged PG 52-40	79
Figure 4.4 Phase angle master curve of RTFO-aged PG 52-40.....	80
Figure 4.5 $ G^* $ master curve of RTFO-aged PG 58-34	80
Figure 4.6 Phase angle master curve of RTFO-aged PG 58-34.....	81
Figure 4.7 Determine critical temperatures of PG 52-28 binder by limiting stiffness obtained from BBR tests.....	83
Figure 4.8 Determine critical temperatures of PG 52-40 binder by limiting stiffness obtained from BBR tests.....	83
Figure 4.9 Determine critical temperatures of PG 58-34 binder by limiting stiffness obtained from BBR tests.....	84
Figure 4.10 Determine critical temperatures of PG 52-28 binder by limiting m -value obtained from BBR tests.....	84

Figure 4.11 Determine critical temperatures of PG 52-40 binder by limiting m -value obtained from BBR tests.....	85
Figure 4.12 Determine critical temperatures of PG 58-34 binder by limiting m -value obtained from BBR tests.....	85
Figure 4.13 Determine critical temperatures of RTFO-aged binder by limiting failure strain from the DTT test	87
Figure 4.14 Determine critical temperatures of RTFO plus PAV-aged binder by limiting failure strain from the DTT test.....	88
Figure 4.15 TSAR input text file	91
Figure 4.16 Plot for critical temperature determination through TSAR.....	93
Figure 4.17 Critical temperature prediction for binder PG 52-28 after RTFO aging.....	95
Figure 4.18 Critical temperature prediction for binder PG 52-40 after RTFO aging.....	96
Figure 4.19 Critical temperature prediction for binder PG 58-34 after RTFO aging.....	97
Figure 4.20 Critical temperature prediction for binder PG 52-28 after RTFO + PAV aging.....	98
Figure 4.21 Critical temperature prediction for binder PG 52-40 after RTFO + PAV aging.....	99
Figure 4.22 Critical temperature prediction for binder PG 58-34 after RTFO + PAV aging.....	100
Figure 4.23 IE*1 data of the Central region mixes	105
Figure 4.24 IE*1 data of the Northern region mixes	106
Figure 4.25 Master curves of the Central region mixes.....	107
Figure 4.26 Master curves of the Northern region mixes.....	108

Figure 4.27 Flow number results of the Central region mixes	110
Figure 4.28 Flow number results of the Northern region mixes.....	110
Figure 4.29 Creep stiffness of asphalt (PG 52-28) concrete at different temperatures.....	112
Figure 4.30 Creep stiffness of asphalt (PG 58-34) concrete at different RAP contents and temperatures (Central region)	115
Figure 4.31 Creep stiffness of asphalt (PG 52-28) concrete at different temperature and RAP contents (Northern region).....	116
Figure 4.32 Creep stiffness of asphalt (PG 52-40) concrete at different temperature and RAP contents (Northern region).....	117
Figure 4.33 Tensile strengths of mixes at different temperatures (Northern region)	119
Figure 4.34 Tensile strengths of mixes at different temperatures (Central region)	121
Figure 4.35 Example of determination of mixture cracking temperature.....	123
Figure 4.36 Determining mixture cracking temperature for Mix 1 in Table 3.1	124
Figure 4.37 Determining mixture cracking temperature for Mix 2 in Table 3.1	124
Figure 4.38 Determining mixture cracking temperature for Mix 3 in Table 3.1	125
Figure 4.39 Determining mixture cracking temperature for Mix 4 in Table 3.1	125
Figure 4.40 Determining mixture cracking temperature for Mix 5 in Table 3.1	126
Figure 4.41 Determining mixture cracking temperature for Mix 6 in Table 3.1	126
Figure 4.42 Determining mixture cracking temperature for Mix 7 in Table 3.1	127
Figure 4.43 Determining mixture cracking temperature for Mix 8 in Table 3.1	127

Figure 4.44 Determining mixture cracking temperature for Mix 9 in Table 3.1	128
Figure 4.45 Determining mixture cracking temperature for Mix 10 in Table 3.1	128
Figure 4.46 Determining mixture cracking temperature for Mix 11 in Table 3.1	129

LIST OF TABLES

Table 2.1 Three blending simulation adopted in NCHRP Project 9-12 (McDaniel and Anderson 2001)	24
Table 2.2 NCAT cost analysis assumptions	40
Table 2.3 Average leachate concentrations ($\mu\text{g/L}$) (Horvath 2003)	46
Table 3.1 Matrix of HMA mixtures	50
Table 3.2 Testing matrix (triplicates for each test)	54
Table 3.3 Laboratory Testing Plan.....	68
Table 4.1 True high temperature grades of tested Alaskan binders.....	77
Table 4.2 Viscoelastic behavior results in terms of $ G^* $ and δ	77
Table 4.3 MSCR results	82
Table 4.4 Critical low temperature by limiting BBR parameters	86
Table 4.5 Critical low temperature by limiting DTT parameter	89
Table 4.6 Critical temperature using different methods	102
Table 4.7 IDT strength test results for materials from the Northern region	118
Table 4.8 IDT strength test results for materials from the Central region	120
Table 4.9 Cracking temperature results of all the 11 mixes	130
Table 4.10 Assumptions for the cost analysis.....	131
Table 4.11 The composition of a control mix without any RAP and 25% RAP mix.....	131

Table 4.12 Calculations 132

EXECUTIVE SUMMARY

Recycled asphalt pavement (RAP) has been used for several decades in hot-mix asphalt (HMA) for paving purposes. In Alaska, the newly established statewide HMA highway specification allows up to 15% RAP content in the wearing course of roadway pavement and up to 25% RAP content in the binder or base course layer(s). As a result, projects are expected to increase the use of these sustainable materials. Designers will typically develop pavement design alternatives using available pavement mechanistic analysis procedures and then use life cycle cost analysis to select the most cost-effective option. Mechanistic analysis procedures (e.g., Alaska Flexible Pavement Design software) require material engineering properties as an input source. Consequently, it is essential to properly establish the engineering properties of HMA mixtures containing RAP material.

This study evaluated three asphalt binders commonly used in Alaska mixes in order to properly characterize Alaskan HMA materials containing RAP. These asphalt binders included one neat binder, PG 52-28, and two polymer-modified binders, PG 52-40 and PG 58-34. The binder tests included the dynamic shear rheometer (DSR) test for verification of true high performance grades (PGs), an evaluation of viscoelastic behavior, master curves, a multiple stress creep recovery (MSCR) test associated with DSR setup, and bending beam rheometer (BBR) and

direct tension (DTT) tests for low-temperature performance evaluation. The binder cracking low temperature was further determined with Thermal Stress Analysis Routine (TSAR) software, using BBR and DTT data. Eleven HMA control and RAP mixtures containing 25% or 35% RAP were produced in the lab or collected from field projects for performance evaluation, covering two mixture types and material sources from the Alaska Department of Transportation & Public Facilities Northern and Central regions. The laboratory mixture performance evaluation included the asphalt mixture pavement test for dynamic modulus and flow number and indirect tension (IDT) tests for creep stiffness and low temperature strengths. The mixture cracking temperature was determined for each mix with IDT testing data. The preliminary material savings of using typical Alaskan HMA containing 25% RAP compared with using HMA without RAP was estimated as the cost analysis for typical Alaskan RAP mix, with consideration of conditions in Alaska.

Based on the DSR testing results, the true high temperature grades of the three Alaskan binders were verified: the high grades of PG 52-28 binder without aging and after rolling thin film oven (RTFO) aging were 56.6°C and 56.9°C, respectively; the true grades of PG 52-40 binder without aging and after RTFO aging were 60.6°C and 56.4°C, respectively; the true grades of PG 58-34 binder without aging and after RTFO aging were 64.3°C and 61.4°C, respectively. The following engineering properties of the three binders were determined based on DSR, BBR, and DTT tests: viscoelastic behavior in terms of the complex modulus ($|G^*|$) and phase angle (δ) at high

performance temperatures, MSCR rate and compliance, BBR stiffness and m -value, and DTT failure stress and strain. The MSCR test results also showed that all the selected binders satisfied the non-recoverable creep compliance (J_{nr}) standard for all traffic levels at corresponding high PGs specified in AASHTO MP 19.

Based on the BBR test results, it was found that the low-temperature cracking resistance of highly modified binder such as PG 52-40 might not be affected by long-term aging, which suggests further use of this binder in RAP mix for better low-temperature cracking performance. Using BBR and DTT data as input in TSAR analyses, the binder cracking temperatures of PG 52-28, PG 52-40, and PG 58-34 was determined: -38.1°C , -38°C , and -35.4°C , respectively, for RTFO-aged, and -28°C , -37°C , and -26°C , respectively, for RTFO plus pressure aging vessel-aged. The critical low temperatures of all binders were also determined by limiting BBR stiffness, BBR m -value, and DTT failure strain. By comparing these methods to determine the critical low temperature of the asphalt binder, it was found that the TSAR method evaluates a different property of the binder than the previous Superpave BBR and/or DTT specification. The TSAR method could be better correlated with binder cracking resistance. Recently updated binder testing methods—MSCR and cracking temperature determination—would give more meaningful understanding of modified binder performance. The use of these methods is recommended for binder evaluation in Alaskan RAP mixes using modified binders.

The incorporation of RAP into Alaskan HMA increased the dynamic modulus and flow number of the mixtures, which indicates that the addition of RAP increased the rut resistance of the Alaskan mixes tested. Typically, the higher the RAP content, the higher the improvement in rutting. Difference in production method, that is, whether the mixture is produced in the lab or in the field, may affect the flow number testing results. The addition of RAP increased the IDT creep stiffness of the mixtures regardless of testing temperature, which could potentially result in lower resistance to low-temperature cracking. The higher the RAP content, the higher the creep stiffness. The mixes produced with varying production parameters such as production method and job mix formula may generate complicated stiffness results. The IDT strength data of each mix were determined as engineering properties. With the IDT strength and creep stiffness data, the mixture cracking temperatures were determined. It was found that the mixture cracking temperature was close to the binder's low PG grade on 52-28 Type II-B and 58-34 Type II-B Central region mixes and 52-40 Northern region Type II-B mixes, while the mixture cracking temperature of the 58-34 Type II-A Central region mixes and 52-28 Northern region mixes was a little higher. This indicates that binder cracking may contribute significantly to the mixture's low-temperature cracking, while with some mixes, the binder may not fail before the mixture fails. Adding certain amounts of RAP did not affect the low-temperature performance of some mixes, while doing so increased the low-temperature cracking temperature of some mixes. This indicates that RAP may not impair the low-temperature performance of some Alaskan mixes. However, RAP mixes are still questionable, as not all grouped mixes showed comparable

cracking temperatures. In addition, the parameters in RAP mix production and construction that significantly contribute to low-temperature cracking are still unknown.

According to a typical cost analysis of Alaskan conditions, a rough estimate of \$13.3/ton savings was reached if 25% RAP is used in an HMA paving job in Alaska. The cost analysis along with the performance evaluation show that using 25% or 35% RAP in an Alaskan HMA is very promising. The rutting resistance of Alaskan mix is enhanced by the addition of RAP. The low-temperature performance of RAP mix may not be impaired by the addition of RAP, but concerns about low-temperature cracking of RAP mix still exist. It is recommended that additional binders and mixtures be tested for a more complete evaluation of Alaskan RAP mix regarding material collection and production method. How virgin binder and RAP binder affect the mixture's performance, especially low-temperature cracking performance, is still unknown. It is recommended that further research be conducted to address this issue. Furthermore, testing efforts on additional Alaskan RAP mixes are needed to verify the conclusions drawn from this preliminary study. Field sections with both RAP mix and control mix included should be developed to correlate the laboratory testing results and the actual field performance of RAP mixes.

CHAPTER 1.0 INTRODUCTION

1.1 Problem Statement

With a decline in the supply of locally sourced quality aggregate, a growing concern over waste disposal, and the rising cost associated with asphalt binder, the use of recycled asphalt pavement (RAP) for new and rehabilitation pavement projects have increased substantially. In Alaska, the new established statewide hot-mix asphalt (HMA) highway specification allows up to 15% RAP content in the wearing course of roadway pavement and up to 25% RAP content in the binder or base course layer(s). As a result, projects are expected to increase the use of these sustainable materials. Designers will typically develop pavement design alternatives using available pavement mechanistic analysis procedures and then use life cycle cost analysis (LCCA) to select the most cost-effective option. Mechanistic analysis procedures (e.g., AK Flexible Pavement Design software) require material engineering properties as an input source. Consequently, it is essential to properly establish the engineering properties of HMA mixtures containing RAP material.

1.2 Background

Recycled asphalt pavement has been used for several decades in HMA for paving purposes. The use of RAP in HMA leads to significant environmental and economic benefits. The major benefits are realized through reduced demand for new or virgin aggregates and asphalt binders (Page and Murphy 1987; Huang et al. 2004; Behnia et al. 2010). Considering material and construction costs, it has been estimated that using RAP provides a savings ranging from 14% to 34% for RAP content of between 20% and 50% in HMA pavements (Kandhal and Mallick 1997). Later economic analyses using various calculation methods showed savings of 24% (Kristjánssdóttir et al. 2007), 26% (Brock and Richmond 2007), or 35% (Willis et al. 2012) with the use of 50% RAP. However, many states specify the allowed RAP content to be used in HMA due to undetermined mix design methods and limited knowledge of production technology (Zaumanis and Mallick 2015). For example, Washington DOT allows 20% RAP by weight of aggregate in HMA without further testing. Oregon currently allows the use of up to 30% RAP in HMA; however, the use of blending charts for RAP proportions greater than 15% is recommended. New Hampshire allows up to 30% RAP from a known source or 15% RAP from an unknown source to be used in a mixture. Nebraska allows 40–50% RAP for primary types of asphalt mixtures. A study done by the FHWA (1993) indicated that up to 80% RAP has been used in some HMA with an acceptable level of performance. Maximum use of RAP materials in asphalt mixtures has been desired, but is not a simple task because of undesirable inherent

characteristics of RAP, that is, aged (stiff) asphalt binder and inconsistent aggregate properties.

The recently completed NCHRP 09-46 project (West et al. 2013) aimed at developing a mix design and analysis procedure for HMA containing high-RAP content (defined as greater than 25% and may exceed 50%) that provides satisfactory long-term performance and proposed changes to existing specifications to account for HMA containing high RAP content.

Numerous research studies have been reported in the literature concerning methods of using RAP and the performance of HMA mixtures containing RAP (Kennedy et al. 1998; McDaniel and Anderson 2001; Al-Qadi et al. 2007; Huang et al. 2011). In general, when RAP was used at low or medium content level in HMA, equivalent (or better) performance compared with the virgin material was expected. However, the degree of improvement is a function of the source, quantity, and quality of RAP incorporated in the mix. Compromised fatigue and low-temperature performance was reported when RAP content was higher (Tam et al. 1992; McDaniel and Anderson 2001; Huang et al. 2011), though different results have been reported from field investigations (Kandhal et al. 1995; Paul 1996). Significant efforts have also been made on production, construction, and properties of RAP mixtures with fiber, rejuvenator, and warm-mix asphalt technology. Another critical question regarding the use of RAP in HMA is, how much old asphalt is actually blended with new (virgin) asphalt during the mixing process? The NCHRP Project 9-12, Incorporation of RAP in the Superpave System, investigated the effects of RAP on binder and mixture properties and the question of whether RAP is “black rock” or whether

blending occurs between the new and RAP binders. Other attempts (Huang et al. 2005, Bonaquist 2007, McDaniel et al. 2012, Mogawer et al. 2012) were made to investigate the blending process of RAP with virgin materials and the degree of blending. It was found that only a small portion of aged asphalt in RAP actually blended in the remixing process; other portions formed a stiff coating around RAP aggregates, and RAP functionally acted as “composite black rock.” Additional concerns that have limited the use of RAP, especially high RAP in HMA, include production technology, potential emissions, and mixture workability (Zaumanis and Mallick 2015). However, recent advances in asphalt plants have made it possible to routinely produce mixtures containing high RAP (50%) (Bonaquist 2007) or full (100%) RAP (Hajj et al. 2008) and comply with the emissions requirements (Zaumanis and Mallick 2015). Meanwhile, the use of softer binder, rejuvenators, and warm-mix additives has proved to be effective in improving the workability of RAP mix (Zaumanis and Mallick 2015; Botella et al. 2016).

In Alaska, a preliminary laboratory study was undertaken to investigate how three RAP contents added to HMA affect the Superpave performance grade (PG) of the blended binder (Saboundjian and Teclemariam 2010). Another project (Connor and Li 2009) evaluated the performance of mix with the addition of 15% RAP for Fairbanks International Airport Runway 1L/19R Reconstruction, and results showed that the addition of 15% RAP did not adversely impact the quality of the HMA. The new statewide HMA highway specification allows up to 15% RAP materials in the wearing course of a roadway pavement, and up to 25% RAP in the binder or

base course layer(s). However, the performance data on HMA containing RAP for surface course applications are limited. It is essential to properly characterize (i.e., develop/establish engineering properties) typical Alaskan HMA mixes containing RAP material.

1.3 Objectives

The main objective of this study was to properly characterize Alaskan HMA materials containing RAP. The characterization provided the following: (1) mix modulus (stiffness) values at different temperatures, to be used in pavement design/analysis procedures, (2) rutting performance at intermediate and high temperatures, and (3) low-temperature thermal cracking performance. This comprehensive characterization can be used for pavement performance prediction and comparisons, using mechanistic empirical pavement procedures.

1.4 Research Methodology

The following major tasks were accomplished to achieve the objectives of this study:

- Task 1: Literature Review
- Task 2: Development of Materials Collection Plan
- Task 3: Specimens Fabrication and Performance Tests
- Task 4: Characterization of Asphalt Binder with RAP

- Task 5: Data Processing and Analyses
- Task 6: Draft of Final Report and Recommendations

1.4.1 Task 1: Literature Review

The review covered current practices and progress in characterization of HMA mixtures containing RAP. A summary of the economic benefit of RAP use in HMA mixtures, the impact of RAP on HMA production, emission control, and mixture compaction are included. This task was accomplished through a critical review of technical literature and research in progress. This task is presented in Chapter 2.

1.4.2 Task 2: Development of Materials Collection Plan

Based on discussions between the research team and professionals from ADOT&PF, variables used in the experimental matrix included the following: Two RAP sources (Northern and Central regions), two RAP contents (25% RAP for Type II-A and Type II-B mixes, and 35% RAP for Type II-B mix), and three regional asphalt binders (PG 52-28, PG 58-34, PG 52-40). The matrix of HMA mixtures with RAP prepared in the study is summarized in Chapter 3. Recycled asphalt pavement and HMA mixtures were collected from several paving projects in both the Central and Northern regions of Alaska. Virgin aggregates and asphalt binder were collected to prepare

mixtures that were not available directly from local paving projects. Details of materials information and job mix formula were provided. This task is presented in Chapter 3.

1.4.3 Task 3: Specimens Fabrication and Performance Tests

Adhering to AASHTO T27 and T308, ignition and sieving analysis tests were performed to verify binder content and gradation for each RAP source. Laboratory-mixed specimens were prepared according to standard procedures. Volumetric properties of mixtures (e.g., air voids and voids in mineral aggregate [VMA]) were verified before further performance tests. The project examined how properties changed as different amounts of RAP were added and what the variation in these properties was if different sources (types) of RAP and virgin materials were used. Tests conducted to assess the performance of HMA containing RAP included the following: (1) dynamic modulus $|E^*|$ and flow number (FN), using the asphalt mixture performance test (c) (AASHTO TP-79) and (2) low-temperature cracking performance (indirect tensile creep/strength), using the indirect tension test (AASHTO T-322). This task is presented in Chapter 3.

1.4.4 Task 4: Characterization of Asphalt Binder with RAP

Based on the binder study conducted by Saboundjian and Teclemariam (2010), this task further categorized the asphalt binder with RAP. The dynamic shear rheometer (DSR) was used to measure the viscoelastic behavior of the rolling thin film oven (RTFO)-aged binder in terms of complex modulus (G^*) and phase angle (δ), and to conduct multiple stress creep recovery (MSCR) tests for modified binders (i.e., PG 58-34, and PG 52-40 in this study) according to RTFO TP70. The bending beam rheometer (BBR) and direct tension (DTT) tests were employed as well for low-temperature cracking analysis in Task 5. The description of the binder tests listed in this task is presented in Chapter 3.

1.4.5 Task 5: Data Processing and Analyses

Laboratory data from Tasks 3 and 4 were processed and analyzed. A catalog of dynamic moduli for typical Alaskan HMA mixtures containing RAP was synthesized. Thermal stress analysis was provided by using TSAR™ software with test results from Task 4 as data inputs. Statistical analysis was conducted to investigate the effects of different mixture variables on the performance of HMA mixtures containing RAP. A preliminary cost comparison of paving jobs with typical Alaskan HMA mixtures with different amounts of RAP and without RAP was also conducted. This task is included in Chapter 4.

1.4.6 Task 6: Draft of Final Report and Recommendations

Upon completion of the aforementioned tasks, a final report was drafted. The report included a literature survey and discussion of the results of other researchers, a description of the research methods and approach for this project, the test procedures and results, this project's findings, and suggestions for further study.

The research findings of this study (including dynamic moduli values of HMA mixtures containing RAP) are intended to be included in a future revision of the Alaska Flexible Pavement Design (AKFPD) software and manual. Recommendations for the use of RAP in new design projects are provided. Specific recommendations have been imparted regarding RAP mix production in hot plants, emission control, and field compaction. Implementation activities (elaborated in Proposed Technology Transfer Activities) were conducted to disseminate research to a broad professional community. The conclusions and recommendations are presented in Chapter 5.

CHAPTER 2.0 LITERATURE REVIEW

Current road construction practice has shown that the use of RAP in the production of new roads has many advantages. The main advantages fall under two broad categories: economic and environmental. The more RAP a project can use, the less high-quality virgin aggregates and binder are necessary in a mixture. Thus, the benefit is immediate to the cost and sustainability of the project due to the reuse of materials and preservation of a natural resource. In addition, the apprehension over waste transport and disposal is reduced since the material will be reused near its original location. This can greatly cut the amount of fuel and employee/equipment hours needed to haul the old material, avoiding landfill use entirely. The use of RAP also benefits the environment by reducing the amount of fossil fuels required to produce fresh HMA. Aurangzeb and Al-Qadi (2014), using life-cycle cost analysis (LCCA), showed a possible \$94,000 per mile reduction in cost for HMA mixes with up to 50% RAP. Their research concluded that the environmental impact of construction could be reduced by up to 28% with higher RAP use when compared with conventional virgin asphalt mixes.

Laboratory research is identifying the benefits of RAP while addressing the sources of resistance to its use. Most agencies currently use small amounts (up to 25% by weight of total mix) of RAP in their HMA mix designs, and the average national usage rate was estimated to be 12% in 2007

(Copeland 2011). The greatest cause of concern for higher RAP use is the pavement's performance. Many researchers have studied the performance of HMA with RAP, generally concluding that an increase of RAP content increases the stiffness and rutting resistance while decreasing the fatigue and low-temperature cracking resistance. Low-temperature cracking resistance of HMA is of special concern in cold climate regions; thus, it is essential to properly characterize Alaskan HMA containing RAP.

2.1 Background of RAP

Recycled asphalt pavement is asphalt pavement materials that have been removed during road resurfacing, rehabilitation, or reconstruction operations. In the United States, use of RAP in HMA gained attention in the 1970s. The rising price of asphalt binder drove the industry to look for cost-saving strategies. Because RAP contains binder, in addition to quality aggregate, its reuse quickly became popular. In 1979, the Federal Highway Administration (FHWA) provided a field demonstration to introduce RAP in paving projects (Hellriegel 1980). According to a report by Hellriegel (1980), the paved shoulder-lane that contained RAP performed "extremely well." Still, the issues of production technology, emission control and pavement performance hindered the wide use of RAP in paving projects during the late 1970s and early 1980s (Howard et al. 2009).

The increasing demand for green technologies in the 1990s made recycling pavement more popular. It was estimated by FHWA and the U.S. Environmental Protection Agency (EPA) (FHWA 1993) that more than 90 million tons of asphalt pavement were reclaimed every year in the early 1990s, making asphalt the most frequently recycled material. Further guidance and information on the practice of pavement recycling were provided by the FHWA in the publication, *Pavement Recycling Executive Summary and Report and Pavement Recycling Guidelines for State and Local Governments: Participant's Reference Book* (Sullivan 1996; Kandhal and Mallick 1997). When the Superior Performing Asphalt Pavements (Superpave) mix design was introduced in 1993 as a product of the Strategic Highway Research Program (SHRP), however, no guidance for the use of RAP in HMA was included, which caused reluctance in state agencies to allow RAP in Superpave mixtures until a design method was developed (Hansen and Newcomb 2011). Furthermore, the Superpave mix design system that was introduced encouraged the use of coarse-graded mixtures, limiting to some degree the amount of RAP that could be used in the mix (Copeland 2011). These issues were addressed in a nationwide study carried out by McDaniel et al. (2000) in National Cooperative Highway Research Program (NCHRP) Project 9-12. The most significant deliverable of the project was NCHRP Report 452, which provided *Recommended Use of Reclaimed Asphalt Pavement in the Superpave Mix Design Method: Technician's Manual* (McDaniel and Anderson 2001).

Many state transportation agencies placed limits on maximum RAP use due to aged binder concerns (Copeland 2011), and economic incentives to use large percentages of RAP were few. However, sharp increases since 2006 in cost of asphalt binder and quality aggregate motivated the asphalt industry to use higher amounts of RAP. A recently completed NCHRP Project 9-46 was conducted to revise and improve current practices for high RAP usage in mix designs. The findings of this project were included in NCHRP Report 752, *Improved Mix Design, Evaluation, and Materials Management Practices for Hot Mix Asphalt with High Reclaimed Asphalt Pavement Content* (West et al. 2013).

2.2 RAP Management

Recycled asphalt pavement management practices differ substantially among HMA producers and agencies state-to-state. Decisions in RAP management practices at a plant include “choices regarding milling and collecting RAP, segregating RAP from different sources, stockpiling, crushing, fractionation, testing, and mix design” (West et al. 2013). Each of these decisions should be assessed individually with a focus on both economics and quality. Those management practices that enable high percentages of RAP and ensure high-quality asphalt mixtures deliver the best long-term value (West et al. 2013).

Recycled asphalt binder is a byproduct generated from milling, from full-depth pavement removal, and from waste HMA materials that are generated at plants. In RAP management, it is important to consider when to keep RAP from a new source separate and when to combine RAP from different sources (Copeland 2011). Besides the RAP source, possible key factors in RAP management include “RAP processing, stockpiling, and mix production for HMA containing RAP for various plant configurations” (West et al. 2013). The National Asphalt Pavement Association (NAPA) published a practical guide, *Recycling Hot Mix Asphalt Pavements, Information Series 123* (NAPA 1996), to address RAP management. This guide is one of the earliest publications to provide a document on “how to recycle,” summarizing for producers and agencies the equipment and methods successfully employed to reclaim, size, store, and process RAP in various types of HMA facilities throughout the country.

In 1998, another guide, *Pavement Recycling Guidelines for State and Local Governments – Participant's Reference Book*, was published by National Center for Asphalt Technology (NCAT) (Kandhal and Mallick 1997). This guide was prepared to provide the following information on recycling of asphalt pavements: performance data, legislation/specification limits, selection of pavement for recycling and recycling strategies, economics of recycling, and structural design of recycled pavements. Included are these recycling methods: hot-mix asphalt recycling (both batch and drum plants), asphalt surface recycling, hot in-place recycling, cold-mix asphalt recycling, and full depth reclamation. Materials and mix design, construction

methods and equipment, case histories and quality control/quality assurance are discussed for all recycling methods.

Further, nationwide RAP management guidance manuals include RAP mix design guides for technicians, originating from NCHRP Project 9-12A (McDaniel and Anderson 2001) and *NAPA's Designing HMA Mixtures with High RAP Content: A Practical Guide, Quality Improvement Series 124* (Newcomb et al. 2007). Both guides provide guidance on sampling RAP stockpiles and techniques. The most recent nationwide guidance, however, was published as one deliverable in NCHRP Report 752 (West et al. 2013): *Best Practices for RAP Management*. This new publication provides management guidance particular to RAP materials from the time of collection through processing, mix design, and quality control practices during production of asphalt mixtures containing RAP. The new guide represents current best practices for RAP management as of 2010; it was prepared by NCAT and reviewed by numerous agencies and industry experts. The aim of the guide is to facilitate the most effective use of RAP and proper RAP management practices.

2.3 RAP Properties

The ability to recycle pavement attracted much attention because both the asphalt binder and quality aggregates in old pavement can be reused. The following section discusses the most important material characteristics found in RAP.

Generally, asphalt binder demonstrates two stages of aging: short-term and long-term (Al-Qadi et al. 2007). Short-term aging occurs mostly during mixing with aggregates, transportation, and laying processes because of exposure to high temperatures (Zaumanis and Mallick 2015). Short-term aging is caused by (a) oxidation which occurs excessively in the asphalt pugmill due to binder spread into thin films; (b) loss of volatile fractions (volatilisation); and (c) absorption of oily constituents, resins, and asphaltenes by aggregates (Read and Whiteoak 2003; Zaumanis and Mallick 2015). Long-term aging mostly occurs in-service and depends on the void content in pavement and on the layer position within the road construction. Long-term aging is caused by (a) oxidation because of constant supply of fresh air; (b) polymerisation; (c) photo-oxidation for surface layers; (d) thixotropy due to the formulation of a structure within asphalt binder over a long period; and (5) syneresis due to exudation of thin oily components (Read and Whiteoak 2003; Zaumanis and Mallick 2015).

As asphalt binder ages, its rheological behavior will inherently differ from virgin materials. This suggests the importance of controlling the blending process between recycled and virgin binders of a mixture (Al-Qadi et al. 2007). If the old binder is too stiff, the blend of old and virgin binders may not perform as anticipated. When blended at intermediate to higher percentages, the aged binder may significantly alter the properties of the blend; however, the small portion of RAP binder (up to 20%) may not have an effect on the properties of the blend (Kennedy et al. 1998).

The RAP aggregates should also be specified to ensure suitable performance. The basic principle is to apply the same requirements to the RAP fractions as those that are specified for virgin aggregates (Willis et al. 2012; Zaumanis and Mallick 2015). In reality, however, excessive fines can be generated during RAP processing (milling and crushing operations) (West 2010), which may result in RAP aggregate fractions that cannot satisfy the aggregate size distribution requirement, dust to binder ratio, and voids in mineral aggregate (VMA) (McDaniel et al. 2002; Zaumanis and Mallick 2015). This issue may limit the use of RAP. Additionally, the variability of RAP gradation is viewed as a concern and has been reported as a problem (Zaumanis and Mallick 2015).

2.4 Design of Mixture with RAP

The current standard for Superpave mix design is AASHTO M 323-07, and the affiliated specification is AASHTO R 35-07 (West et al. 2013). AASHTO M 323-07 includes guidance on using RAP in Superpave mixes, which was based on NCHRP Project 9-12 (McDaniel et al. 2000). One of the most important recommendations is the selection of virgin binders based on RAP content. For RAP content below 15%, the virgin binder grade should be the same as for a virgin mix. For intermediate RAP content between 15% and 25%, the virgin binder should be one full grade lower than for a virgin mix. For RAP content above 25%, blending charts or equations should be used to determine the appropriate virgin binder grade. These practical recommendations were primarily based on the binder blending study previously discussed (McDaniel et al. 2000).

One of the key issues with regard to RAP mix designs is how much actual blending occurs between the RAP binder and the virgin binder. This issue was first addressed in NCHRP Project 9-12 (McDaniel and Anderson 2001). The purpose of the project was to research whether RAP acts like black rock or whether some blending does occur between the RAP binder and the virgin binder. Three types of mixture specimens were fabricated simulating actual practice, black rock, and total blending (Table 2.1). After the Superpave shear tests and indirect tensile creep and strength tests, it was concluded that RAP does not act like black rock under blending conditions;

it partially blends to a significant extent, rather than total blending of the RAP binder and the virgin binder. Soleymani et al. (2000) also suggested partial blending in a similar performance-based study.

Table 2.1 Three blending simulations adopted in NCHRP Project 9-12 (McDaniel and Anderson 2001)

Mixture Type	Preparation Method
Actual Practice	Blending RAP, virgin aggregate and virgin binder, simulating actual practice
Black Rock	Removal of RAP binder, blending virgin binder with recovered RAP aggregate and virgin aggregate, simulating no blending
Total Blending	Removal of RAP binder, physically blending the extracted and recovered RAP binder into the virgin binder, then combining the blended binder into the virgin aggregate, simulating total blending

Other studies on RAP-virgin binder blending focused on qualitative evaluation, by developing a mechanical model (Bonaquist 2007), using a $G^*/\sin(\delta)$ index (Shirodkar et al. 2011), direct observation through atomic force microscopy (AFM) (Nahar et al. 2013), and chemical characterization using gel permeation chromatography (GPC) (Zhao et al. 2016). Recent research conducted by Zhao et al. (2015) directly quantified the RAP binder mobilization rate during mixing. This GPC-based method led to a conclusion that the RAP binder mobilization rate decreased with the increase in RAP percentage in the mixtures evaluated in the study, which could approximate 100% at low RAP content (10% and 20%), while dropped from 73% to 24% when the RAP percentage increased from 30% to 80%. The quantified RAP binder mobilization

rate defines how much aged binder is available during the mixing process. This parameter may be used in RAP mix design if the accuracy of the data quantification is satisfied.

2.5 Laboratory Evaluation of RAP Mixtures

Laboratory evaluations of asphalt mixtures containing RAP vary widely in scope and procedure. Most are performed to evaluate the following: (a) stiffness, (b) rutting resistance, (c) fatigue resistance, (d) low-temperature cracking, and (e) moisture resistance.

2.5.1 Stiffness – Dynamic Modulus

In the NCHRP 9-12 project (McDaniel et al. 2000), shear tests and indirect tensile tests were conducted to assess the effects of RAP on mixture stiffness at high, intermediate, and low temperatures. The findings from testing mixtures with three RAP samples and two virgin binders indicated that all the selected tests showed a stiffening effect from the RAP binder at higher RAP content (McDaniel et al. 2000). At low RAP content, the mixture properties were not significantly different from those of mixtures with no RAP.

With the intent to examine how the addition of RAP changes the volumetric and mechanistic properties of asphalt mixtures, Daniel and Lachance (2005) evaluated one Superpave mixture

containing two types of RAP: a processed RAP and an unprocessed RAP. Testing included dynamic modulus in tension and compression, creep compliance in compression, and creep flow in compression. Dynamic modulus and creep compliance master curves were constructed with the use of the time-temperature superposition principle to describe the behavior of each mix over a range of temperatures. The dynamic modulus of the processed RAP mixtures increased from the control to a 15% RAP level, but the 25% and 40% RAP mixtures had dynamic modulus curves similar to that of the control mixture in both tension and compression. The creep compliance curves showed similar trends. A combination of gradation, asphalt content, and volumetric properties is likely the cause of these trends.

Li et al. (2008) studied the effect of RAP percentages and sources on the stiffness of asphalt mixtures. Ten asphalt mixtures, with two different binder grades (PG 58-28, PG 58-34) from two different sources, with three RAP content percentages (0%, 20%, 40%) were evaluated.

Experimental results indicated that asphalt mixtures containing RAP have higher dynamic modulus values than the control mixtures containing no RAP. The stiffer asphalt binder results in higher dynamic modulus values for both the control and the RAP-modified mixtures.

Experimental data reveal that the RAP source is not a significant factor for the dynamic modulus at low temperatures, although it significantly affects dynamic modulus values at high temperatures. No significant statistical relationship between dynamic modulus and fracture energy was determined.

Mogawer et al. (2012) compared laboratory-testing results from eighteen plant-produced mixtures obtained from three locations in the northeast United States. The RAP content varied from zero to 40%. The stiffness of the mixtures increased as the percentage of RAP increased, but not when the discharge temperatures of the mixtures were inconsistent. Additionally, reheating the mixtures in the laboratory caused a significant increase in the stiffness of the mixtures.

Colbert and You (2012) investigated the influence of fractionated RAP materials on asphalt mixture performance. The RAP mixture percentages assessed in the study were 15%, 35%, and 50%. It was found that, on average between all RAP mixtures, the addition of RAP increased the resilient modulus by 52% due to the addition of RAP asphalt binder and aggregates, which stiffened the mixture under higher temperature and heavier loading conditions. Dynamic modulus results indicated a statistical significant difference for high percentage RAP mixtures.

2.5.2 Rutting Resistance

Stroup-Gardiner and Wagner (1999) conducted a study to investigate the use of reclaimed asphalt pavement in Superpave HMA applications. Two sources of RAP (Georgia and Minnesota) were used so that a wide range of asphalt and aggregate properties would be represented. Results showed that the mixes containing RAP had significantly lower rutting

depths in the Asphalt Pavement Analyzer (APA) tests, which indicated the higher rutting resistance of RAP mixes.

In NCHRP Report 452 (McDaniel et al. 2000), shear tests were conducted on mixtures containing different RAP content (0%, 10%, 20%, and 40%). The shear testing results indicated an increase in stiffness and decrease in shear deformation as the RAP content increased. This indicates that a higher RAP content mixture exhibits a greater resistance to rutting.

Further research has determined that a correlation exists between increased rutting resistance and increased percentage of RAP content in the mixture. Mogawer et al. (2012) found that rutting resistance improved as the percentage of RAP in the mixtures increased. Colbert and You (2012) found that, on average between all RAP mixtures (RAP content ranging from 15% to 50%), the addition of RAP decreased rutting by 24%.

Apeagyei et al. (2011) developed nineteen projects to evaluate the rutting resistance of plant-produced asphalt mixtures in the laboratory. These mixtures contained RAP amounts that ranged from 0% to 25%. Tests on the mixtures included the dynamic modulus ($|E^*|$) test at multiple temperatures and the flow number (FN) test at 54°C to characterize stiffness and rutting resistance, respectively. Mixtures with lower FNs either contained no RAP, contained 25% RAP, or had PG 64-22 as the design binder grade. Mixtures that contained moderate amounts of RAP

(10% and 15%), regardless of design binder grade, had higher FNs than mixtures with either high or low RAP amounts. Statistical analysis showed that the RAP amount was the most significant factor to affect rutting resistance in the mixtures studied. The effect of RAP on FN was unexpected, because it showed the rutting resistance to decrease with increased RAP.

Possible reasons for this result might have been the use of softer asphalt binder in mixtures with higher RAP and the observed decrease in both P_b and $G^*/\sin \delta$ with increased RAP amounts.

Before conclusions can be drawn, caution is advised concerning rutting performance of RAP mixtures (Zaumanis and Mallick 2015). If reduced binder grade or rejuvenators are used, rejuvenator or virgin binder will continue to penetrate (diffuse) the aged binder film even after placement of the pavement. The dominant effect of the softer outer layer may lead to increased dynamics of developing permanent deformations in early stages of pavement life up to the point when equilibrium is reached (Shah et al. 2007; Zaumanis and Mallick 2015).

2.5.3 Fatigue Resistance

Fatigue cracking is mainly caused by repeated traffic loading and can lead to significant reduction in the serviceability of flexible pavements (Shu et al. 2008). For HMA containing RAP, the stiff RAP binder is prone to cracking under long-term traffic conditions, thus causing more severe fatigue issues. The beam fatigue testing results from the NCHRP 9-12 Project report

(McDaniel et al. 2000) support this conclusion, since beam fatigue life decreased with higher RAP content when no change was made in the virgin binder grade.

Shu et al. (2008) conducted a laboratory study evaluating the fatigue characteristics of plant-prepared HMA mixtures containing 0%, 10%, 20%, and 30% RAP with one source of aggregate, limestone, and one type of binder, PG 64-22. This study used different testing methods with Superpave indirect tension (IDT) tests and beam fatigue testing. The fatigue properties tested included indirect tensile strength (ITS), failure strain, toughness index (TI), resilient modulus, $DCSE_f$, energy ratio, plateau value, and load cycles to failure. The results indicate that both Superpave IDT and beam fatigue tests agree in ranking the fatigue resistance of mixtures when proper procedures are followed.

With the decision by the Virginia DOT to allow higher percentages—more than 20%—of RAP in HMA with no change in binder grade, Maupin et al. (2009) conducted a study to estimate the effect of increased RAP percentages on performance and relative cost. Laboratory tests revealed no significant difference between the higher RAP mixtures and the control mixtures for fatigue performance. The study reported that value engineering proposals received for jobs not advertised with a high RAP specification seemed to indicate that using more than 20% RAP could reduce costs in some cases.

2.5.4 Low Temperature Cracking

Aged RAP binder typically increases stiffness of asphalt mixtures, leading to potential concerns regarding low-temperature brittleness (Tam et al. 1992). The results of using recycled hot-mix (RHM) at five sites constructed by the Ontario Ministry of Transportation between 1981 and 1983—sites participating in early asphalt recycling programs—are presented in Tam et al. (1992). The laboratory findings involved a comparison between the two types of results and the use of McLeod's limiting stiffness criteria and fracture temperature method. The study confirms the common belief that RHM is less resistant to thermal cracking than nonrecycled mixes are. The fracture temperature method was found to be better than McLeod's limiting stiffness approach for evaluating low-temperature cracking. Recommendations to improve RHM low-temperature performance were made.

In NCHRP Report 452 (McDaniel et al. 2000), indirect tensile testing to evaluate mixtures with varied RAP content is described. It was found that at low RAP content, the testing results of RAP mixtures did not vary significantly from the results of control mixtures. However, results showed increased stiffness for higher RAP content mixtures, which could lead to an increase in low-temperature cracking—if no adjustment is made in the virgin binder grade.

Mogawer et al. (2012) conducted a RAP study to document the effects of mixture production parameters on mixture performance, including cracking resistance. In the study, RAP content (zero to 40%) varied and softer binders were used. The study found that cracking resistance was reduced as the percentage of RAP in the mixtures increased.

Willis et al. (2013) pointed out that most highway agencies have decades of experience with HMA whose percentage of RAP has remained low to moderate because of the general perception that RAP mixtures may be more susceptible to various modes of cracking, including low-temperature cracking. Two methods are proposed in Willis et al. (2013) to increase the durability of RAP mixtures: (a) increase the amount of virgin binder in the asphalt mixture and (b) decrease the performance grade of the virgin binder. Through testing of several RAP mixtures with the use of energy ratio concepts and an overlay tester, it was concluded that when RAP binder exceeds 30%, a softer grade of asphalt should be used to increase the mixture's resistance to cracking.

2.5.5 Moisture Resistance

Moisture damage affects the properties of aged binder in RAP prior to recycling (Al-Qadi et al. 2007). In principle, stripped HMA should not be recycled because of the probability of this distress recurrence in the new HMA. However, when a small percentage of RAP was used (15%

to 20%) together with an anti-strip agent, samples with moisture-damaged HMA provided comparable strength and moisture resistance to samples made with virgin materials. For mixtures containing RAP, as RAP aggregates are already covered with asphalt, there is less chance of water penetration in the particles. Therefore, in general, highly recycled asphalt mixtures are not susceptible to more stripping than conventional asphalt (Zaumanis and Mallick 2015).

Al-Qadi et al. (2012) conducted a study to investigate the impact of high RAP content on structural and performance properties of asphalt mixtures. Moisture damage of RAP mixes is evaluated in terms of tensile strength ratio (TSR). In general, tensile strength and TSR of the HMA increased as RAP content increased. Apart from one mix type (District 5 HMAs) with 40% RAP, all tested HMAs exceeded the Illinois DOT's minimum TSR criterion of 85%. However, the District 5 control mix failed to pass the minimum tensile strength criterion of 60 psi (414 kPa). Visual inspections conducted on failed split TSR specimen faces showed similar stripping behavior between the control mixtures and the mixtures containing RAP, which shows that mixtures with RAP expressed comparable moisture resistance to control mixes.

Mogawer et al. (2012) used a Hamburg Wheel Tracking Device to investigate the moisture susceptibility of HMA that contained various amounts of RAP. It was found that water damage resistance improved as the percentage of RAP in the mixtures increased.

The NCHRP 9-46 project also used TSR (West et al. 2013) to evaluate the moisture susceptibility of RAP mixtures with different aggregates, varied RAP content, and virgin binder grades. With the addition of anti-stripping additive, the RAP mixtures could reach the 0.8 TSR threshold. However, it was noted by the authors that the tensile strength of the conditioned or unconditioned RAP samples was always higher than that of the virgin control mixtures. The use of TSR to assess moisture susceptibility was only questioned by the authors.

One study conducted by Xiao and Amirkhanian (2009) focused on the effect of RAP on moisture damage in rubberized asphalt mixtures. The testing conducted included the determination of binder viscosity, toughness, and ITS analysis. Several mixtures containing different crumb rubber types, two different RAP sources, and various percentages of rubber and RAP were evaluated. The results indicated that, in general, the addition of RAP improved the ITS values and reduced the moisture susceptibility of the mixture, although the addition of crumb rubber had a slightly negative effect.

2.6 Field Evaluation

A study by Paul (1996) was among the earliest to examine the variations found in recycled asphaltic concrete mixtures based on field evaluation. Five recycling projects constructed in the late 1970s and early 1980s were selected for examination, with five conventional construction

projects used as controls. The five-year field evaluation examined performance from the perspective of structure, serviceability, and distress. Findings indicate that pavements containing reclaimed materials performed similarly to conventional mixtures for a period of 6 to 9 years of service life.

The California Department of Transportation (Caltrans) initiated a study (Zaghloul et al. 2007) to evaluate the performance of in-service pavements in California, and hence the success of Caltrans' pavement design and rehabilitation procedures. This effort also included the investigation of the field performance of RAP. As part of this study, sixty RAP test sections located in three of California's environmental zones—Desert (DS), Mountain (MT), and North Coast (NC)—along four routes (one in each of Caltrans Districts 1, 7, 9, and 11) were considered. Deflection, roughness, distress, and cores/bores were among the data attributes collected from the test sections. Based on field data, it was found that the RAP sections triggered for ride quality, distress, and structural adequacy in the NC, DS, and MT environmental zones, respectively. The NC RAP sections were observed to perform better than the DS and MT RAP sections. The authors attributed this to the use of cement treated base (CTB), since CTB typically has a higher modulus than an aggregate base course.

Appea et al. (2009) provided several case studies of field locations with high RAP mixtures used in 2007 on selected routes in Virginia. A description of RAP processing at different plants was

given, including how the production of high RAP material (RAP which makes up 20% or more of the asphalt mix) was monitored at the plant location and in the field. Additionally, the study offered a view of the types of asphalt plants operated by varying contractors, showing how each location maintained quality control in high RAP production. Results show that placement of high RAP went well, and field monitoring mechanisms are being put in place to continue monitoring these sites for long-term performance.

A study conducted by NCAT in 2009 compared virgin and recycled asphalt pavements using data from the Long-Term Pavement Performance (LTPP) program (West 2009). The data were collected over a period of approximately 20 years. The study examined the impacts of several other important factors (location, age, overlay thickness, and milling of the existing pavement). Seven pavement performance measurements were analyzed: International Roughness Index (IRI), rutting, fatigue cracking, longitudinal cracking, transverse cracking, block cracking, and raveling. The statistical analyses showed that RAP mixes performed better than or equal to virgin mixtures for the majority of the data obtained. From the results, in most cases, using at least 30% recycled material in asphalt pavement provides the same overall performance as virgin pavement.

2.7 State Specifications

Economic analyses using various calculation methods showed that with the use of 50% RAP, there was a savings of 24% (Kristjánssdóttir et al. 2007), 26% (Brock and Richmond 2007), or 35% (Willis et al. 2012). However, in many states, undetermined mix design methods and limited knowledge of the production process dictate allowable RAP content (Zaumanis and Mallick 2015). For example, Washington DOT allows 20% RAP by weight of aggregate in HMA without further testing, while Oregon currently allows up to 30% RAP to be used in HMA, although the use of blending charts for RAP proportions greater than 15% is recommended. New Hampshire allows up to 30% RAP from a known recyclable source or 15% RAP from an unknown source to be used in a mixture. Nebraska allows up to 40–50% of RAP for primary types of asphalt mixtures. A study done by the FHWA (1993) indicated that up to 80% RAP has been used in some HMA with an acceptable level of performance. Overall, the maximum use of RAP materials in asphalt mixtures is desired, but is not a simple task because of the undesirable innate characteristics of RAP, that is, aged (stiff) asphalt binder and inconsistent aggregate properties. The recently completed NCHRP 09-46 project (West et al. 2013) aimed at developing a mix design and analysis procedure for HMA containing high RAP content (defined as greater than 25% and may exceed 50%). The project also targeted satisfactory long-term performance goals and proposed changes to existing specifications to account for HMA containing high RAP content.

The most updated information about state specifications on RAP usage can be found in a recent Asphalt Pavement Industry Survey initiated by NAPA (Hansen and Copeland 2015). Figure 1 shows the estimated average percent of RAP by state from 2009 to 2014; the detailed data are arranged in Figure 2. The accuracy of the data is dependent on the responses. It can be seen that the number of states that average more than 20% RAP in HMA/WMA (colored green and dark green) increased steadily from seven states in 2009 to 23 states in 2014. The use of increased amounts of RAP has spread quickly in the Midwest and West. For 2013 and 2014, all (100%) of the contractors/branches responding to the survey reported using RAP, and more than 91% of contractors reported having excess RAP on hand in 2014. In 2011 and 2012, 98% of respondents reported using RAP. From 2013 to 2014, the amount of RAP used in HMA/WMA increased from 67.8 million to 71.9 million tons. The average percent RAP used in mixtures increased from 19.3% in 2013 to 20.4% in 2014.

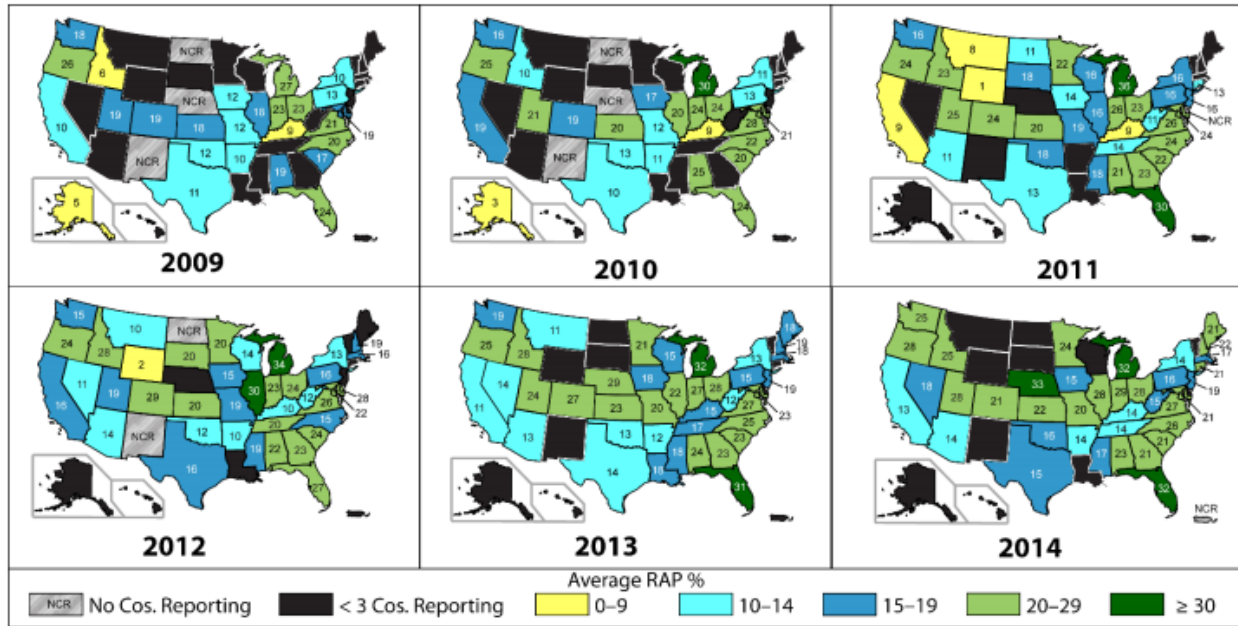


Figure 2.1 Estimated average percent of RAP by state (Hansen and Copeland 2015)

State	Average RAP Percent						State	Average RAP Percent					
	2009	2010	2011	2012	2013	2014		2009	2010	2011	2012	2013	2014
Alabama	19%	25%	21%	22%	24%	23%	Montana			8%	10%	11%	
Alaska	5%	3%					Nebraska	NCR	NCR			29%	33%
Arizona			11%	14%	13%	14%	Nevada				11%	14%	18%
Arkansas	10%	11%		10%	12%	14%	New Hampshire				19%	19%	22%
California	10%	19%	9%	16%	11%	13%	New Jersey			16%		19%	19%
Colorado	19%	19%	24%	29%	27%	21%	New Mexico	NCR	NCR		NCR		
Connecticut			13%			21%	New York	10%	11%	16%	13%	13%	14%
Delaware			NCR	28%			North Carolina	20%	22%	24%	15%	25%	26%
District of Columbia	NCR	NCR	NCR	NCR		NCR	North Dakota	NCR	NCR	11%	NCR		
Florida	24%	24%	30%	27%	31%	32%	Ohio	23%	24%	23%	24%	28%	28%
Georgia			23%	23%	23%	21%	Oklahoma	12%	13%	18%	12%	13%	16%
Hawaii							Oregon	26%	25%	24%	24%	25%	28%
Idaho	6%	10%	23%	28%	28%	25%	Pennsylvania	13%	13%	16%	16%	15%	16%
Illinois	18%	20%	16%	30%	22%	28%	Puerto Rico						NCR
Indiana	23%	24%	26%	23%	27%	29%	Rhode Island						
Iowa	12%	17%	14%	15%	18%	15%	South Carolina	17%	20%	22%	24%	23%	21%
Kansas	18%	20%	20%	20%	23%	22%	South Dakota			18%	20%		
Kentucky	9%	9%	9%	10%	15%	14%	Tennessee			14%	20%	17%	14%
Louisiana					18%		Texas	11%	10%	13%	16%	14%	15%
Maine					18%	21%	Utah	19%	21%	25%	19%	24%	28%
Maryland	19%	21%	24%	22%	23%	21%	Vermont						
Massachusetts				16%	18%	17%	Virginia	21%	28%	26%	26%	27%	27%
Michigan	27%	30%	36%	34%	32%	32%	Washington	18%	16%	16%	15%	19%	25%
Minnesota			22%	20%	21%	24%	West Virginia			11%	12%	12%	15%
Mississippi			18%	19%	18%	17%	Wisconsin			16%	14%	15%	
Missouri	12%	12%	19%	19%	20%	20%	Wyoming			1%	2%		
No Contractors Reporting		< 3 Contractors Reporting		0-9%	10-14%	15-19%	20-29%						≥ 30%

Figure 2.2 Average estimated RAP percent (Hansen and Copeland 2015)

2.8 Economic Analysis of Using RAP

Due to the economic and environmental benefits of recycling, state agencies are focusing increasing efforts to incorporate higher levels of RAP in new construction projects. To provide support for this movement, several researchers have studied new methods to analyze the cost (or cost savings) associated with increasing RAP use. The many influential factors include, for instance, which technologies are available for the inclusion of RAP and where in the pavement structure the benefits of RAP use can be maximized. To properly evaluate the life cycle costs of using RAP in highway construction, both economic and environmental aspects must be considered.

The National Center for Asphalt Technology (NCAT) website

(<http://www.morerap.us/files/faq.pdf>) provides an example of the cost savings realized by using 20% RAP in a traditional hot mix with a target binder content of 5%. In this case, the cost saving was determined as \$5.11 per ton.

Table 2.2 NCAT cost analysis assumptions

Mix Type	Assumptions
Virgin Mix	Virgin aggregate: \$13 per ton; Virgin binder: \$435 per ton; Virgin mix cost: \$34.10 per ton
RAP Mix	Virgin aggregate: \$13 per ton; Processed RAP: \$9 per ton; RAP with 5% binder content; 20% RAP mix cost: \$28.99

The Alaska Department of Transportation & Public Facilities (ADOT&PF) provides a straightforward model for comparing alternative design strategies for cost analysis purposes. The ADOT&PF model can be found in the Alaska Flexible Pavement Design Manual (2004). This model is based on engineering economics and is useful when comparing costs associated with alternative designs. The use of recycled materials can easily be evaluated using this model. The ADOT&PF model suggests a seven-step analysis for conducting a cost analysis: (1) establish alternative design strategies, (2) determine performance periods and activity timing, (3) estimate agency and user cost, (4) develop cash flow diagrams, (5) compute net present value cost for each alternative, (6) perform a sensitivity analysis, and (7) analyze the results and reevaluate the strategies.

Several researchers have identified issues incorporating recycled asphalt into cost analysis models. These issues arise because of the various methods of RAP use in the construction process. Morian and Ramirez (2016) have identified three main technologies for this purpose: cold in-place recycling, cold plant recycling, and hot in-place recycling. The proposed model incorporates several costs associated with each construction alternative and provides a methodology for evaluating these costs using a cost/benefit analysis. All HMA containing RAP production costs are compared with that of virgin materials to provide a clear assessment for economic evaluation. The proposed model is as follows:

$$TIC = RAP + MC + PC + MobC + HC + PavC \quad (\text{Eq. 2.1})$$

where TIC = total initial cost (\$/ton), RAP = RAP removal cost (\$/ton), MC = recycled mix cost (\$/ton), PC = plant cost (\$/ton), $MobC$ = mobilization cost (\$/ton), HC = hauling cost (\$/ton), and $PavC$ = paving cost (\$/ton). Each of the factors considered in this equation represent variables evaluated by the following functions: $RAP = f(\text{removal depth, equipment cost})$; $MC = g(\text{mix design, RAP\%, material costs})$; $PC = h(\text{RAP sizing, RAP stockpiling costs, plant modification cost, laboratory test cost})$; $MobC = i(\text{distance to jobsite, permits cost, cost per mile})$; $HC = j(\text{hauling cycle duration, project length, trucking costs})$; $\text{Hauling cycle duration} = k(\text{truck capacity, delay at plant, loading time, distance to job site, delay at job site, dump time})$; $PavC = l(\text{placement costs, compaction costs})$.

Once the total initial cost (TIC) was determined for each construction alternative, an equivalent annual cost (EAC) was calculated. To do this, the performance life of each alternative was estimated based on a literature survey. The proposed EAC equation is as follows:

$$\text{Equivalent Annual Cost (EAC)} = \frac{\text{Total Initial Cost } \left(\frac{\$}{\text{ton}}\right)}{\text{Expected performance life (years)}} \quad (\text{Eq. 2.2})$$

Using the EAC, a cost benefit analysis was conducted to evaluate the economic benefit of each construction alternative compared with conventional virgin HMA. The following equation shows this procedure:

$$\frac{B}{C} = \frac{(EAC \text{ Recycling Method})}{(EAC \text{ Virgin HMA})} \quad (\text{Eq. 2.3})$$

The authors further refined this model by incorporating the structural contribution of the various asphalt pavement products to overall pavement performance. Following recommendations by the 1993 AASHTO Guide, virgin HMA was assigned a structural coefficient of 0.44 per inch of thickness, and underlying asphalt-treated base layers were assigned a value of 0.4 per inch of thickness. The authors used a layer coefficient of 0.3 per inch of thickness for recycled asphalt pavement products. Using the structural layer coefficient, the cost benefit equation became:

$$\frac{B}{C} = \frac{(EAC \text{ Recycling Method}) * (Structural Layer Coefficient Virgin HMA)}{(EAC \text{ Virgin HMA}) * (Structural Layer Coefficient Recycling Method)} \quad (\text{Eq. 2.4})$$

Using data from the literature, the authors evaluated each construction method on a cost/benefit basis. In general, it was concluded that when compared with virgin HMA mixtures, all recycling options were beneficial from an economic standpoint, but the greatest cost savings could be realized using hot in-place recycling. The authors were clear to point out that several project-specific factors may influence the perceived benefits of using RAP. Some of these factors include percentage of RAP allowed in the mix design and haul distance to transport RAP. These as well as other project-specific variables must be analyzed carefully by the owner and design team to determine the most cost-effective alternative. It is also important to keep in mind the

technologies available for inclusion of RAP. Some technologies, such as hot in-place recycling, may not be in use at every agency.

Other researchers have investigated best uses with regard to pavement structure for reclaimed asphalt. Franke and Ksaibati (2014) researched the most cost-effective applications for RAP.

Using a method proposed by NAPA, they assessed the benefits of using RAP in hot plant mixes.

They compared these findings with the benefits of using RAP in gravel roads and as base material. It was concluded that the most substantial cost savings when using RAP for highway construction projects is realized in its use in hot plant mix. In the study, a cost savings of \$40.87 per ton of RAP was determined when RAP was incorporated in the hot plant mix. When RAP was used in the construction of gravel roads, a cost savings of \$17.07 was realized, and \$15.71 per ton of RAP was saved by incorporating RAP in the base materials. It is important to keep in mind project-specific variables (e.g., haul distances), which can affect the results of this type of analysis.

In addition to the economic costs associated with highway construction, environmental costs must be evaluated. Willis (2015) researched the effect of recycled materials on pavement life cycle. In this study, the author assessed the environmental impact of highway construction activities based on energy consumption and equivalent emitted carbon. The research database was composed of a 2012 NCAT test section designed to reduce the life-cycle costs of the

pavement structure. Using the life-cycle assessment software Roadprint, a comparison was made on the material and construction phases of an idealized virgin hot-mix construction project.

Based on this study, Willis concluded that the CO₂ produced during raw material extraction and processing is greatly reduced when recycled materials are used to replace virgin aggregate.

Carbon dioxide production was reduced by 5% to 29%, and energy consumption was reduced by 9% to 26% by using recycled materials. In addition to energy consumption and CO₂ emission, other environmental concerns arise regarding the use of RAP. Issues regarding the potential of certain toxic constituents to leach into soil and groundwater have been evaluated. This concern includes the processing and transporting of recycled materials, including RAP.

Research by Horvath (2003) shows average metal leachate concentrations and how they compare with the limits established by the Texas Risk Reduction Program (TRRP). The results are summarized in Table 2.3.

These environmental concerns can be difficult to quantify economically. The author recommends the use of a software package titled, Pavement Life-cycle Assessment Tool for Environmental and Economic Effects (PaLATE). This software estimates energy consumption and emissions of CO₂, NO_x, PM₁₀, SO₂, CO, and average leachate for various construction materials including RAP. PaLATE can be used to help highway designers evaluate the environmental implications of design alternatives.

Table 2.3 Average leachate concentrations ($\mu\text{g/L}$) (Horvath 2003)

Metal	TRRP Limits	RAP
Al	24000	2000
Sb	6	5.74
As	50	25
Ba	2000	2007
Be	4	1
Cd	5	1.51
Cr	100	5.5
Pb	15	20.4
Mn	1100	106.7
Hg	2	2
Mo	120	10
Ni	100	50
Se	50	25
V	26	25.17
Zn	7300	633

Based on the literature review of this section, it is clear that cost analysis (both economic and environmental) is crucial to any roadway design project. Job-specific variables must be considered carefully to determine which design applications of recycled materials will maximize the benefits. For example, in Alaska many construction projects occur in remote areas. Because of this remoteness, factors such as haul distances can become major considerations in cost analysis. In addition, due to the poor subgrade materials in many areas, the use of RAP may prove most beneficial in pavement layers beneath the wearing course. To properly evaluate the life-cycle costs of road construction, many factors must be considered. It is the responsibility of

the design team to examine all feasible alternatives for potential benefits to cost as well as the environment.

CHAPTER 3.0 EXPERIMENTAL DETAILS

3.1 Materials

The ADOT&PF divides the state into three regions: Southcoast, Central, and Northern. For this project, materials from the Central and Northern regions were selected for characterization.

Southcoast region materials were excluded based on availability and logistical difficulties as well as the recommendation of ADOT&PF professionals. The inclusion of RAP in HMA mix designs is also significantly more prevalent in the Central and Northern regions. Six mixes were proposed for the Central region and five mixes were proposed for the Northern region in considering RAP content as high as 35% and various mix and binder types. The materials studied in this experiment are summarized in Table 3.1.

The Central region included six mixes covering two binder grades, PG 52-28 and PG 58-34, and two mix designations, Type II-A and Type II-B. The six mixes were composed of three control mixes without RAP and three RAP mixes, with one control mix paired with one RAP mix. Type II-A was tested with 25% RAP and the binder designation PG 58-34. This mix was acquired from the field as a plant-produced mix. Type II-B was tested with 25% RAP with the PG 58-34 binder and 35% RAP with the PG 52-28 binder. The mixture with 25% RAP was acquired from

the field, and 35% RAP was produced in the lab following the job mix formula (JMF) of mix No. 1 with the same binder grade and mix type. All RAP mixtures were tested against a control containing no RAP. Control specimens Type II-A with PG 58-34 binder and Type II-B with PG 52-28 binder were acquired in the field. Control Type II-B (No. 2) with binder designation PG 58-34 was produced in the lab following the JMF of mix No. 5 with the same binder grade and type mix.

The Northern region mixes used two different binder grades: PG 52-28 and PG 52-40. The Type II-B mix designation was used for all mixes from this region with differing amounts of RAP. The PG 52-28 binder was tested with 25% and 35% RAP, while the PG 52-40 was tested at 25%. Both mixtures were tested against a control mix containing 0% RAP. Due to the lack of highway construction projects in the Northern region, all asphalt mixtures were produced in the laboratory. One JMF was used for mixes with the same binder type, provided by the same contractor that supplied the aggregates. Table 3.1 provides a summary of the Northern region mixes studied in this experiment.

Table 3.1 Matrix of HMA mixtures

Mix #	Region	Mix Type	Mix Name	RAP %	Binder PG Supplier	Aggregate Source	Project Name/No./Contractor/Year
1	Central	Control	Type II-B	0	PG 52-28 Tesoro	MP 78 Parks Pit (KASH)/C Str. QAP	A-Street Resurfacing/ 56000/ QAP/ 2014
2		Control	Type II-B	0	PG 58-34 EP	MP 78 Parks Pit (Dyno- Nobel)/C Str. QAP	Lab Produced
3		Control	Type II-A	0	PG 58-34 Denali	MP 39 Glenn Hwy / AS&G	Lake Hood A&B Parking Rehab / 54465 / Granite / 2015
4		RAP25	Type II-A	25	PG 58-34 Denali	MP 39 Glenn Hwy / AS&G	AIA 7L/25R Runway Rehab/ 53598 / Granite / 2015
5		RAP25	Type II-B	25	PG 58-34 Denali	MP 39 Glenn Hwy / AS&G	W. Dowling Ph.II Recon. / 51030 / Granite / 2015
6		RAP35	Type II-B	35	PG 52-28 Tesoro	MP 78 Parks Pit (Dyno- Nobel)/C Str. QAP	Lab Produced
7	Northern	Control	Type II-B	0	PG 52-28 EP	Tanana River Valley (Exclusive Paving)	Lab Produced
8		Control	Type II-B	0	PG 52-40 EP	Tanana River Valley (Exclusive Paving)	Lab Produced
9		RAP25	Type II-B	25	PG 52-28 EP	Tanana River Valley (Exclusive Paving)	Lab Produced
10		RAP25	Type II-B	25	PG 52-40 EP	Tanana River Valley (Exclusive Paving)	Lab Produced
11		RAP35	Type II-B	35	PG 52-28 EP	Tanana River Valley (Exclusive Paving)	Lab Produced

* Type II: NMAS 19mm; Class A: 75 blows; Class B: 50 blow

The materials used for plant-produced mixes were selected by the contractors in charge. The materials used for lab-produced mixes were selected according to local availability. All the aggregates were collected from the same contractors who selected the JMFs (Figure 3.1). Binders were provided by the contractors according to their availability. Recycled asphalt pavement used in both the Central and the Northern regions was collected from the Northern region (Figure 3.2), as RAP collected from the Central region was not fractionated. Ignition (Figure 3.3) and sieving analysis (Figure 3.4) tests were performed to verify binder content and gradation for selected RAP. The binder content of RAP was determined to be 4.75%. Descriptions of all JMFs used in this study can be found in Appendix A.



Figure 3.1 Collected aggregates



Figure 3.2 Collected RAP



Figure 3.3 Binder content determination with ignition test



Figure 3.4 Gradation verification of RAP

3.2 Binder Tests

Table 3.2 presents the binder-testing matrix based on discussion with ADOT&PF engineers.

Three typical Alaskan binders provided by Emulsion Product that were used in many of the selected mixes were tested, including PG 52-28, PG 52-40, and PG 58-34. A DSR was used to verify the binder high-temperature grading, to test for viscoelastic behavior and master curve, and to determine rutting potential using the MSCR method. The BBR and DTT were used to determine the binder's low-temperature performance, and this data were analyzed using Thermal Stress Analysis Routine (TSAR) software to determine the binder's critical cracking temperature.

Table 3.2 Testing matrix (triplicates for each test)

Properties	Parameters	Equipment	Binder status	Binders	Testing T (°C)	Standard
Binder Grading		DSR		PG 52-28 PG 52-40 PG 58-34		ASTM D 7643
Viscoelastic behavior	complex modulus (G^*) and phase angle (δ)	DSR	RTFO	PG 52-28 PG 52-40 PG 58-34	Three for each ($\pm 6^\circ\text{C}$ and high PG) ¹	AASHTO T 315
Master Curve		DSR	RTFO	PG 52-28 PG 52-40 PG 58-34		AASHTO T 315
MSCR	See standard	DSR	RTFO	PG 52-40 PG 58-34 ²	Two for each (-6°C and high PG) ³	AASHTO MP 19
Low Temperature	See standard ⁴	BBR	See standard	PG 52-28 PG 52-40 PG 58-34	See standard	AASHTO T 313
Low Temperature	See standard	DTT	See standard	PG 52-28 PG 52-40 PG 58-34	See standard	AASHTO T 314

¹ For example, PG 52-28 should be tested at 46°C, 52°C, and 58°C.

² PG 52-28 can be tested for reference.

³ For example, PG 52-40 should be tested at 52°C and 46°C.

⁴ For BBR, need to collect data for each point used to develop the curve. Provide the $S(t)$ vs. time variation for each binder. The collected data will be used for further analysis with TSAR™ software.

3.2.1 Dynamic Shear Rheometer

The dynamic shear rheometer (DSR) test was used to analyze the viscoelastic behavior at mid- to high-level temperatures. Adhering to ASTM D-7643 and AASHTO T 315, three asphalt binders—PG 58-34, PG 52-28, and PG 52-40—were subjected to DSR testing (Figure 3.5). Six specimens per binder grade were tested, with three specimens acting as a virgin binder group and

three specimens undergoing the RTFO aging method (Figure 3.6). Figure 3.7 shows the DSR specimens. For each binder grade group, a mid and high temperature were chosen irrespective of in-service placement temperature and applied to the control group and RTFO-aged specimens. For the test, a thin film of binder specimen was placed between two plates of the DSR device, the lower plate fixed, and a torque was applied to the upper plate at a frequency of 10 radians per second. The applied torque and resulting shearing strain measured by the DSR test, contribute to the complex modulus (G^*) and phase angle (δ) computation. The G^* is a measurement of total resistance to deformation under constant shear, while δ is the interval between the applied shearing stress and the resulting shearing strain due to applied torque. For the original binder group, the binder specification requires a minimum value of 1.0 kPa for $G^*/\sin\delta$ for the corresponding temperature. For the RTFO-aged binder group, the binder specification requires a minimum value of 2.20 kPa for $G^*/\sin\delta$ for the corresponding temperature. G^* and δ values tested at all the high temperatures were recorded to display the viscoelastic behavior of the binders. The binder master curve for G^* and δ was developed with a reference temperature of 25°C by the DSR software, with testing results obtained at -10°C, 5°C, 20°C, and 35°C.



Figure 3.5 DSR equipment



Figure 3.6 Rolling thin film oven (RTFO)



Figure 3.7 DSR specimen

The MSCR test was conducted according to AASHTO MP 19. This test is a new high-temperature binder specification that more accurately indicates the rutting performance of the asphalt binder and is blind to modification. The same DSR was used for the MSCR test on the three binders evaluated in this study. A 1-second creep load was applied to the asphalt binder sample. After the 1-second load was removed, the sample was allowed to recover for 9 seconds. The test was started with the application of low stress (0.1 kPa) for 10 creep/recovery cycles; then the stress was increased to 3.2 kPa and repeated for an additional 10 cycles.

3.2.2 Bending Beam Rheometer

In accordance with AASHTO T 313, the BBR test (Figure 3.8) was used to determine stiffness on three asphalt binders, PG 52-28, PG 52-40, and PG 58-34. In the BBR test, a small beam (Figure 3.9) of binder subjected to a constant creep load and the resulting deflection were measured. Two types of specimens were produced for each binder to employ two different means of aging. One specimen was aged by using the PAV (Figure 3.10) and RTFO methods and the other specimen was aged solely by using the RTFO. Two temperatures per aging method were chosen with respect to anticipated lowest pavement service temperature. Three sample beams were created and assigned to the chosen temperature and properly aged via their respective method. Application of simple beam theory allows the creep stiffness (S) and the creep rate (m -value), which is defined as the rate of change of stiffness with time, to be

calculated. The measured S value at 60 seconds must be less than 300 MPa and the m -value at this time of loading must be at least 0.30 for binder specifications to hold (AASHTO M 320). If the stiffness falls between 300 MPa and 600 MPa, then the DTT (AASHTO TP3) should be conferred. The DTT consists of a dog-bone-shaped sample of binder pulled at a slow rate of 1 mm/minute at low temperatures to determine failure strain (defined at the maximum recorded load during the test). The specification requires that the failure strain be at least 1%. The m -value requirement must be satisfied in both cases.



Figure 3.8 Bending beam rheometer (BBR)



Figure 3.9 BBR specimen

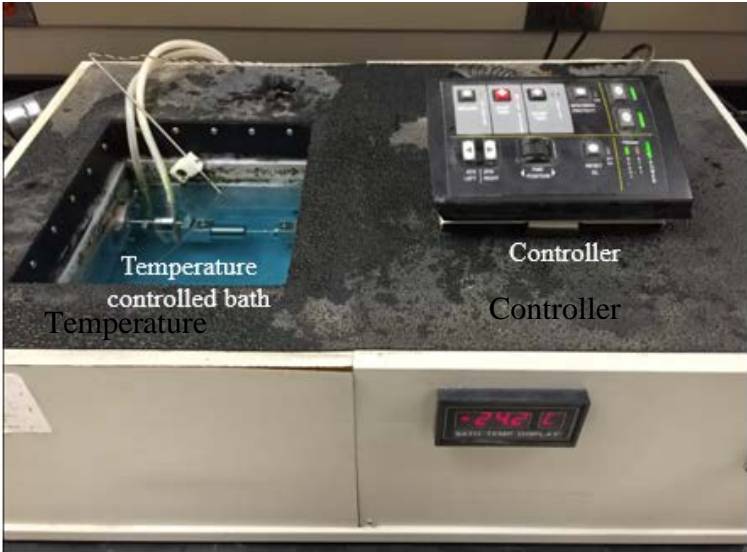


Figure 3.10 Pressure aging vessel (PAV) aging

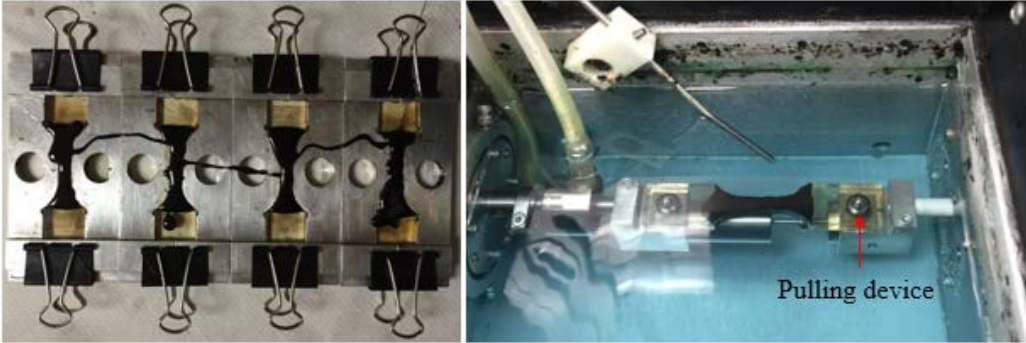
3.2.3 Direct Tension Test

Direct tension (DTT) tests were conducted according to AASHTO T 314. Figure 3.11(a) shows the tester used. The bath controls the temperature during testing and conditions the asphalt binder specimens. A sample of asphalt binder is molded into a necked shape, as shown in Figure 3.11(b), for mounting on a pulling device as shown in Figure 3.11(c). This sample is then pulled apart at a constant strain rate of 3% per minute until it fails, at which point the strain at failure is recorded. During testing, the strain and stress were recorded. Failure of the sample can occur by two means: fracture (breaks apart in 2 pieces) or unrestrained flow without fracture. In the case of fracture, failure strain is defined as the strain at the moment of fracture. In the case of flow without fracture, failure strain is defined as the strain corresponding to the maximum stress

observed. The test should not be continued past 10% strain; if the sample has not failed by 10% strain, record failure strain as “greater than 10 percent.”



(a) Direct tension tester



(b) Asphalt binder specimens in the molds; (c) Temperature controlled bath

Figure 3.11 Direct tension test

3.3 Mixture Specimen Fabrication

The laboratory-produced mixtures were fabricated following the JMF. Each aggregate gradation was weighed and placed in an oven at 165°C for 2 hours. Asphalt binder was heated at 165°C for 1 hour to gain enough workability. The RAP was heated in a separate oven at 110°C for 1 hour according to general RAP processing rule of thumb. The three components (i.e., aggregate, binder, and RAP) were then mixed using a commercial-grade mixer manufactured by Hobart (Figure 3.12). The loose asphalt mix was placed in the oven at 165°C for an additional 2 hours to simulate short-term aging. The only procedure for field mix prior to sample fabrication involved placing the mix in an oven at 165°C for 2 hours. The HMA test specimens (both lab and field produced) were fabricated following AASHTO PP 60, *Preparation of Cylindrical Performance Test Specimens Using the Superpave Gyratory Compactor (SGC)* (Figure 3.13).



Figure 3.12 Asphalt mixer



Figure 3.13 Superpave gyratory compactor

The design air void (VTM) for this experiment was $7.0 \pm 0.5\%$. The following method was followed to achieve target air void content:

The maximum specific gravity, G_{mm} , was either provided on the JMF or measured following AASHTO T209, *Theoretical Maximum Specific Gravity (G_{mm}) and Density of Hot Mix Asphalt (HMA)*. An estimate of the HMA required was determined using the G_{mm} , target height, and target air void content using Eq. 3.1.

$$Mass = \left[\frac{100 - (Va_t + F)}{100} \right] * G_{mm} * 176.7147 * H \quad (\text{Eq. 3.1})$$

where

Mass = estimated mass of mixture to prepare a test specimen to target air voids

Va_t = target air void content for the test specimen, percent by volume

G_{mm} = maximum specific gravity of the mixture

H = height of the gyratory specimen, cm

F = air void adjustment factor: 1.0 for fine-graded; 1.5 for coarse-graded

Using the estimated mass from Eq. 3.2, a trial specimen was prepared. The bulk specific gravity was measured, and the air void content was determined. The mass was then adjusted using the following equation:

$$Mass_{adj} = \left[\frac{100 - Va_t}{100 - Va_m} \right] * Mass \quad (\text{Eq. 3.2})$$

where

$Mass_{adj}$ = adjusted gyratory specimen mass, g

V_{a_t} = target air void content for the test specimen, percent by volume

V_{a_m} = measured trial test specimen air void content, percent by volume

$Mass$ = mass used to prepare the gyratory specimen for the trial test specimen

Using the adjusted mass from Eq. 3.2, a second trial gyratory specimen was fabricated. The bulk specific gravity was measured and the air void content was determined. If the air void tolerance was not satisfied, the mass was again adjusted. The process was repeated until the air void content was within the acceptable range.

The specimens produced for AMPT tests from the SGC had a diameter of 150 mm and were compacted to a height of 170 mm (Figure 3.14). The compacted samples were cored using a floor-mounted coring drill (Figure 3.15) to a final diameter of 100 mm and cut to a final height of 150 mm using a masonry saw (Figure 3.16). Studs for mounting linear variable differential transformers (LVDTs) were then attached to the AMPT specimens using a gauge point fixing jig supplied by IPC Global (Figure 3.17). The studs were placed radially at 120°. The specimens used for $|E^*|$ tests were also used for FN.



Figure 3.14 Representative specimens for AMPT tests



Figure 3.15 Asphalt specimen core drill



Figure 3.16 Masonry saw



Figure 3.17 Gauge point fixing jig

The specimens produced for the IDT tests from the SGC had a diameter of 150 mm and a height of 160 mm. The compacted sample was cut three times along its horizontal axis to produce two test specimens having a diameter of 150 mm and a height of 38–50 mm (Figure 3.18). The LVDT mounting hardware was attached using a jig designed to provide a consistent mounting location (Figure 3.19).



Figure 3.18 Specimens for IDT tests



Figure 3.19 LVDT hardware mounting jig

The air voids of all test specimens were confirmed following AASHTO T 269, *Percent Air Voids in Compacted Dense and Open Asphalt Mixtures*. The air voids of test specimens were determined using Eq. 3.3. The air voids of all the test specimens are presented in Appendix B.

$$\text{Percent Air Voids} = 100 \left(1 - \frac{G_{mb}}{G_{mm}} \right) \quad (\text{Eq. 3.3})$$

3.4 Laboratory Mixture Performance Tests

Table 3.3 presents the laboratory testing plan. Laboratory tests included the dynamic modulus (IE*1) test from which the IE*1 master curve could be developed, the flow number test for rutting evaluation, and the IDT creep stiffness test for low-temperature cracking evaluation. Cylindrical samples were produced with the SGC and sliced into target thicknesses for each specific test.

Table 3.3 Laboratory testing plan

Test	Properties	Testing Temperature (°C)
Dynamic Modulus (IE*1)	Modulus	4.4
		21.1
		37.8
		54
Flow Number	Rutting	40
IDT Creep Stiffness and Strength	Low-Temperature Thermal Cracking	0
		-10
		-20
		-30

3.4.1 Asphalt Mixture Performance Tests

The asphalt mixture performance tests (AMPTs) were performed using the simple performance test (SPT) apparatus manufactured by IPC Global of Australia (Figure 3.20). The testing system consists of a digital servo hydraulic control with a continuous electronic control and data acquisition system (CDAS). Two AMPTs were used to evaluate the materials: dynamic modulus and flow number.

Hot-mix asphalt (HMA) is a viscoelastic material. Viscous materials are characterized by the tendency to flow under their own weight. Elastic materials rebound. When a material is subjected to vibratory conditions, a purely viscous material will exhibit a phase difference between stress and strain, where strain lags stress by 90° . A purely elastic material experiences no lag; the stress and strain are in phase and occur simultaneously. The behavior of HMA is between these two extremes. The ratio of stress to strain experienced by an HMA sample while under continuous sinusoidal uniaxial loading results in a complex number, $|E^*|$. By definition, a complex number is a combination of a real number and an imaginary number. The real number part of $|E^*|$ is representative of the elastic stiffness; the imaginary number part defines the internal damping of the material. In this study, the dynamic modulus was tested for each specimen at four temperatures: 4.4°C , 21.1°C , 37.8°C , and 54°C .



Figure 3.20 Sample setup for AMPT test

Master curves for the dynamic modulus were created using the time-temperature superposition (t-TS) principle. Asphalt is a linear viscoelastic material. One implication of this is that the modulus measured at low temperature and high frequency is equal to the modulus measured at high temperature and low frequency. Because of this association, the time-temperature superposition principle can be implemented to characterize the $|E^*|$ over a wide range of loading frequency. At a given reference temperature (usually 20°C, which was selected in this study), the $|E^*|$ values collected over a range of temperatures and frequencies can be shifted with respect to the independent variable axis (frequency/time) to form a smooth S-shaped curve. This curve is commonly referred to as the “master curve” of $|E^*|$. The master curve is used to analyze the temperature and frequency effects on asphalt as well as an input for the Mechanistic-Empirical Pavement Design Guide (MEPDG).

The flow number (FN) test procedure was derived from AASHTO TP 79-13. The samples used to determine the dynamic modulus were also used to test FN. The testing was performed in triplicate. The FN test is used to evaluate the creep characteristics of HMA and results in permanent deformation of the test specimen. A uniaxial compressive load is applied in haversine form, with a loading time of 0.1 seconds and a rest duration of 0.9 seconds for a maximum of 10,000 cycles or until a 50,000 microstrain deformation is reached. No confining stress was applied. Tests were conducted at 40°C, which closely matched the high adjusted PG temperature for Fairbanks, Alaska, and surrounding areas. Average maximum effective pavement temperature was determined using LTPP Bind Version 3.1 software. Figure 3.21 shows flow number samples before and after the test.

Samples used to determine FN exhibit three distinct stages of permanent deformation. First, denoted as the primary zone, the specimen experiences a rapid accumulation of strain. The secondary zone follows and is characterized by a constant accumulated strain rate. The tertiary zone is marked by an increase in strain rate. It is at this juncture, from secondary to tertiary, that the FN is defined. More specifically, the FN for the mixture is the point at which the permanent strain rate is at a minimum, and the tertiary flow begins.



Figure 3.21 Flow number samples before and after the test

3.4.2 Indirect Tension Tests

The indirect tension (IDT) test was used to evaluate the low-temperature performance of asphalt concrete containing RAP, using aggregates from the Central and Northern regions. The setup for IDT creep or strength tests is shown in Figure 3.22. An environmental chamber, in which the temperature could be controlled, was used to condition the specimens to the target temperatures. To determine the tensile creep stiffness $S(t)$ and tensile strength St according to AASHTO specification T 322-07, a programmed data acquisition system was used to record the load and deformation of the specimens during testing.

The IDT creep test is performed by loading the cylindrical specimen with a constant compressive load. The applied compressive load causes the specimen to fail by splitting along the vertical direction. Specimens were approximately 50 mm in height and 150 mm in diameter. The tensile

creep compliance $D(t)$ of each mixture was monitored at three different temperatures at 10°C intervals (i.e., -20, -10, 0°C and -30, -20, 10°C) according to the binder's low temperature grade. At each testing temperature, normalized horizontal and vertical deformations from 6 specimen faces (3 specimens, 2 faces/specimen) were measured with the LVDT as shown in Figure 3.22.

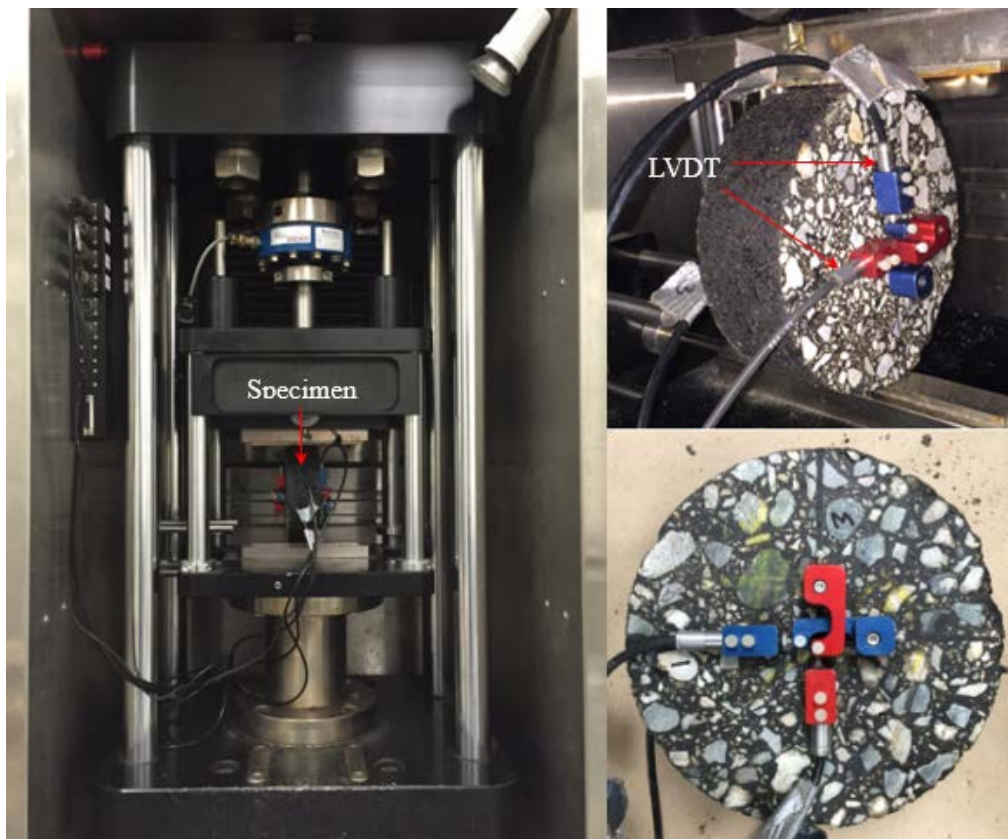


Figure 3.22 IDT setup for creep stiffness test

The creep compliance $D(t)$ of each mixture was tested and calculated according to the test specification of the formula:

$$D(t) = \frac{\Delta X \times D_{avg} \times b_{avg}}{P_{avg} \times GL} \times C_{cmpl} \quad (\text{Eq. 3.4})$$

where

$D(t)$ = creep compliance (kPa),

ΔX = trimmed mean of the horizontal deformations (meter),

D_{avg} = average specimen diameters (meter),

b_{avg} = average specimen thickness (meter),

P_{avg} = average force during the test (kN),

GL = gage length (38mm), and

C_{cmpl} = creep compliance parameter at any given time, computed as

$$C_{cmpl} = 0.6354 \times \left(\frac{X}{Y}\right)^{-1} - 0.332 \quad (\text{Eq. 3.5})$$

where

X = horizontal deformation, and

Y = vertical deformation

Creep stiffness $S(t)$ at the time t was calculated as the inverse of the creep compliance $D(t)$, i.e.,

$$S(t) = \frac{1}{D(t)} \quad (\text{Eq. 3.6})$$

Besides creep stiffness, tensile strength is a generally accepted measuring factor for asphalt mix for low-temperature cracking resistance. Higher tensile strength at low temperatures indicates higher resistance to thermal cracking. Since the creep test is nondestructive, further testing was conducted on the same set of test specimens to determine the indirect tensile strength by applying a load to the specimen at a rate of 12.5 mm/min of vertical movement. The indirect tensile strength S was calculated using Equation 3.7.

$$S = \frac{2 \times P_{fail}}{\pi \times b \times D} \quad (\text{Eq. 3.7})$$

where

P_{fail} = failure (peak) load,

b = specimen thickness, and

D = specimen diameter.

CHAPTER 4.0 RESULTS AND ANALYSIS

4.1 Binder Tests

The three binders tested in this study were all used. However, the tests conducted on virgin binders were only proposed to further develop the materials library in Alaska for typical binders that can be used with RAP. The binder properties of asphalt mixtures containing RAP were not evaluated.

4.1.1 High-Temperature Binder Grade

According to $G^*/\sin\delta$ values obtained on virgin (original) and RTFO-aged binders, the true high-temperature grades of the tested binders were calculated. The grades are presented in Table 4.1.

These results verified the high PG grades of the three typical Alaskan binders. Detailed data information can be found in Appendix C.

Table 4.1 True high-temperature grades of tested Alaskan binders

Binders	True High Temperature Grade (Original) (°C)	True High Temperature Grade (RTFO) (°C)	High PG (°C)
PG 52-28	56.6	56.9	52
PG 52-40	60.6	56.4	52
PG 58-34	64.3	61.4	58

4.1.2 Viscoelastic Behavior

The viscoelastic behavior of the three Alaskan binders were tested using a dynamic shear rheometer (DSR) and obtained in terms of complex modulus (G^*) and phase angle (δ). Tested binders were RTFO-conditioned. Table 4.2 presents the results tested at three temperatures, including the high PG temperature and plus/minus 6°C of the high PG. As the critical parameters of asphalt binder, these $|G^*|$ and δ values can be used to develop the local material catalog for further analysis. Detailed data information can be found in Appendix C.

Table 4.2 Viscoelastic behavior results in terms of $|G^*|$ and δ

Binders	T (°C)	G^* (kPa)	δ (rad)
PG 52-28	46	10.53	1.46
	52	4.39	1.49
	58	1.88	1.51
PG 52-40	46	4.36	1.05
	52	2.65	1.03
	58	1.65	1.01
PG 58-34	52	4.50	1.09
	58	2.56	1.08
	64	1.54	1.06

4.1.3 Master Curves

Figures 4.1 through 4.6 present the RTFO-aged binder $|G^*|$ and δ master curves at 25°C generated by the DSR software. These master curves were developed based on testing data at 10°C, 5°C, 20°C, and 35°C according to the time-temperature superposition principle. These master curves can be used as a reference for comparison purposes and to predict curves at some extreme frequency zones that are technically interesting but experimentally out of reach.

Detailed data information can be found in Appendix C.

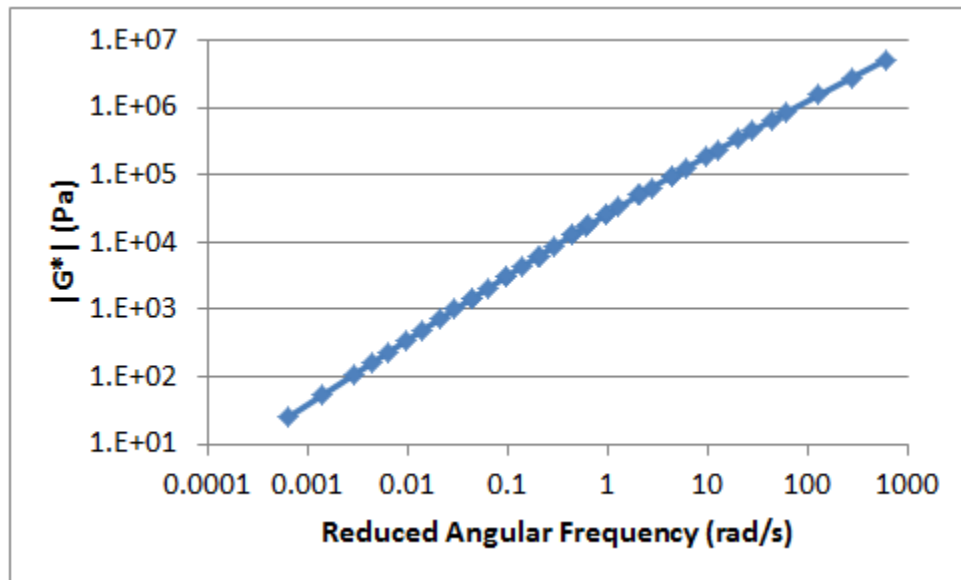


Figure 4.1 $|G^*|$ master curve of RTFO-aged PG 52-28

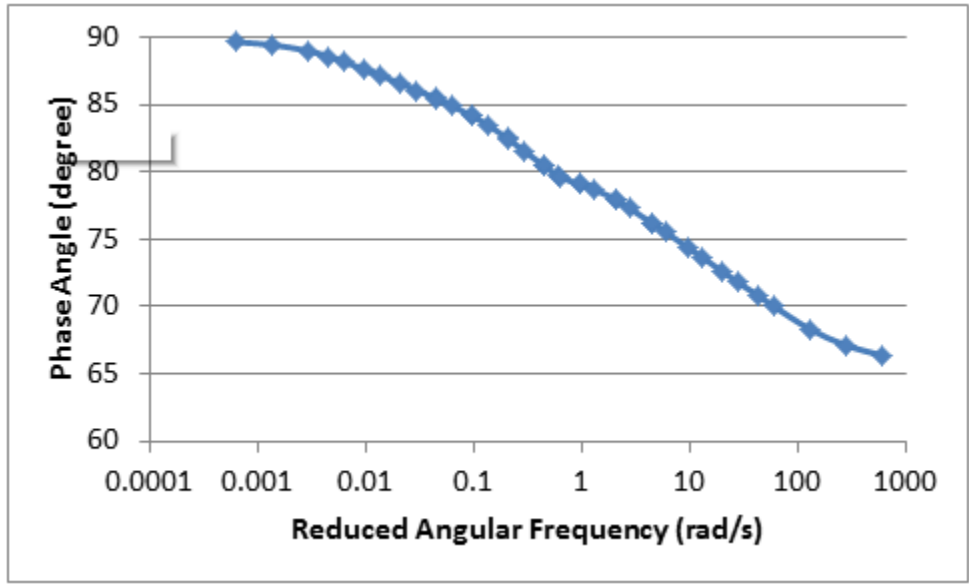


Figure 4.2 Phase angle master curve of RTFO-aged PG 52-28

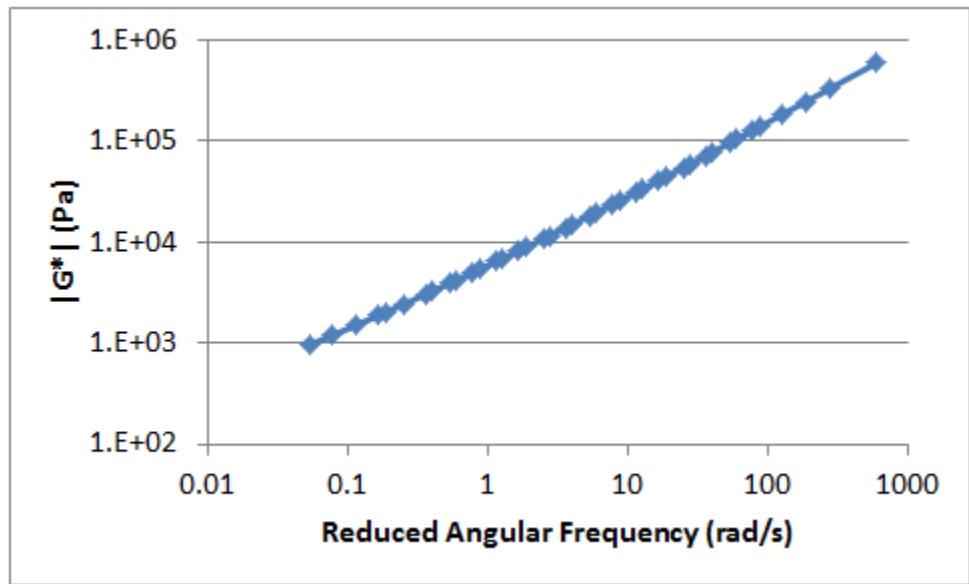


Figure 4.3 $|G^*|$ master curve of RTFO-aged PG 52-40

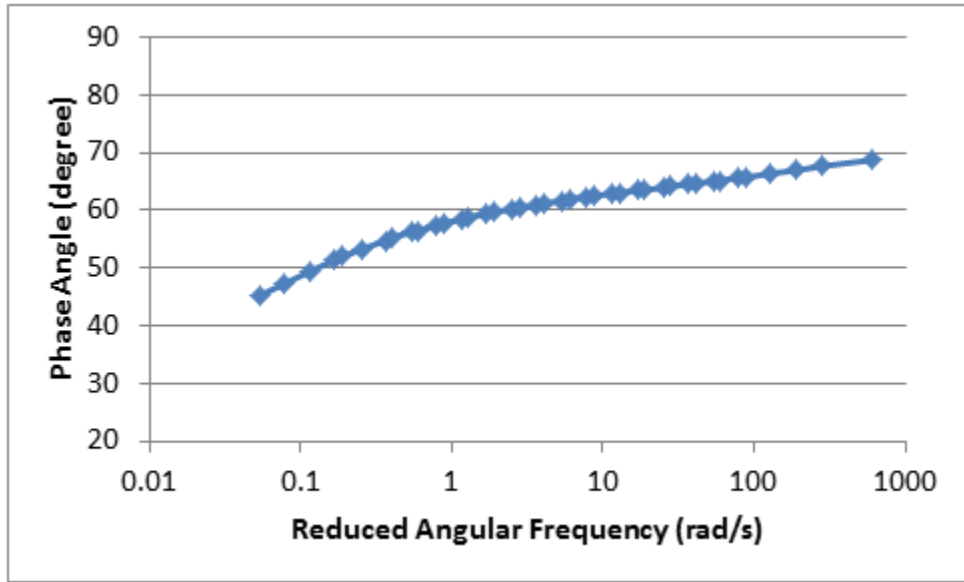


Figure 4.4 Phase angle master curve of RTFO-aged PG 52-40

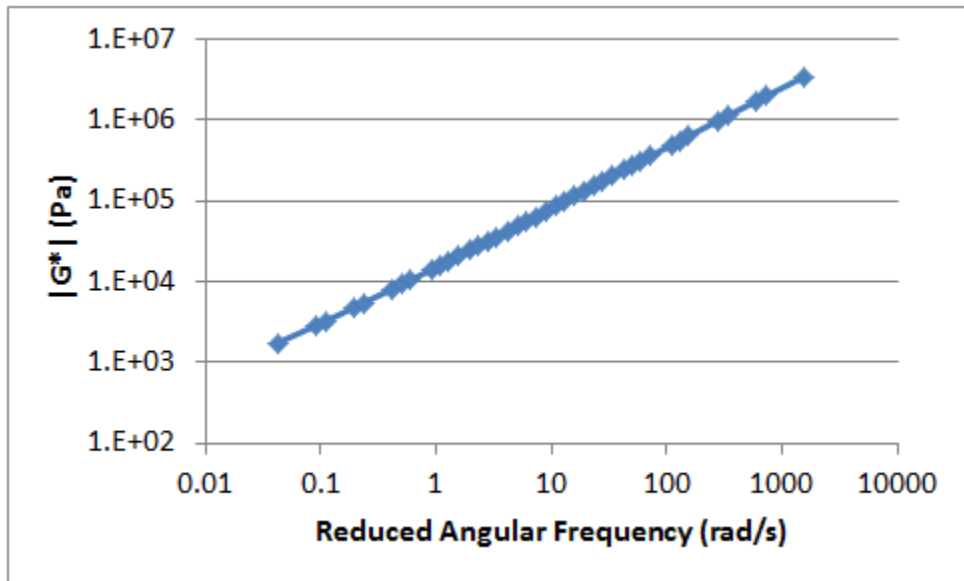


Figure 4.5 |G*| master curve of RTFO-aged PG 58-34

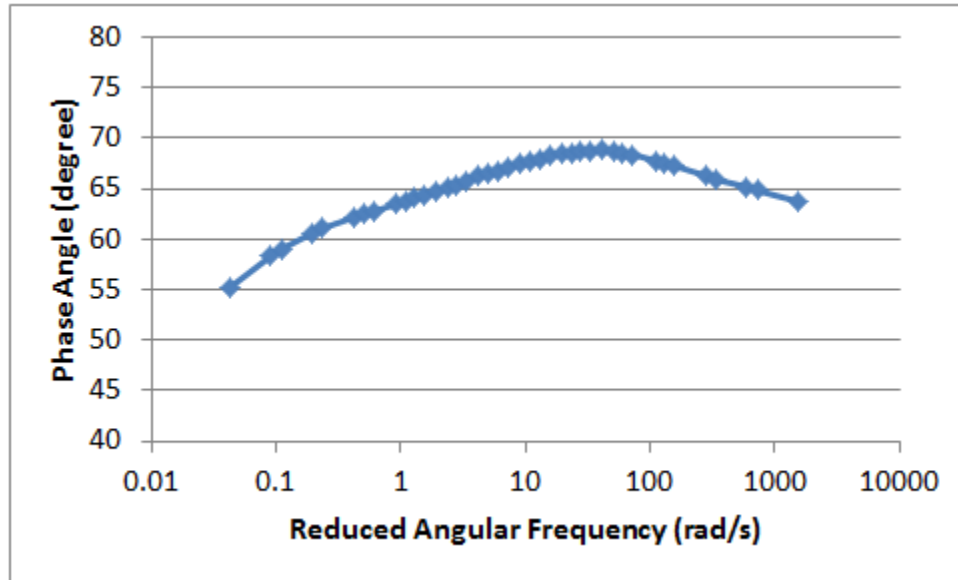


Figure 4.6 Phase angle master curve of RTFO-aged PG 58-34

4.1.4 MSCR

Multiple stress creep recovery (MSCR) tests were performed on three rolling thin film oven (RTFO)-aged asphalt binders—PG 58-34, PG 52-28, and PG 52-40—in accordance with ASTM D-7405. Three specimens were prepared for testing for each RTFO-aged binder in the infrastructural materials lab at the University of Tennessee Knoxville. The tests results are listed in Table 4, typically interpreted by nonrecoverable creep compliance (J_{nr}) and recovery percentage under different stress levels. The AASHTO MP 19, *Performance-Graded Asphalt Binder Using Multiple Stress Creep Recovery (MSCR) Test*, specifies maximum J_{nr} values for each high-performance temperature under different traffic levels. The test results obtained in this study satisfy the J_{nr} standard for all traffic levels at the corresponding high PG grade specified in

AASHTO MP 19. The unmodified binder shows a very low recovery rate (R100 and R3200), which is expected, as the MSCR test is specifically designed for the evaluation of modified binder rutting resistance. Detailed data and graphs can be found in Appendix C.

Table 4.3 MSCR results

Binder Type	T (°C)	R100 (%)	R3200 (%)	R_{diff} (%)	J_{nr}100 (1/kPa)	J_{nr}3200 (1/kPa)	J_{nr}-diff (%)
PG 52-28	46	6.93	4.57	34.33	0.64	0.68	7.07
	52	3.23	0.83	74.27	1.80	1.98	10.27
PG 52-40	46	91.37	90.40	1.03	0.07	0.09	17.33
	52	94.97	93.07	2.00	0.07	0.11	44.10
PG 58-34	52	90.87	90.50	0.40	0.09	0.10	10.17
	58	95.07	94.10	1.03	0.09	0.11	23.17

4.1.5 BBR Results

Figures 4.7 through 4.12 present the process used to determine critical temperature by limiting the critical parameters of the bending beam rheometer (BBR) test, creep stiffness, and *m*-value obtained at 60 seconds.

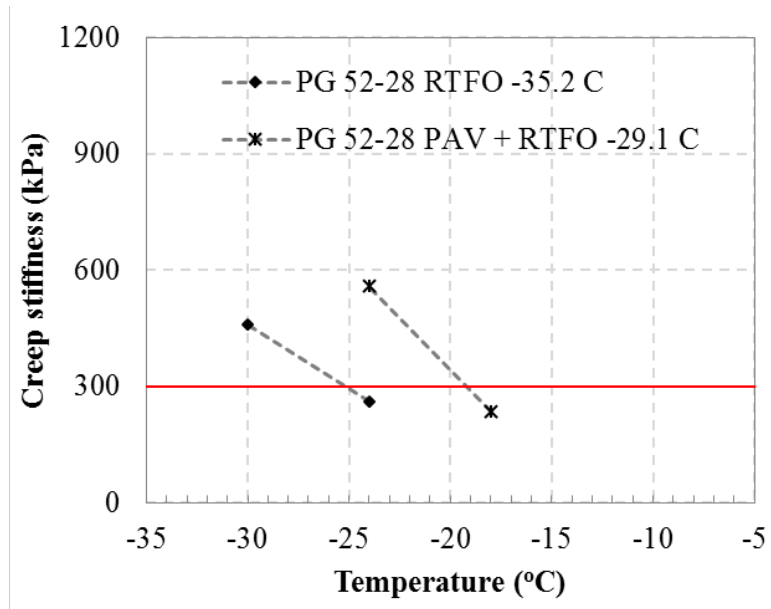


Figure 4.7 Determine critical temperatures of PG 52-28 binder by limiting stiffness obtained from BBR tests

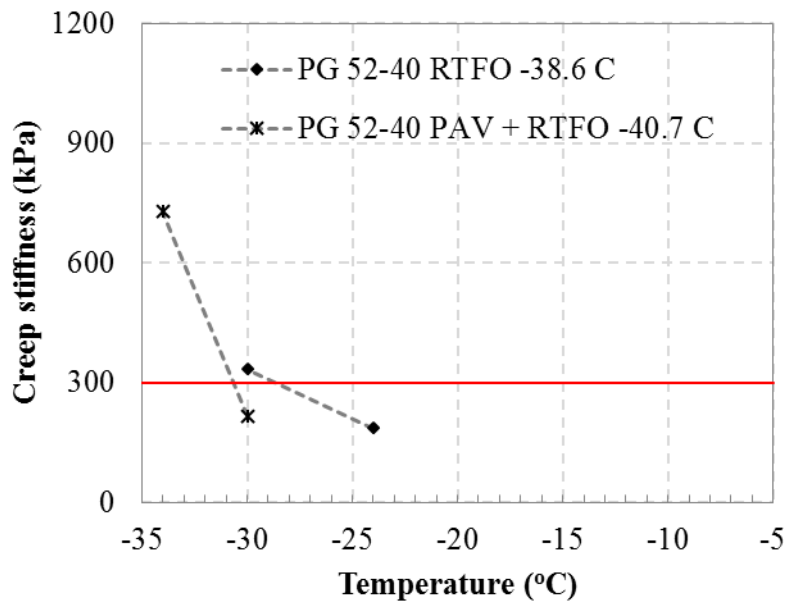


Figure 4.8 Determine critical temperatures of PG 52-40 binder by limiting stiffness obtained from BBR tests

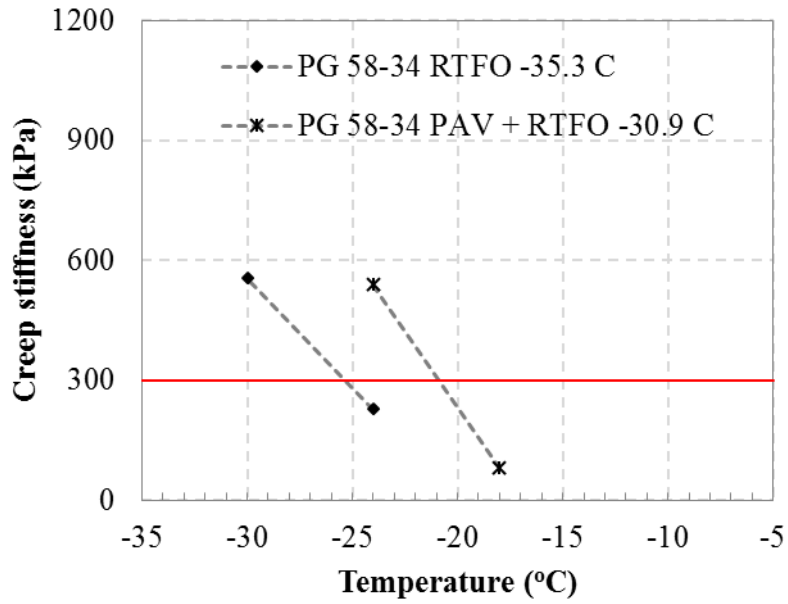


Figure 4.9 Determine critical temperatures of PG 58-34 binder by limiting stiffness obtained from BBR tests

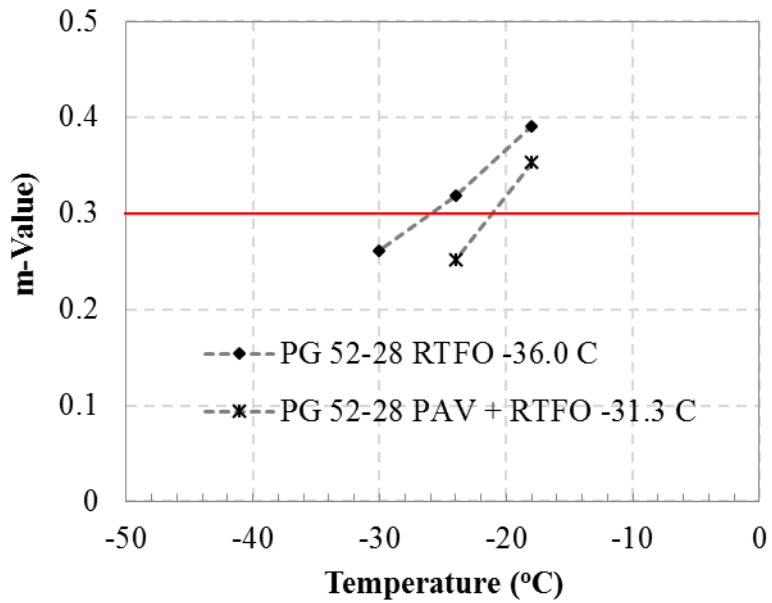


Figure 4.10 Determine critical temperatures of PG 52-28 binder by limiting *m*-value obtained from BBR tests

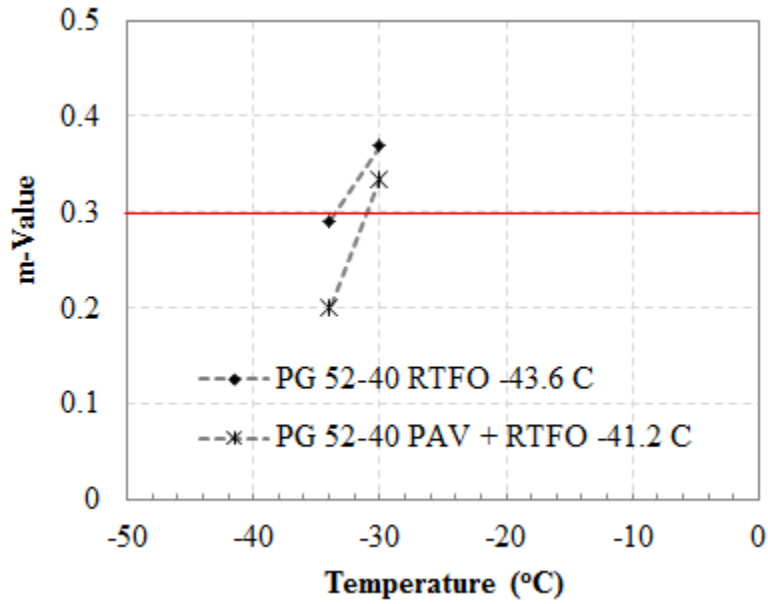


Figure 4.11 Determine critical temperatures of PG 52-40 binder by limiting m -value obtained from BBR tests

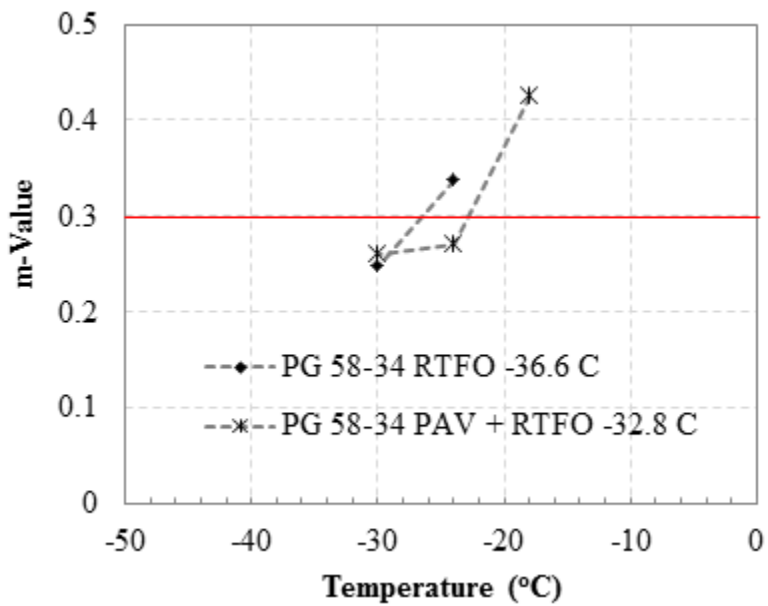


Figure 4.12 Determine critical temperatures of PG 58-34 binder by limiting m -value obtained from BBR tests

Table 4.4 presents the critical temperature of each binder by limiting binder stiffness (300 kPa) at 60 seconds and m -value (0.3). It can be seen that the two criteria give similar results, both close to the PG low temperature of the corresponding binder. The RTFO-aged PG 52-28 and PG 58-34 show a higher critical temperature than RTFO plus PAV-aged, which is expected. For PG 52-40, RTFO and RTFO plus PAV-aged samples show similar results, which indicates that for modified binder with very low PG grade such as PG 52-40, long-term aging may not reduce thermal cracking resistance significantly.

Table 4.4 Critical low temperature by limiting BBR parameters

Binder	Aging Condition	Critical Temperature Limiting Stiffness at 300 kPa, °C	Critical Temperature Limiting m-value at 0.3, °C	PG Low Temperature, °C
PG 52-28	RTFO	-35.2	-36	N/A
	RTFO + PAV	-29.1	-31.3	-28
PG 52-40	RTFO	-38.6	-43.6	N/A
	RTFO + PAV	-40.7	-41.2	-40
PG 58-34	RTFO	-35.3	-36.6	N/A
	RTFO + PAV	-30.9	-32.8	-34

4.1.6 DTT Results

Figures 4.13 through 4.15 present the process used to determine critical temperature by limiting the failure strain of the specimen at 1%. The data curve obtained from the PG 52-40 binder does not show its trend of intercepting the 1% failure strain level, so the critical temperature cannot be

determined. As PG 52-40 has a very low low-temperature grade, the testing temperature should be reduced, which is beyond the limit of the testing equipment used in this study and might cause this issue.

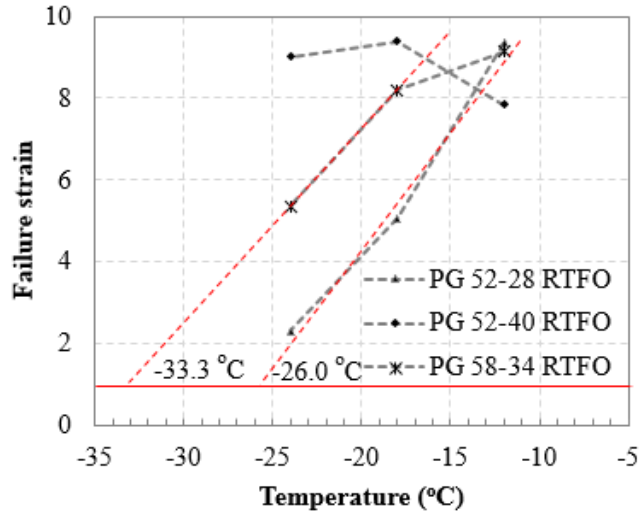


Figure 4.13 Determine critical temperatures of RTFO-aged binder by limiting failure strain from the DTT test

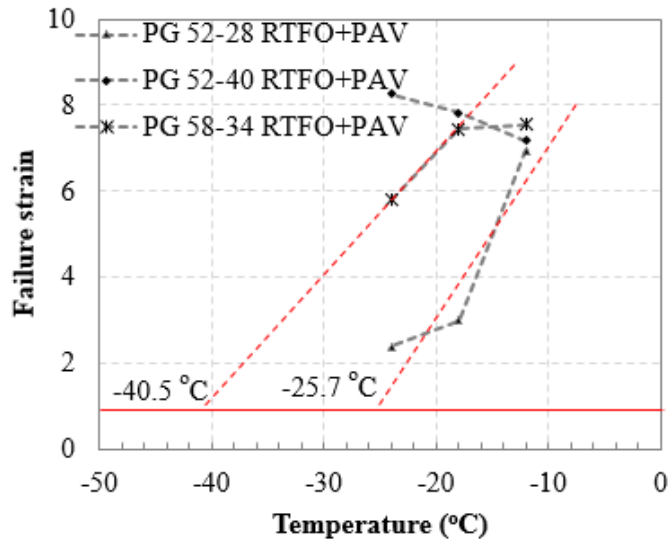


Figure 4.14 Determine critical temperatures of RTFO plus PAV-aged binder by limiting failure strain from the DTT test

Table 4.5 presents the critical temperature of each binder by limiting the failure strain. It can be seen that the critical temperature of PG 52-28 binder is close to its low temperature end, and results obtained on both aging conditions are similar. For PG 58-34 binder, the RTFO-PAV-aged binder showed a lower critical temperature, which was not expected. This might indicate that DTT is not suitable for determining the critical temperature of a binder. More testing data should be obtained to validate this observation.

Table 4.5 Critical low temperature by limiting DTT parameter

Binder	Aging Condition	Critical Temperature Limiting Failure Strain at 1%, °C	PG Low Temperature, °C
PG 52-28	RTFO	-26	N/A
	RTFO + PAV	-25.7	-28
PG 52-40	RTFO	N/A	N/A
	RTFO + PAV	N/A	-40
PG 58-34	RTFO	-33.3	N/A
	RTFO + PAV	-40.5	-34

4.1.7 TSAR Analysis

Thermal Stress Analysis Routine (TSAR™) software is a rapid, user-friendly method developed by Abatech Consulting Engineers to determine the critical temperature that corresponds to thermal cracking based on the bending beam rheometer (BBR) test and the direct tension test (DTT) for the proposed new AASHTO binder specification

(<http://www.abatech.com/TSAR.htm>). Recently, low-temperature requirements have been refined to predict the temperature at which a binder fails in single-event thermal cracking. This temperature will replace the stiffness, *m*-value, and failure strain. An example of this prediction based on BBR and DTT results using TSAR software is presented as follows:

To use the TSAR software, create a text file, as shown in Figure 4.15, and save it as a *.TSA file. In this file, the first 15 rows define the basic properties of the asphalt binder. The basic properties include linear expansion coefficient, glass transition temperature, reference temperature, cooling

rate, temperature step size, initial temperature, final temperature to allow, maximum stress to allow, interval for string results, and pavement constant. The user can set a linear expansion coefficient above and below a glass transition temperature. This value varies with mixture and binder type and has a significant effect on the calculated results. However, measurement is complex and time-consuming. The default value is $0.00017/^\circ\text{C}$. The glass transition temperature (T Glass) can be used to define the point at which the linear expansion coefficient changes. If the same value of linear expansion is used either side of the T Glass, then this parameter has no effect on the calculation. The reference temperature does not affect the calculated thermal stresses significantly. Users may wish to have the output of master curves at a particular reference temperature for a variety of reasons. The reference temperature must lie within the range of temperatures for which isotherms are available. The cooling rate significantly affects the calculated result. In the AASHTO procedure, a rate of 1°C/hr was considered appropriate. However, users may wish to investigate the effect of different rates upon the expected cracking temperature. The initial temperature used in the calculation process should be high enough to ensure that the starting value does not have a significant effect on the computed result. A value of 0°C was selected as the default. The final temperature allowed affects the graphical output, x-axis, and has no effect on the calculated numbers. The maximum stress allowed affects the graphical output, y-axis, and has no effect on the calculated numbers. For the interval for storing results, a change in this number has a minor effect on the results. The pavement constant is a calibration constant used to adjust binder results to field conditions. This has a significant effect

on the calculated results. When the .TSR file is ready, the user can run the TSAR Plus™ software and open the .TSR file.

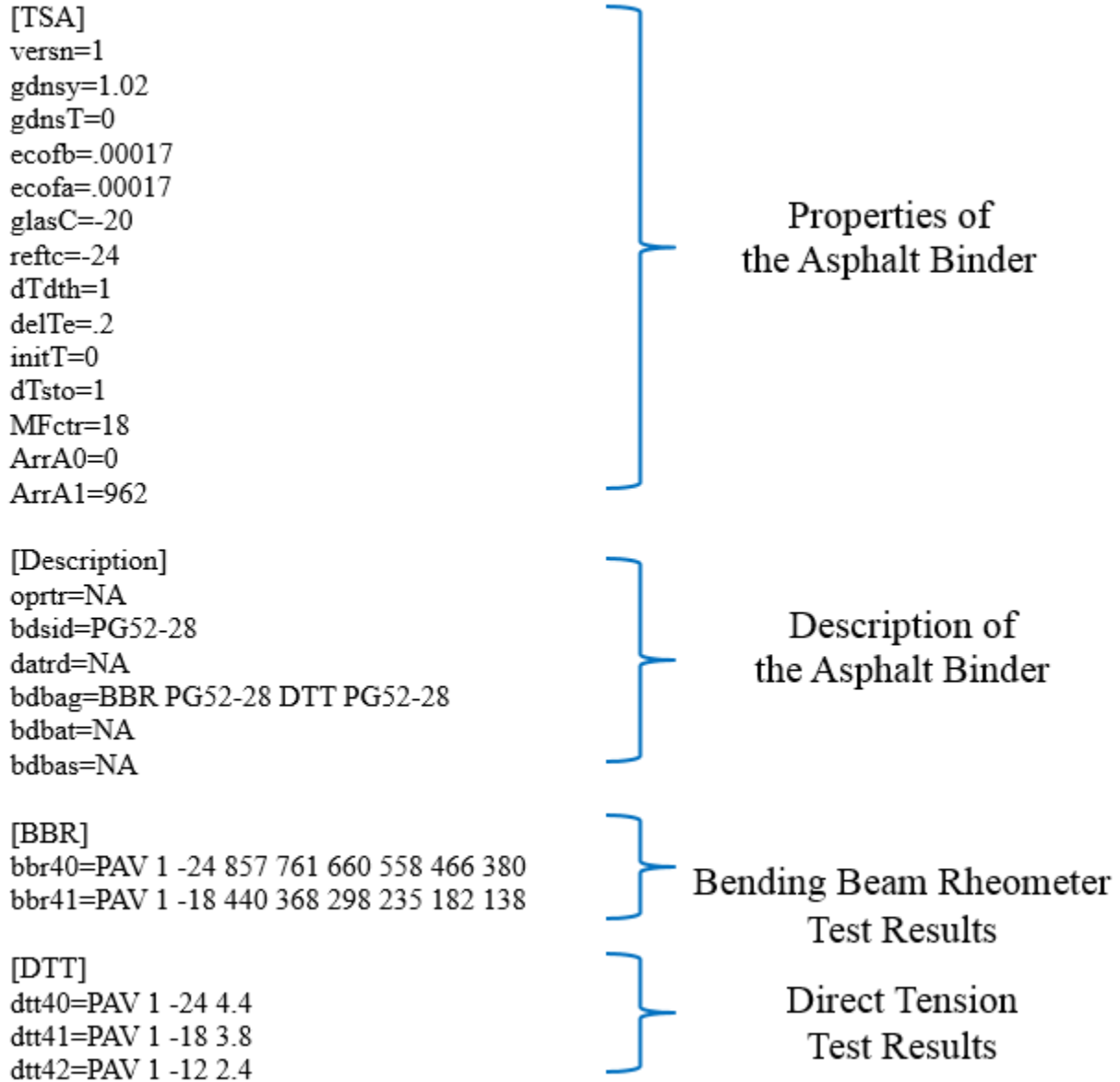


Figure 4.15 TSAR input text file

The user can run the program to predict critical thermal stress based on the BBR and DTT results. TSAR Plus™ software automatically creates a “stiffness master curve,” as shown in Figure 4.16, using the BBR test results. Actually, in the software, four models are available to predict the binder stiffness at different time conditions. The four models are the Christensen-Anderson (CA), as presented in Eq. 4.1; the Christensen-Anderson-Marasteanu (CAM), as presented in Eq. 4.2; the Christensen-Anderson-Sharrock (CAS), as presented in Eq. 4.3; and the Discrete spectrum (DS), as presented in Eq. 4. In Eq. 4.1, S_{glassy} is a constant (3×10^3 MPa), and λ and β are fitted. This type of model enables the low-temperature properties of asphalt binders to be modeled with reasonable accuracy. However, note that models of this form should not be applied to the total binder master curve. In Eq. 4.2, S_{glassy} is a constant (3×10^3 MPa), and λ , β , and κ are fitted. This method works well with data collected over a wide time range. In Eq. 4.3, S_{glassy} , λ , and β are fitted. In Eq. 4.4, n is numerically optimized, and the relaxation strengths, S_i , and relaxation times, λ_i , are estimated. In all the models, ξ represents reduced time. The selection of the master curve analysis method is made using the options provided under preferences. The default model used in the software is the CAM model. Note that the output presented in the report depends on the model selected.

$$S(\xi) = S_{\text{glassy}} \left[1 + (\xi / \lambda)^\beta \right]^{-1/\beta} \quad (\text{Eq. 4.1})$$

$$S(\xi) = S_{\text{glassy}} \left[1 + (\xi / \lambda)^\beta \right]^{-\kappa/\beta} \quad (\text{Eq. 4.2})$$

$$S(\xi) = S_{\text{glassy}} \left[1 + (\xi / \lambda)^\beta \right]^{-1/\beta} \quad (\text{Eq. 4.3})$$

$$S(\xi) = S_{glassy} \sum_{i=1}^n S_i \cdot e^{-\xi/\lambda_i} \quad (\text{Eq. 4.4})$$

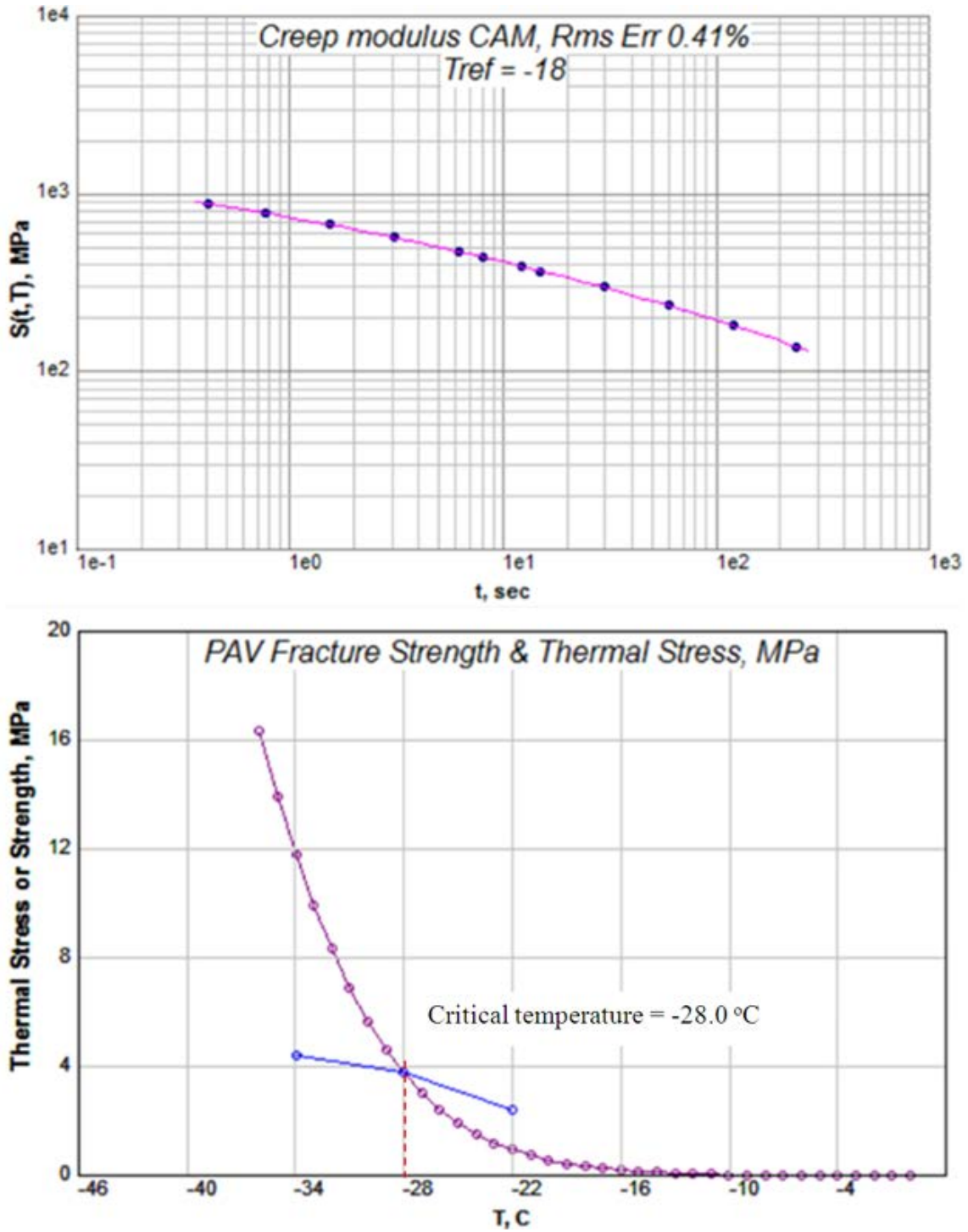


Figure 4.16 Plot for critical temperature determination through TSAR

In TSAR Plus™, the thermal stress calculation is dependent upon a number of factors that can be varied in the software. As addressed before, some of these factors can significantly affect the results of the calculation, whereas, others have only a minor influence on the results. After the stress calculation, a new graph is created as shown in Figure 4.16. In this figure, the fracture strength and the thermal stress curves are plotted together. The intercept of two curves, which is at -28.0°C, is the “critical temperature,” as shown on the figure.

Figure 4.17 through 4.22 present the process of determining the critical temperature of all three binders using TSAR software after RTFO aging or RTFO + PAV aging.

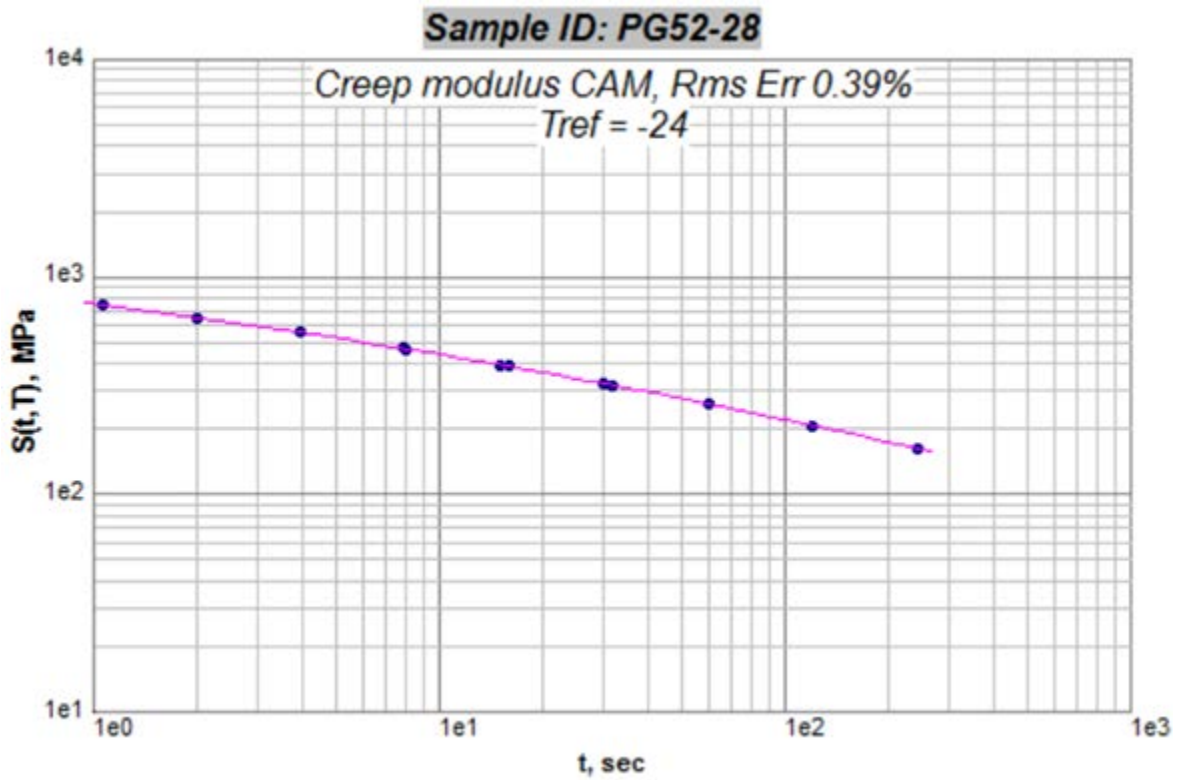
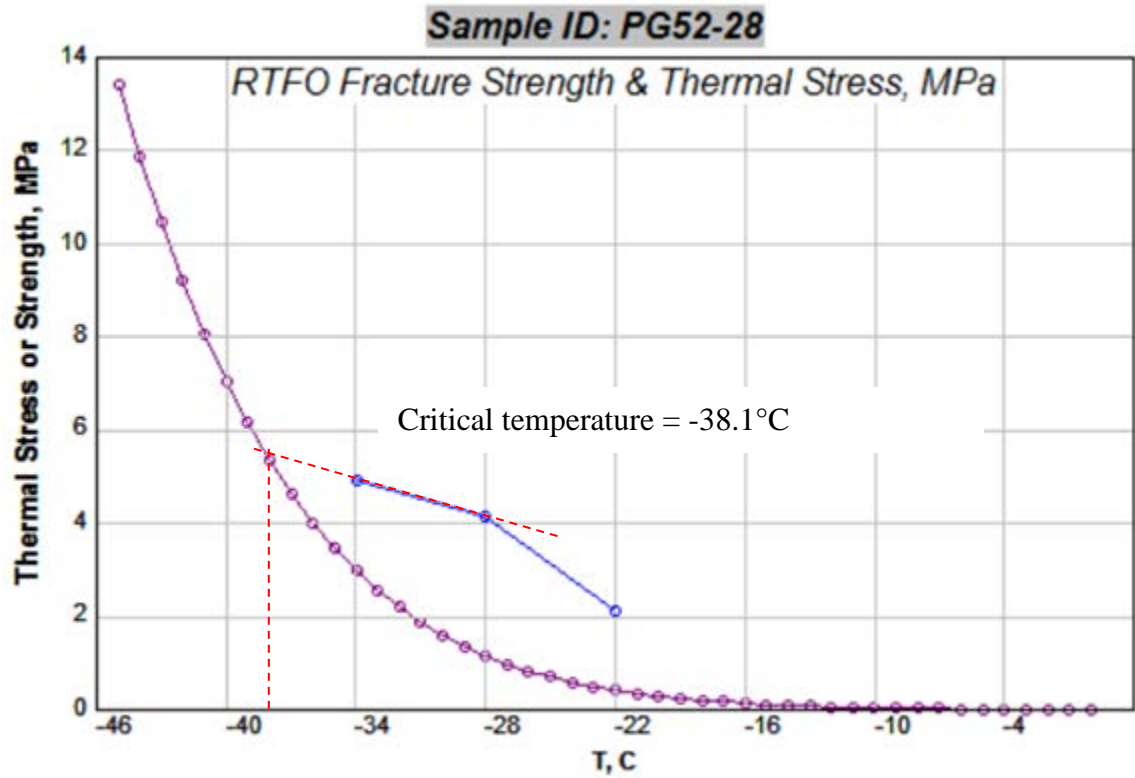


Figure 4.17 Critical temperature prediction for binder PG 52-28 after RTFO aging

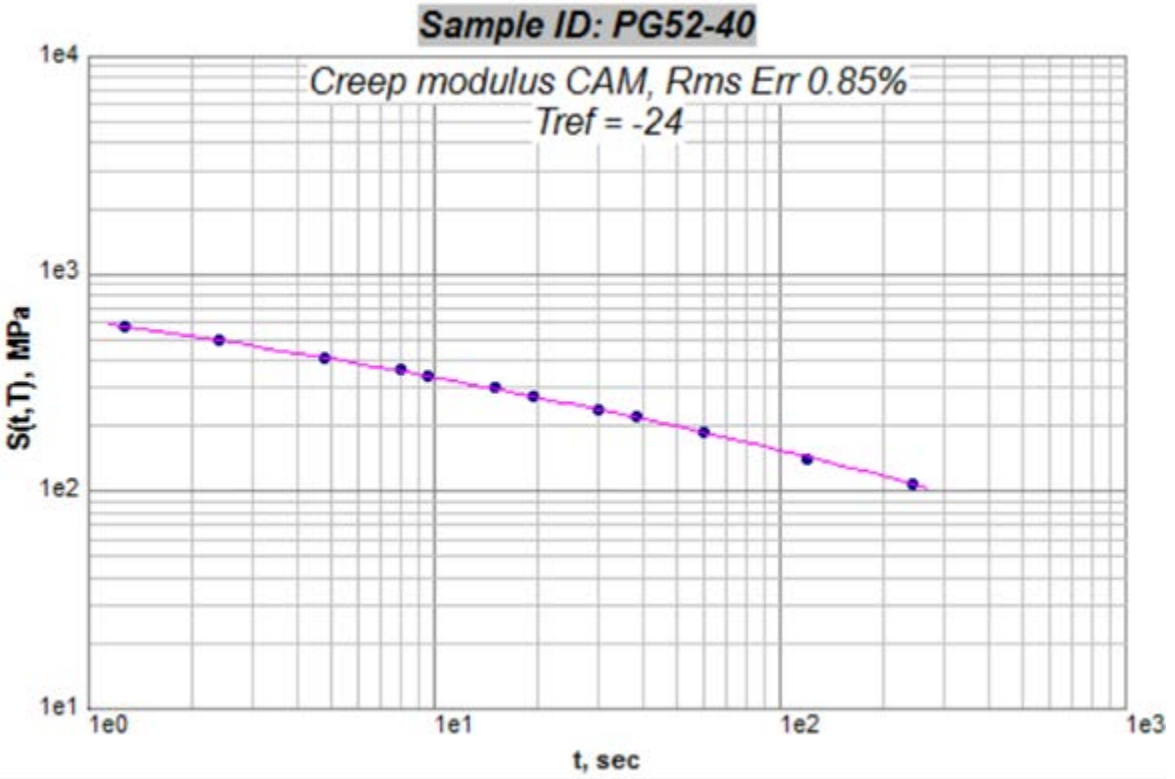
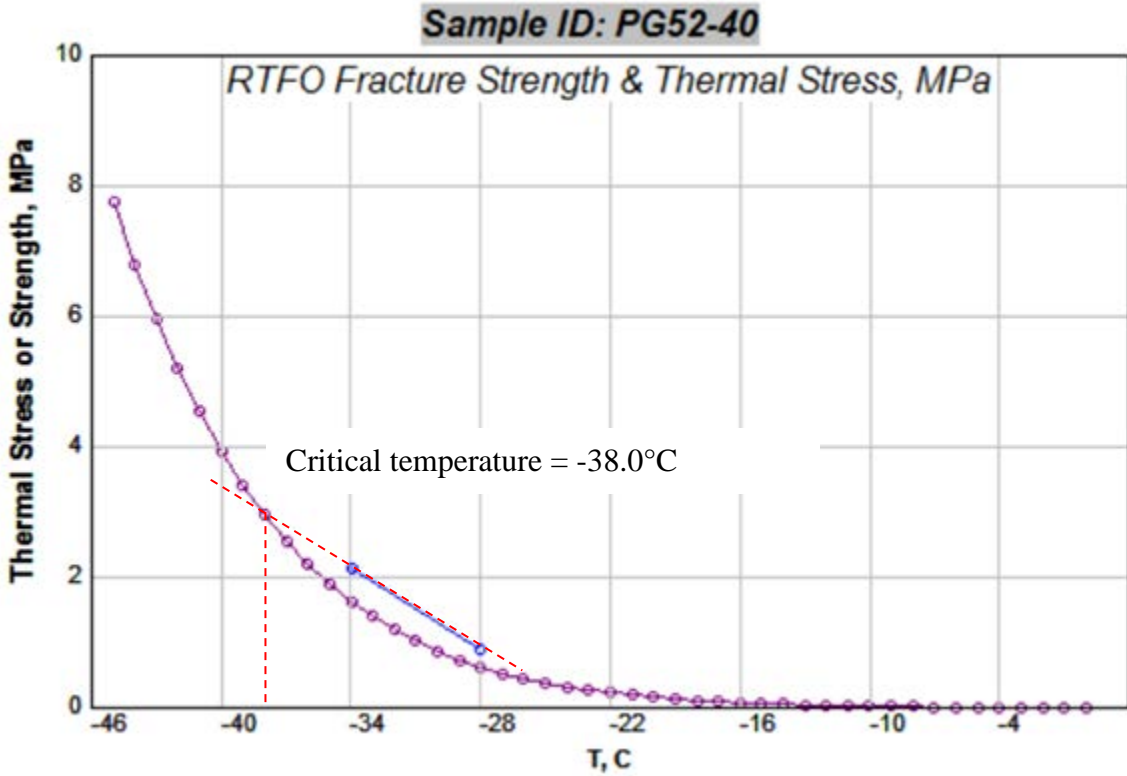


Figure 4.18 Critical temperature prediction for binder PG 52-40 after RTFO aging

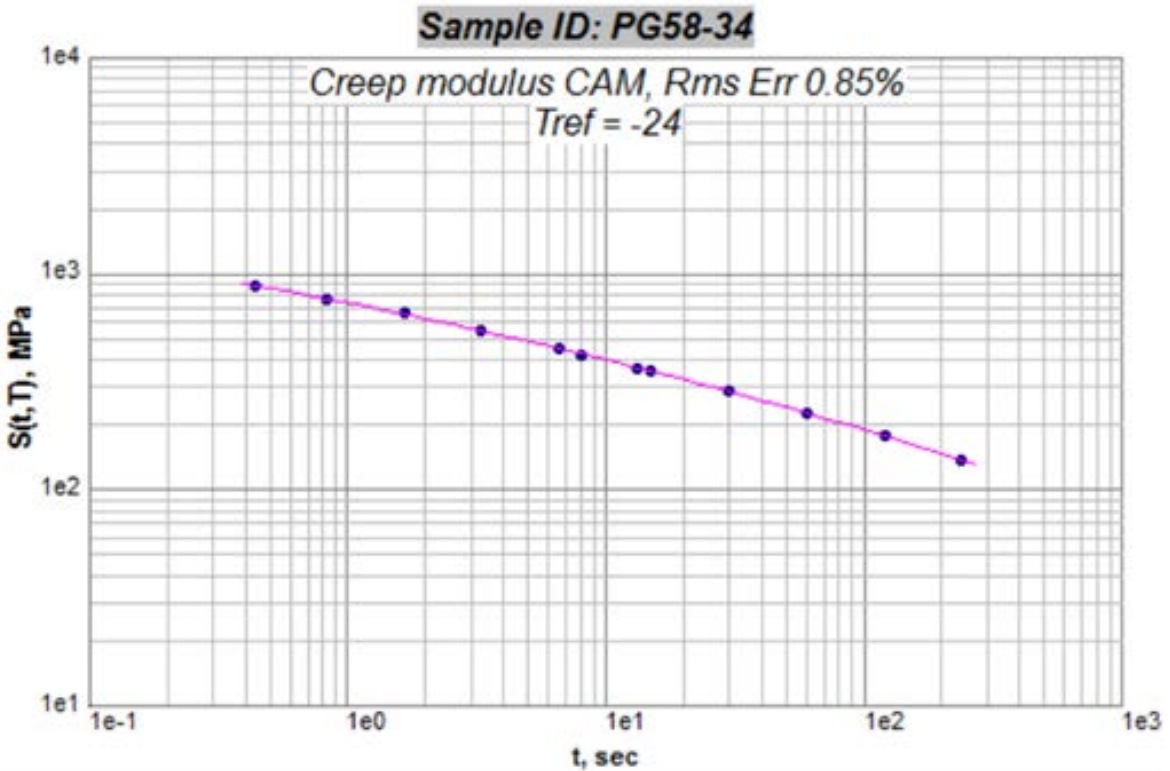
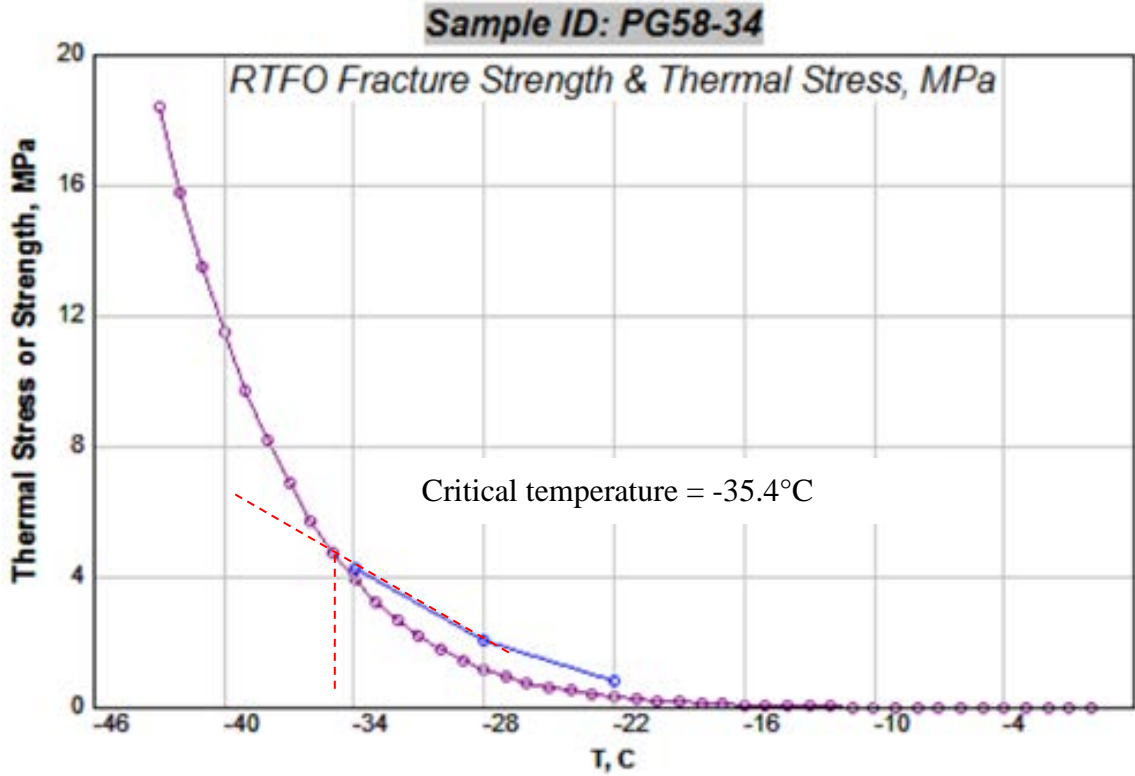


Figure 4.19 Critical temperature prediction for binder PG 58-34 after RTFO aging

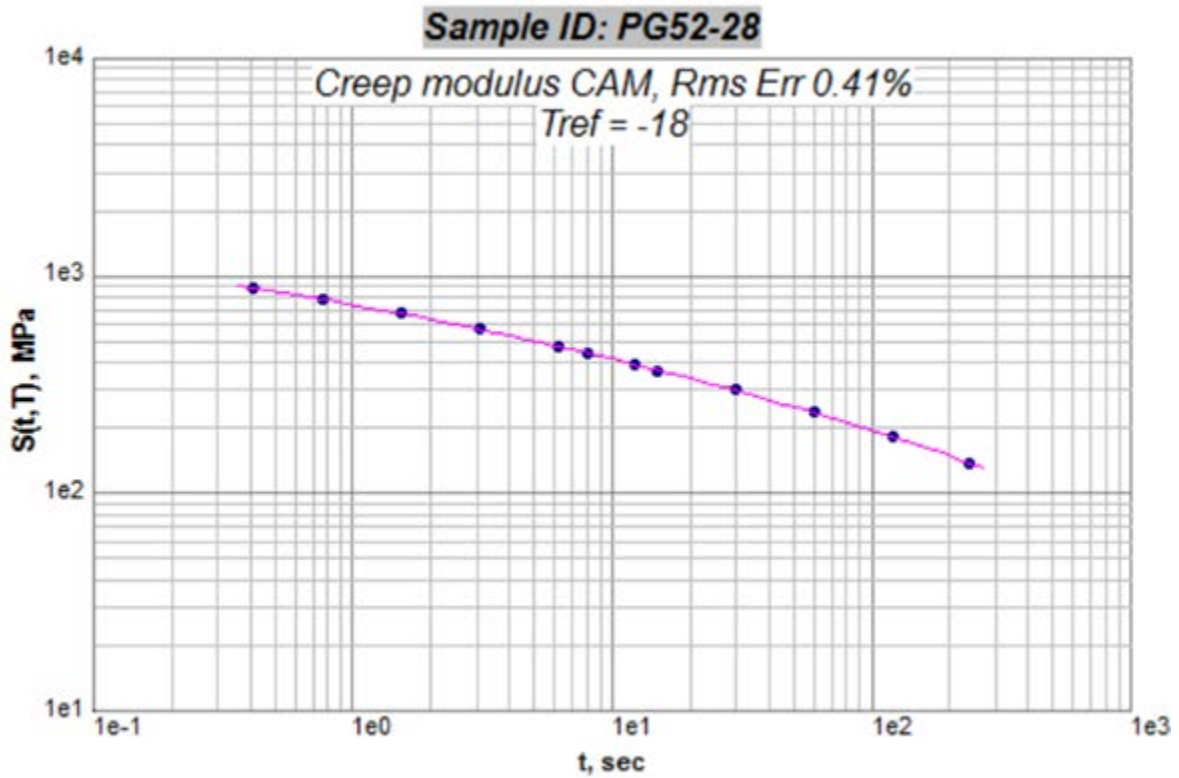
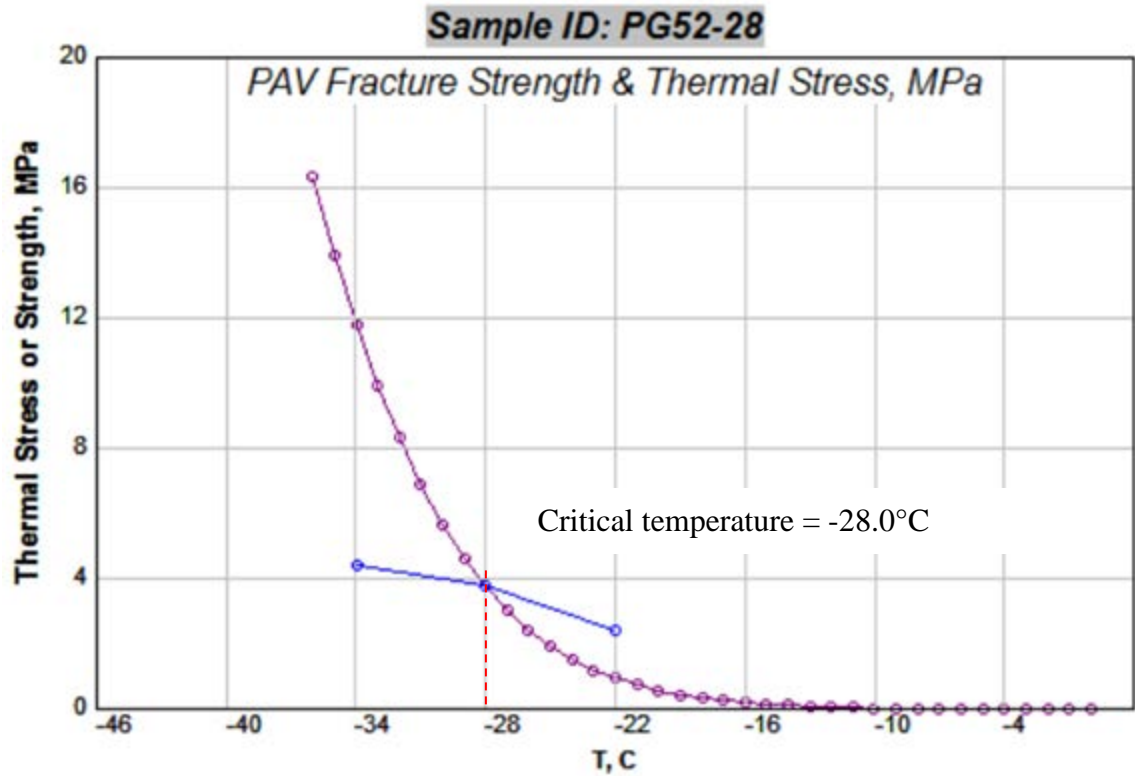


Figure 4.20 Critical temperature prediction for binder PG 52-28 after RTFO + PAV aging

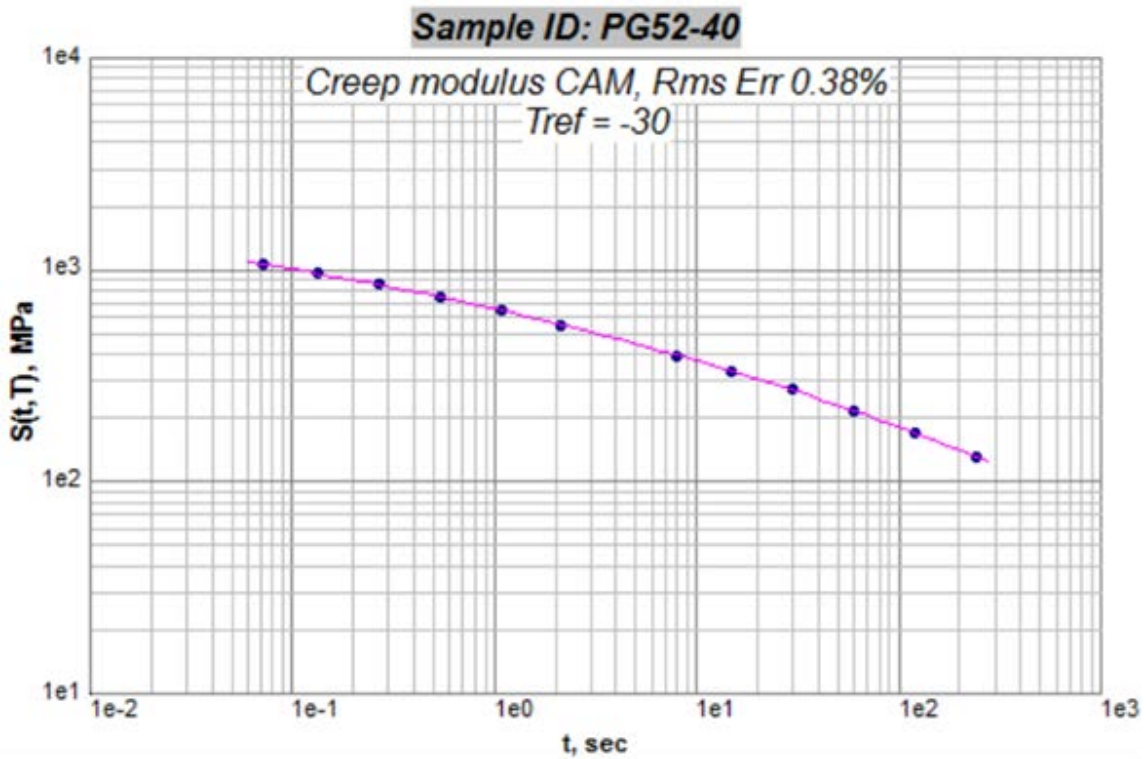
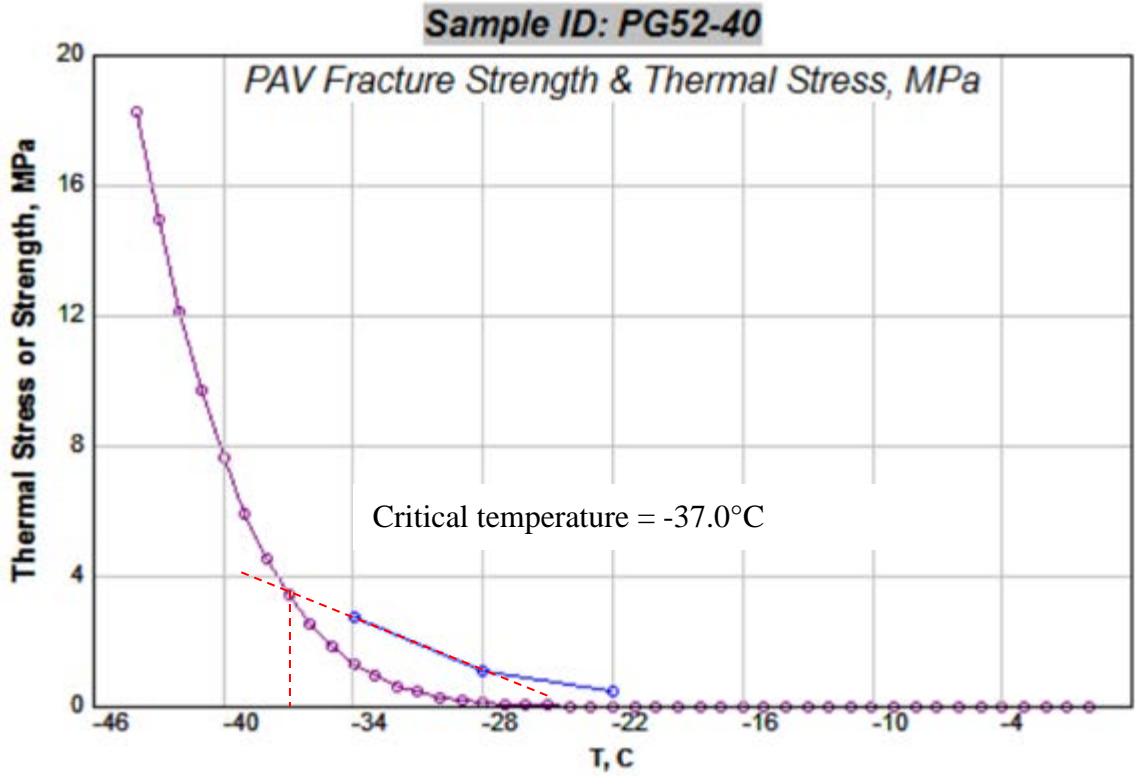


Figure 4.21 Critical temperature prediction for binder PG 52-40 after RTFO + PAV aging

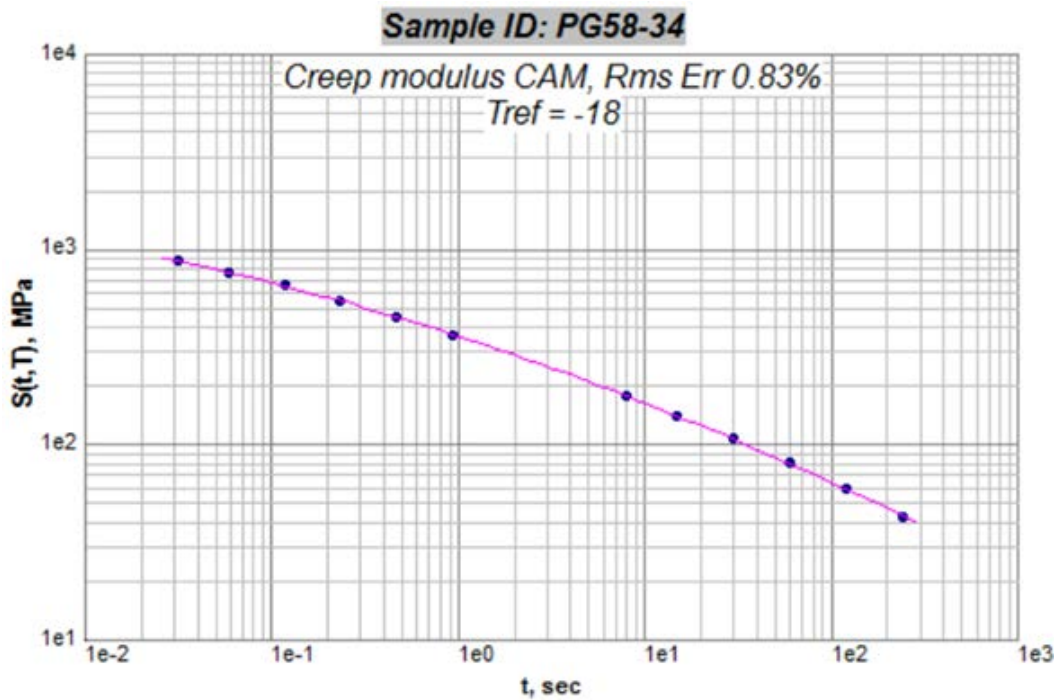
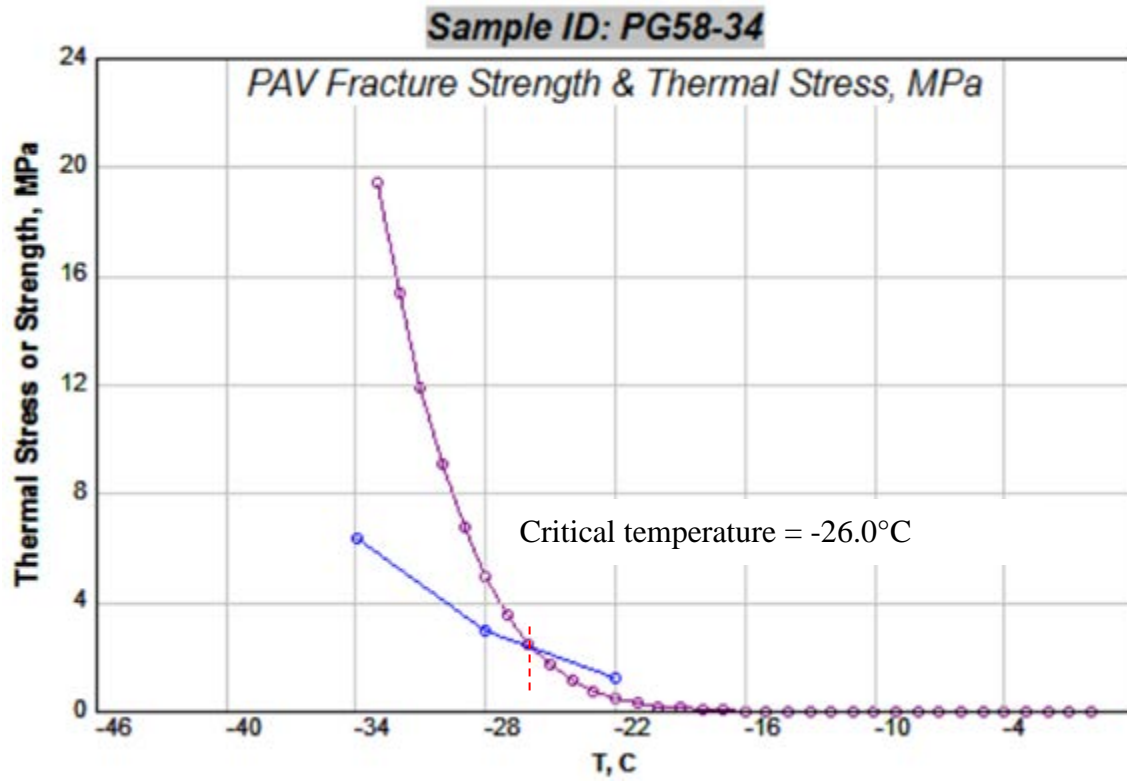


Figure 4.22 Critical temperature prediction for binder PG 58-34 after RTFO + PAV aging

The TSAR critical cracking temperature and the critical temperatures determined based on BBR and DTT data are organized in Table 4.6. The critical cracking temperature is currently used by AASHTO to specify the low-temperature grade of the binder as a replacement of old BBR or DTT methods. From the results shown in Table 4.6, it can be seen that the critical cracking temperatures of the three binders are not close to the BBR and DTT critical temperatures. For PG 52-28 and PG 52-40, the PAV-aged TSAR cracking temperatures were close to their PG low grades, but an 8°C difference was found between the cracking temperature and PG low grade of PG 58-34 binder. This indicates that the new method is evaluating a different property of the binder. Another observation is that the cracking temperatures of RTFO-aged PG 52-28 and PG 58-34 binders were significantly lower than the PAV-aged binders, but a slight difference was found on the pair of PG 52-40 binder. This means that long-term aging may not affect the thermal cracking resistance of highly modified binder such as PG 52-40. All of the binder cracking temperatures would be more meaningful if compared with mixture cracking temperatures.

Table 4.6 Critical temperature using different methods

Binder	Aging Condition	Critical T Limiting BBR Stiffness °C	Critical T Limiting BBR m-value °C	Critical T Limiting DTT failure strain °C	Critical Cracking T, TSAR °C	PG Low Grade °C
PG 52-28	RTFO	-35.2	-36	-26	-38.1	N/A
	RTFO + PAV	-29.1	-31.3	-25.7	-28	-28
PG 52-40	RTFO	-38.6	-43.6	N/A	-38	N/A
	RTFO + PAV	-40.7	-41.2	N/A	-37	-40
PG 58-34	RTFO	-35.3	-36.6	-33.3	-35.4	N/A
	RTFO + PAV	-30.9	-32.8	-40.5	-26	-34

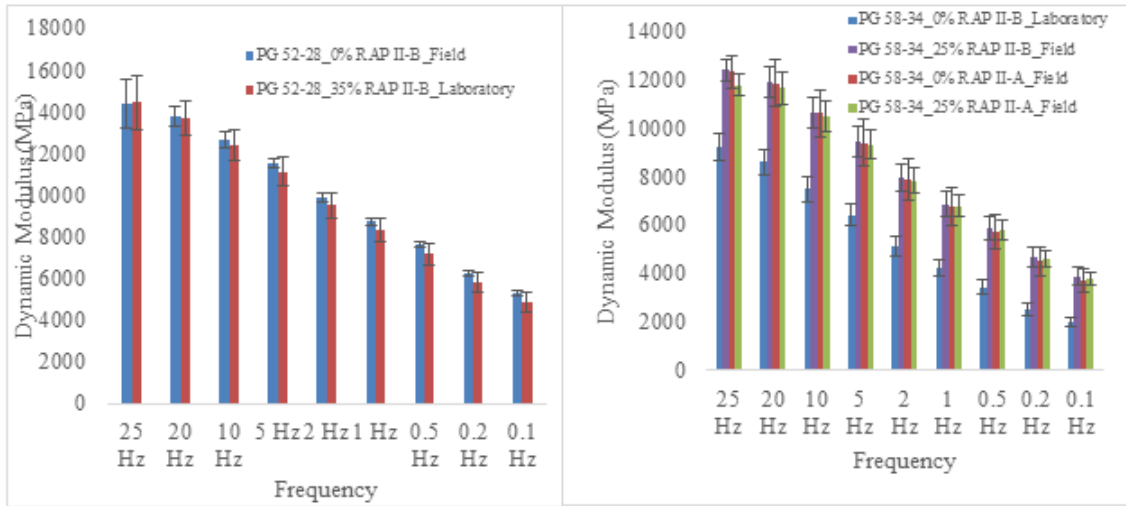
4.2 Asphalt Mixture Performance Tests

The asphalt mixture performance tests (AMPTs) include dynamic modulus ($|E^*|$) and flow number (FN). The dynamic modulus data as well as the summarized data in the form of the master curve are presented here.

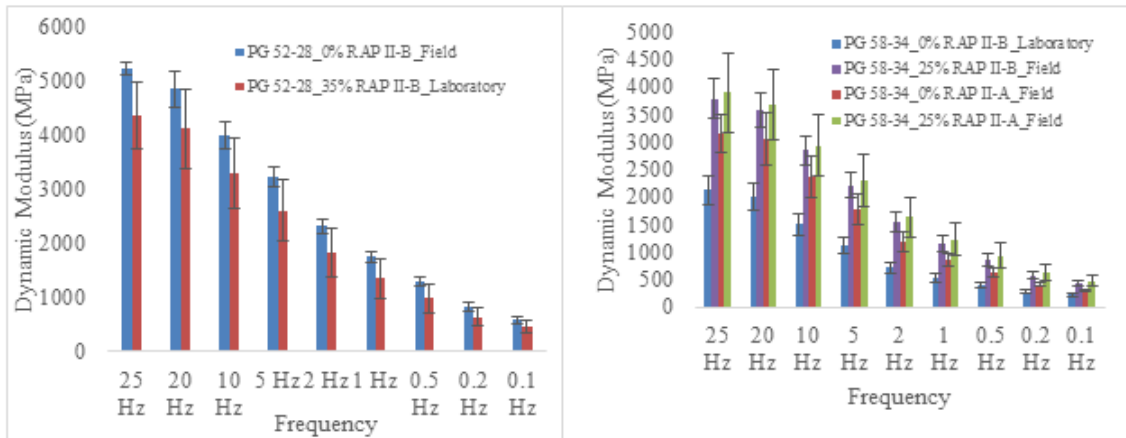
4.2.1 Dynamic Modulus

The $|E^*|$ test was performed as detailed in Chapter 3. Eleven mixtures (see Table 3.1) were tested for $|E^*|$. Figure 4.23 and Figure 4.24 present $|E^*|$ data obtained from the Central region mixes and the Northern region mixes, respectively. It is clear that the dynamic modulus of all the mixtures follows the general trend; i.e., the dynamic modulus increases with the increase in loading frequency. It can be seen that the dynamic modulus of most mixes generally increased with the addition of RAP. The higher the RAP content, the higher the dynamic modulus.

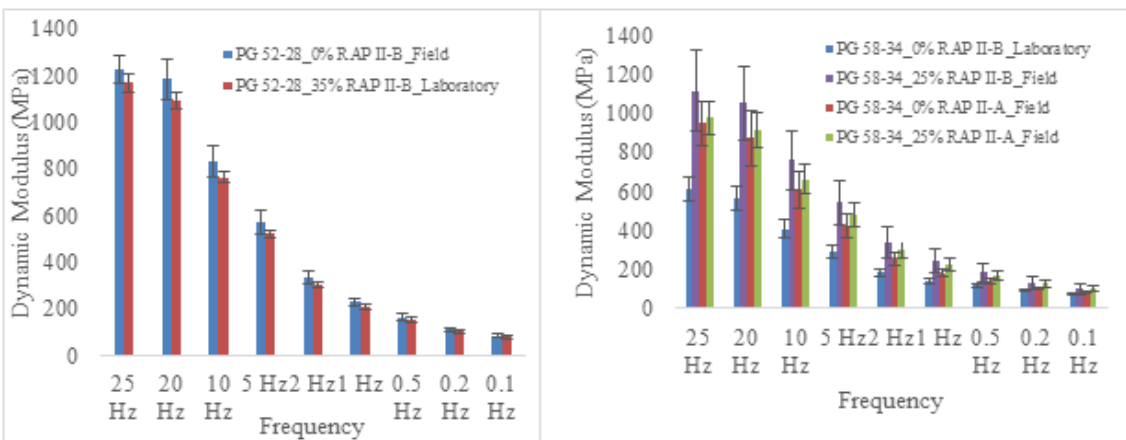
However, one exception was found with the PG 52-28 mixes from the Central region. Note that the control mix in this pair was produced in the field, and the 35% RAP mix was produced in the lab. Generally, the field mix is mixed more completely than the lab mix, but it is difficult to tell if this factor mainly caused the higher dynamic modulus observed on the control mix. Testing on more mixtures should be done to validate this observation.



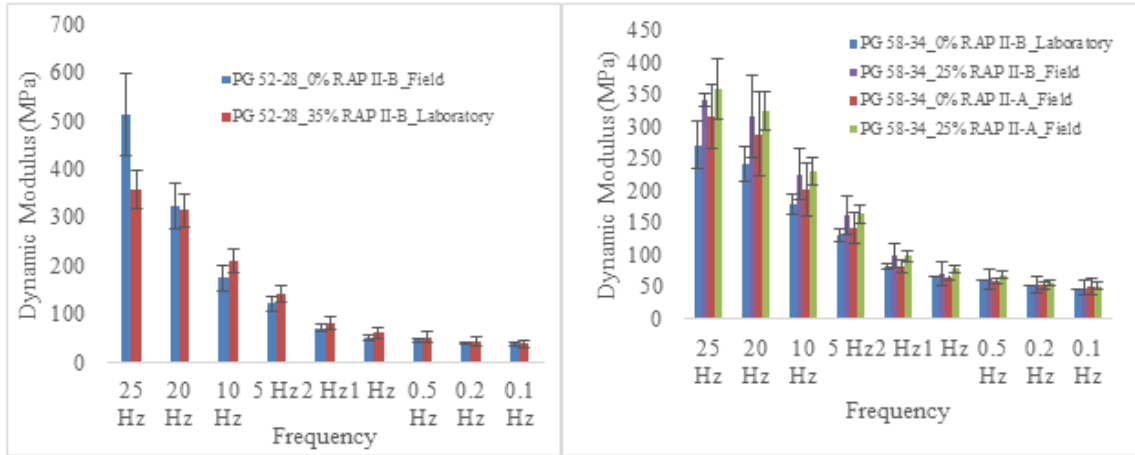
(a) Results Tested at 4.4°C



(b) Results Tested at 21.1°C

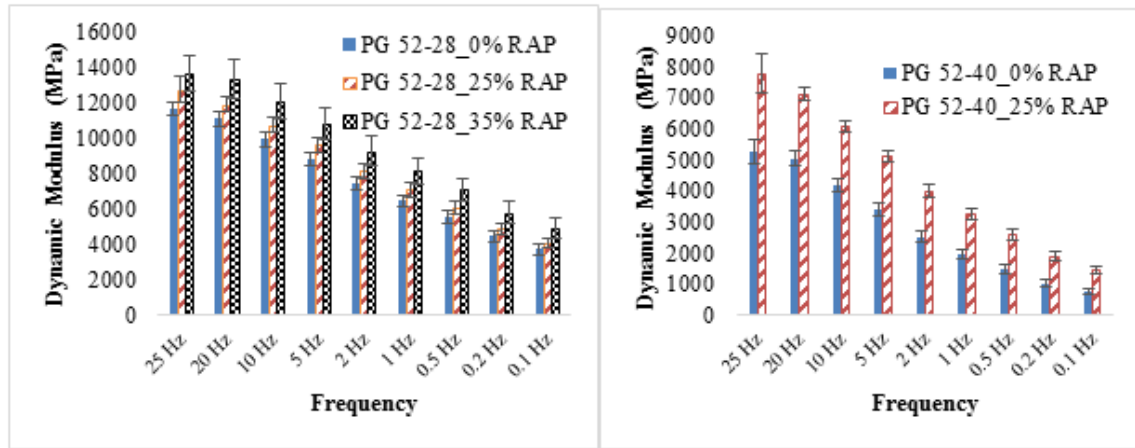


(c) Results Tested at 37.8°C



(d) Results Tested at 54°C

Figure 4.23 IE*1 data of the Central region mixes



(a) Results Tested at 4.4°C

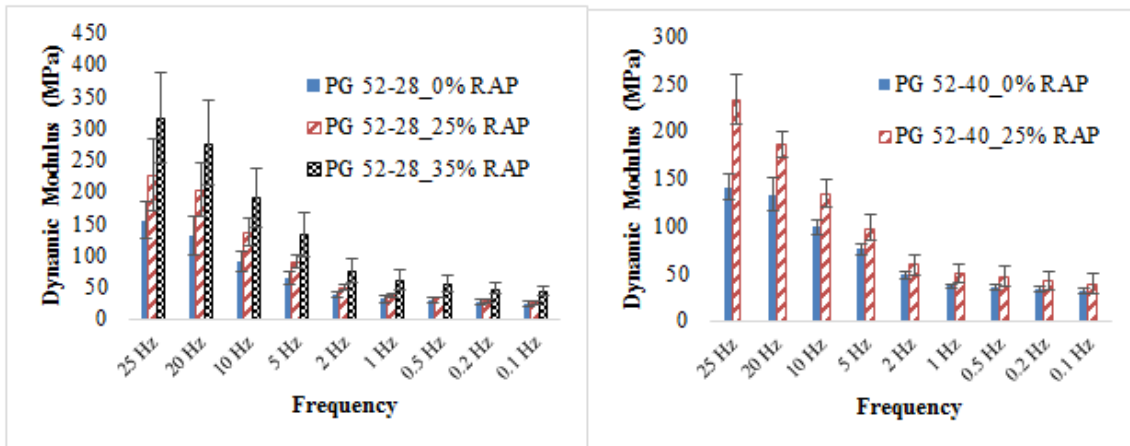
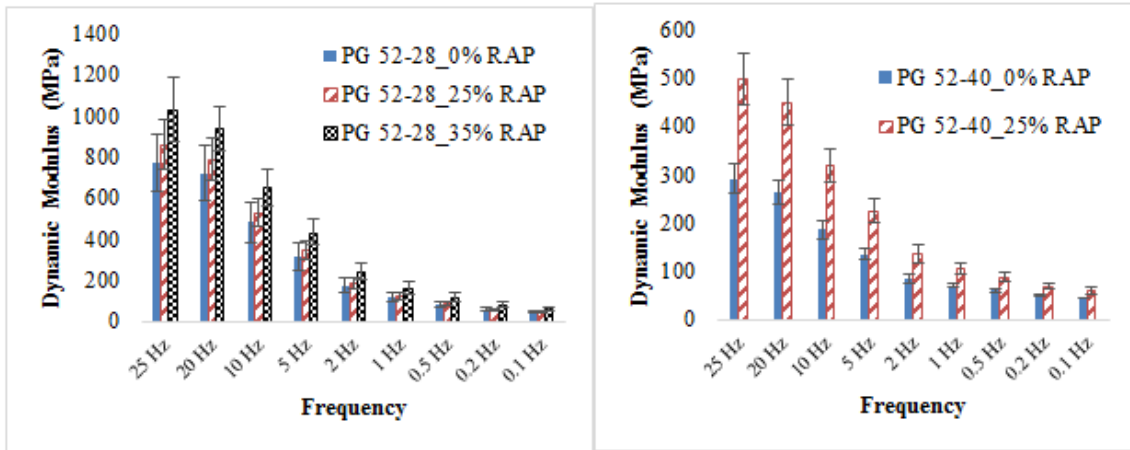
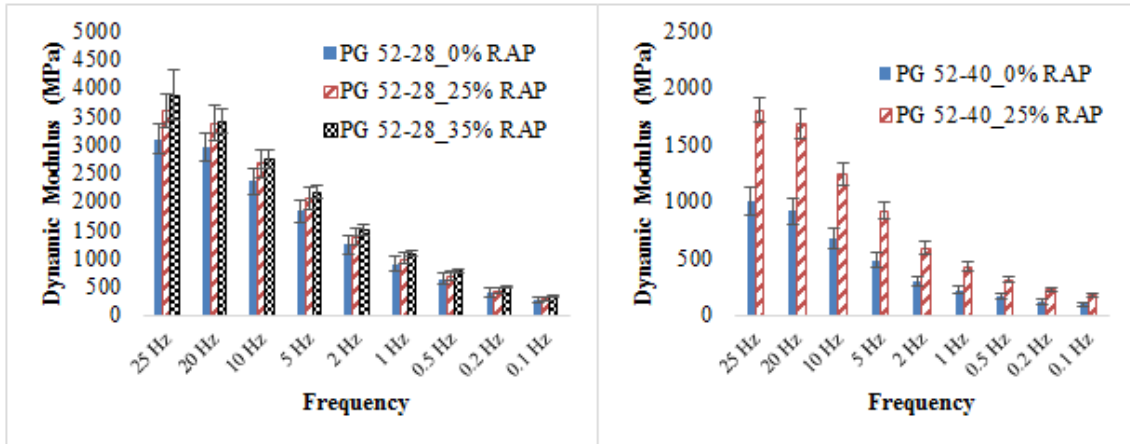
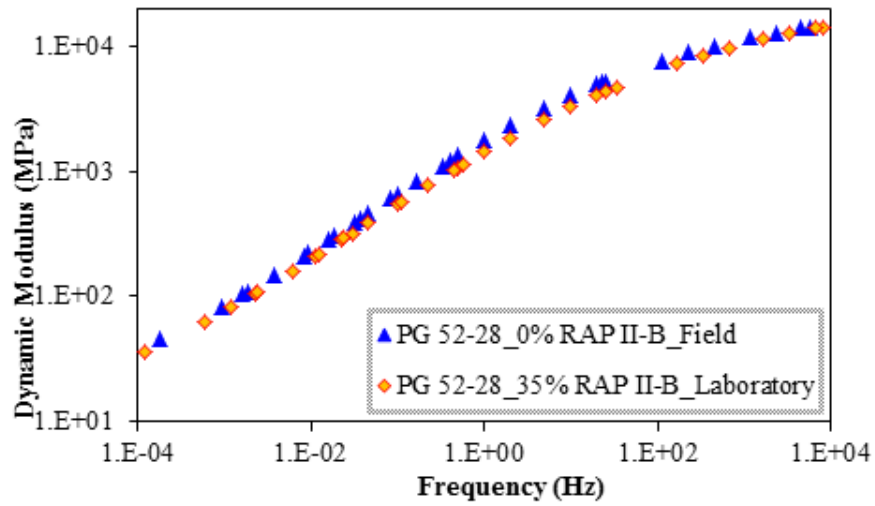
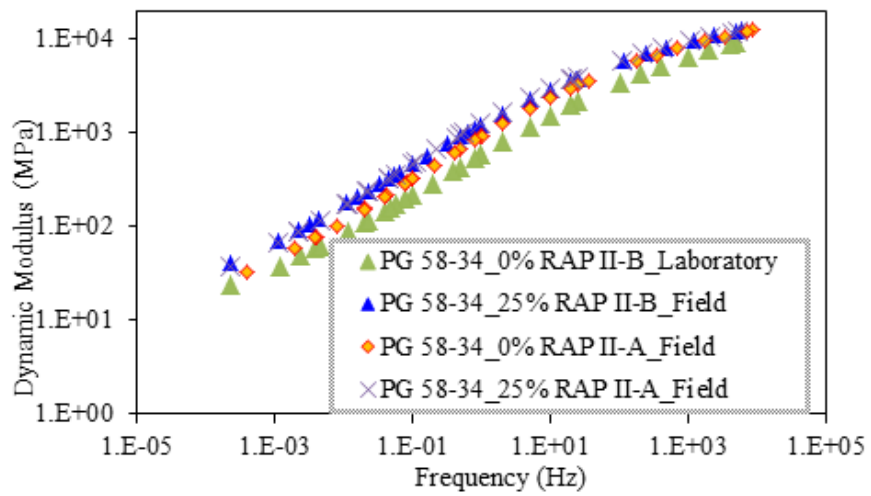


Figure 4.24 IE*1 data of the Northern region mixes

Figures 4.25 and 4.26 present the master curves at reference temperature 21.1°C obtained from the Central region and Northern region mixes, respectively. These data can be used for further pavement analysis of HMA containing RAP. The trend master curves were consistent with the dynamic modulus results.

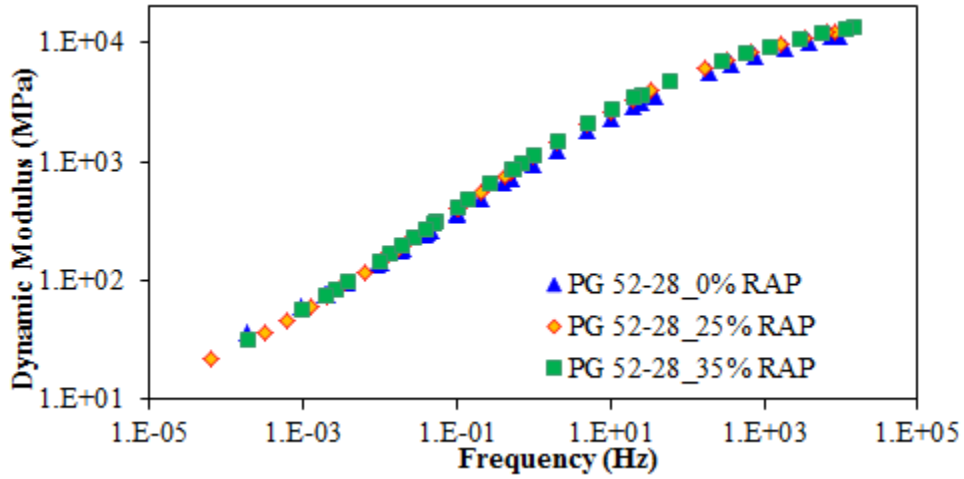


(a) Master curve of PG 52-28 mixes

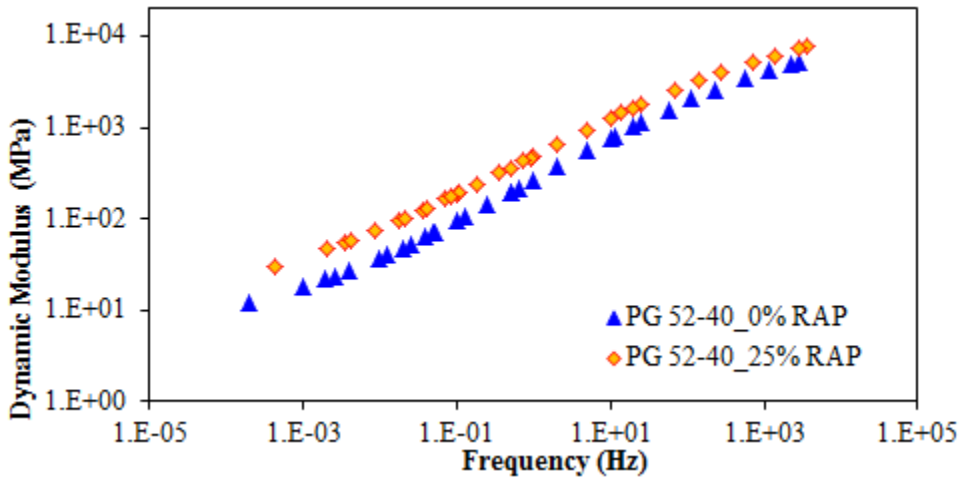


(b) Master curve of PG 58-34 mixes

Figure 4.25 Master curves of the Central region mixes



(a) Master curve of PG 52-28 mixes



(b) Master curve of PG 52-40 mixes

Figure 4.26 Master curves of the Northern region mixes

4.2.2 Flow Number (FN)

The FN test was used to evaluate the rutting resistance of the HMA mixtures. This test examines permanent deformation characteristics by applying a repeated dynamic load. The FN for the mixture is the point at which the permanent strain rate is at a minimum.

Figure 4.27 presents the flow number results for mixes in the Central region. It can be seen that two pairs out of three show that the flow number of the control mix is lower than the flow number of the RAP mix. The pair of type II-B PG 58-34 mixes is the exception. However, it can be seen that the control mix in this pair was produced in the laboratory and the RAP mix was produced in the field. This difference might cause a significant difference in the mixture's performance. A comparison of more mixes is recommended for improved understanding of RAP's effect on flow number variation.

Figure 4.28 shows the flow number results for mixes in the Northern region. The addition of RAP was found to increase the flow number of both PG 52-28 and PG 52-40 mixes, with higher RAP content leading to higher flow number, namely higher rut resistance. This finding was consistent with that from dynamic modulus results. With higher RAP content, a higher flow number is observed.

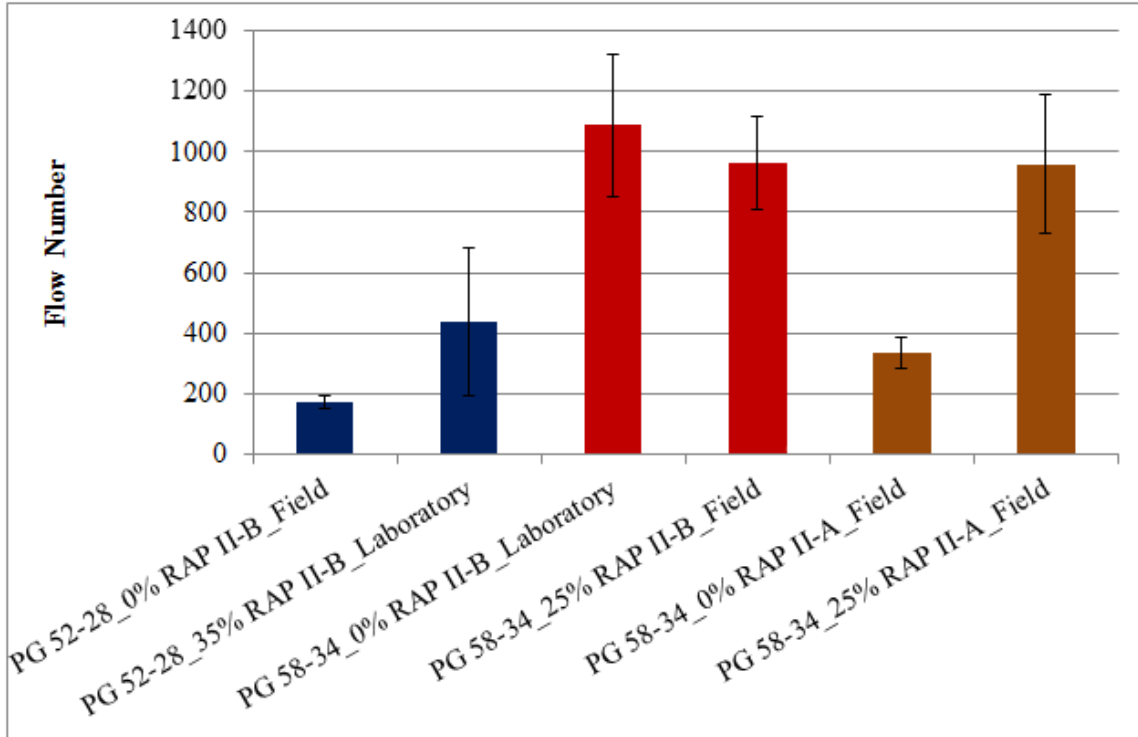


Figure 4.27 Flow number results of the Central region mixes

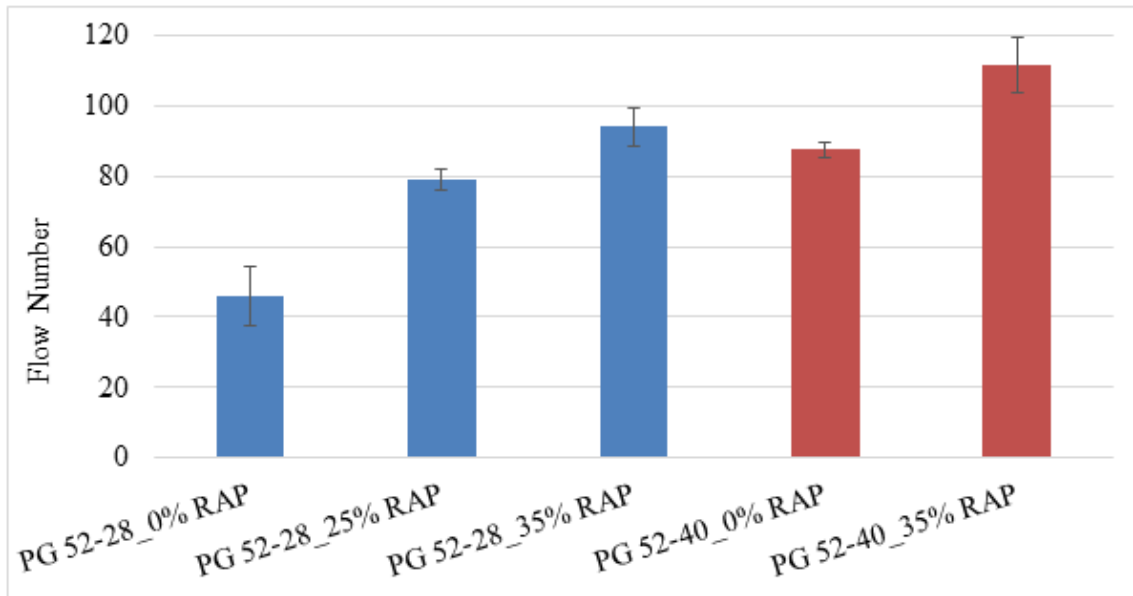


Figure 4.28 Flow number results of the Northern region mixes

4.3 Indirect Tension Tests

4.3.1 Creep Stiffness

Figure 4.29 compares the creep stiffness $S(t)$ of Central region mixes, prepared using asphalt binder PG 52-28, as a function of loading time under three temperatures (0°C, -10°C, and -20°C). In Figure 4.29, the stiffness of the PG 52-28 HMA materials with different RAP content using materials collected from the field or mixed in the laboratory are very close at different temperatures. The influences of RAP content and laboratory or field mixing on the stiffness of the mixes were coupled. The influence of RAP content and laboratory or field mixing cannot be separated from the results presented in Figure 4.29. It was found that the creep stiffness of Central region mixtures decreases with increases in temperature and time, as shown in Figure 4.29.

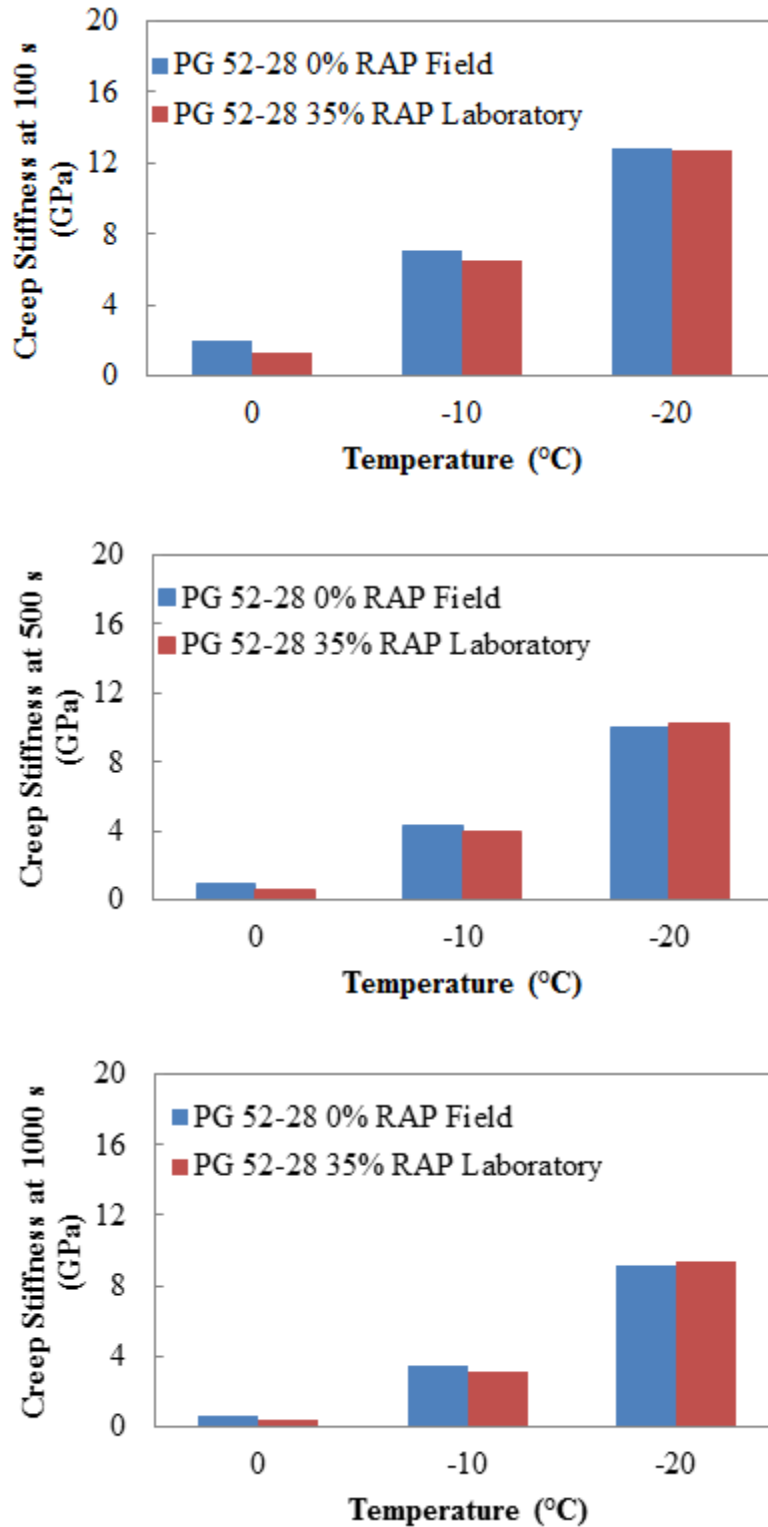
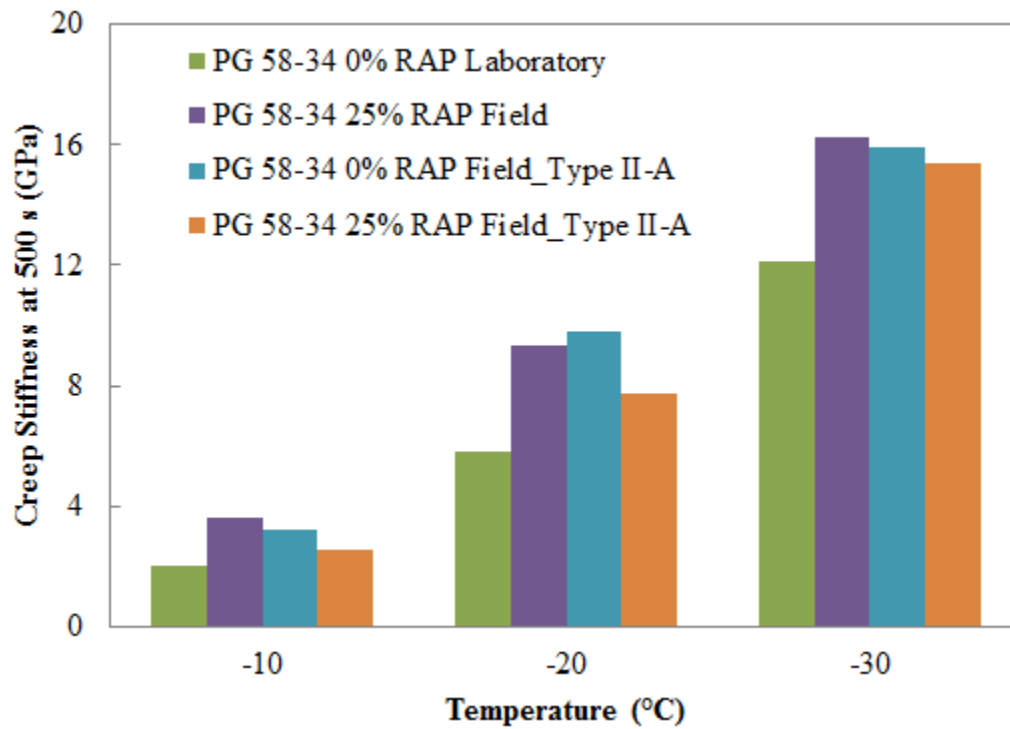
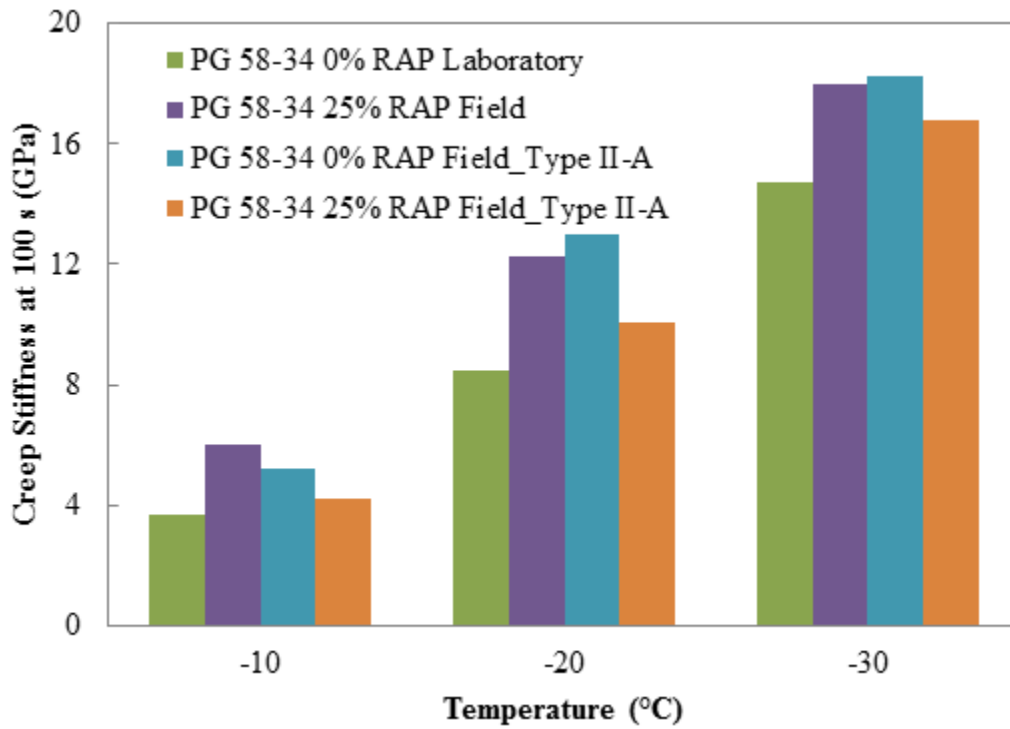


Figure 4.29 Creep stiffness of asphalt (PG 52-28) concrete at different temperatures (Central region)

Figure 4.30 compares the creep stiffness $S(t)$ of Central region mixes, prepared using asphalt binder PG 58-34, as a function of loading time under three temperatures (-10°C, -20°C, and -30°C). In Figure 4.30, the stiffness of the PG 58-34 HMA material with RAP content of 25% and mixed in the field is significantly higher than that of the material with no RAP and mixed in the laboratory. Again, since the influences of RAP content and laboratory or field mixing on the stiffness of the mixes were coupled, the influence of RAP content and laboratory or field mixing cannot be separated from the results presented in Figure 4.30. For the mixes compacted using the Type II-A method as shown in Figure 4.30, the stiffness of the mix with 25% RAP is slightly lower than the mix with no RAP. The difference in stiffness of the two mixes became smaller with time. In addition, the creep stiffness of Central region mixtures prepared using the PG 58-34 binder decrease with the increase of temperature and time, as shown in Figure 4.29.



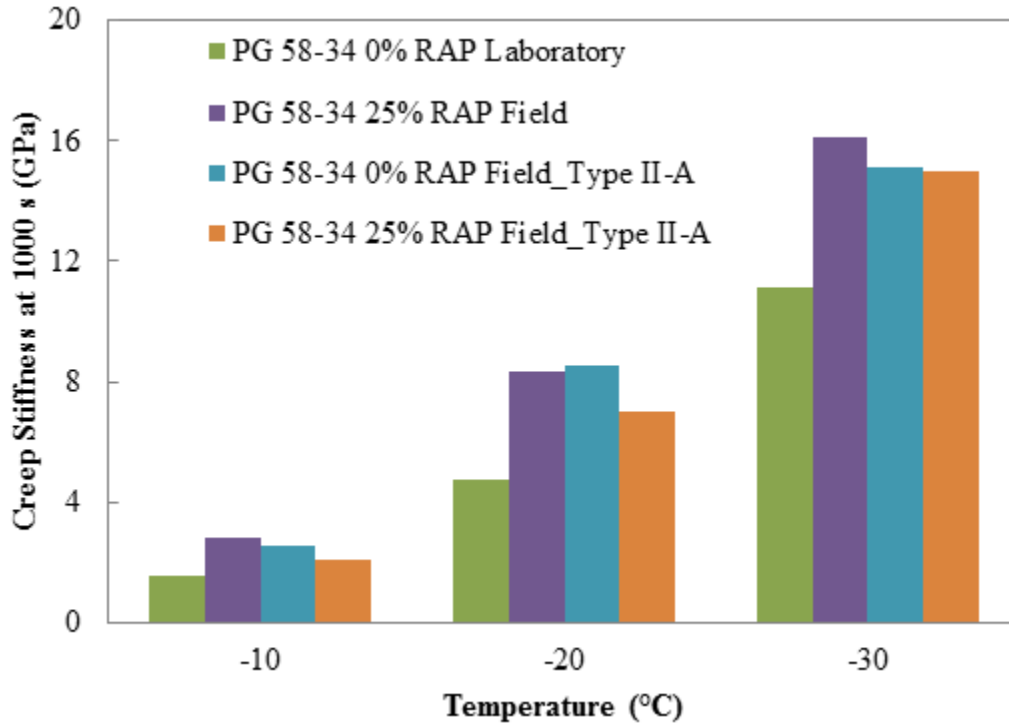


Figure 4.30 Creep stiffness of asphalt (PG 58-34) concrete at different RAP contents and temperatures (Central region)

Figures 4.31 and 4.32 compare the creep stiffness $S(t)$ of Northern region mixes, prepared using asphalt binder PG 52-28 and PG 52-40, as a function of loading time under three temperatures (0°C , -10°C , and -20°C). In general, the creep stiffness of Northern region mixes decreased with the increase of temperature and time. At each temperature level, the creep stiffness increases with an increase of RAP content except for the mixture tested at -20°C and 100 s, as shown in Figure 4.31. Note that the stiffness of the mixture with RAP content of 25% was close to that of the mixture without RAP. However, when RAP content increases to 35%, a significant increase of stiffness is observed (see Figure 4.31).

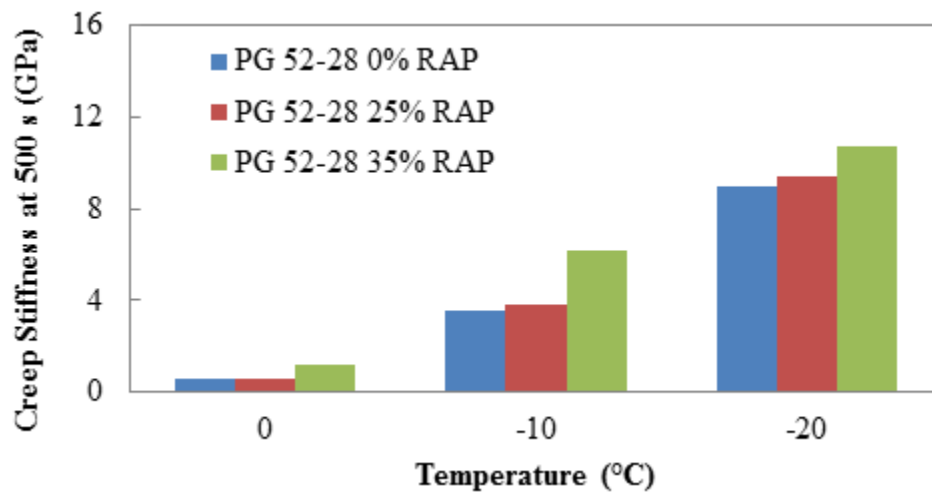
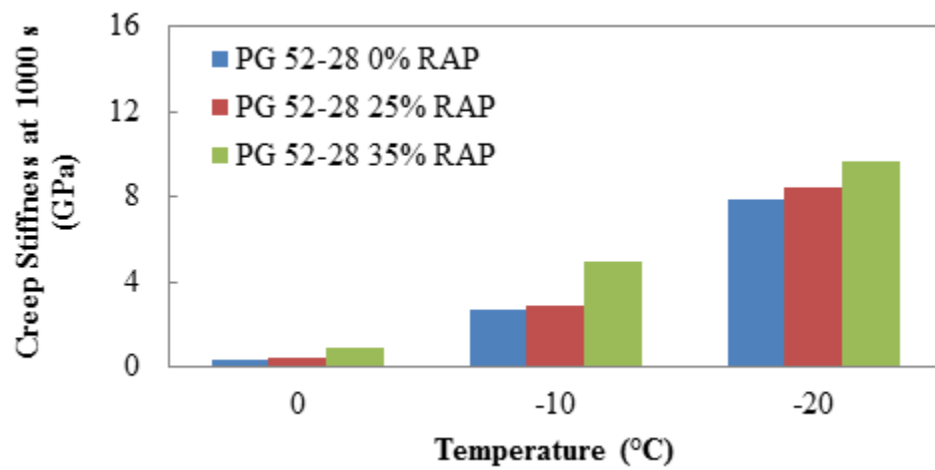
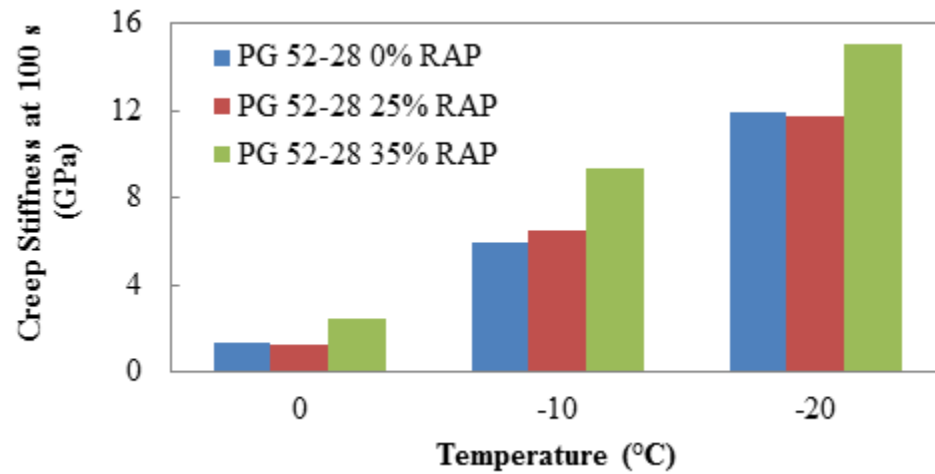


Figure 4.31 Creep stiffness of asphalt (PG 52-28) concrete at different temperature and RAP contents (Northern region)

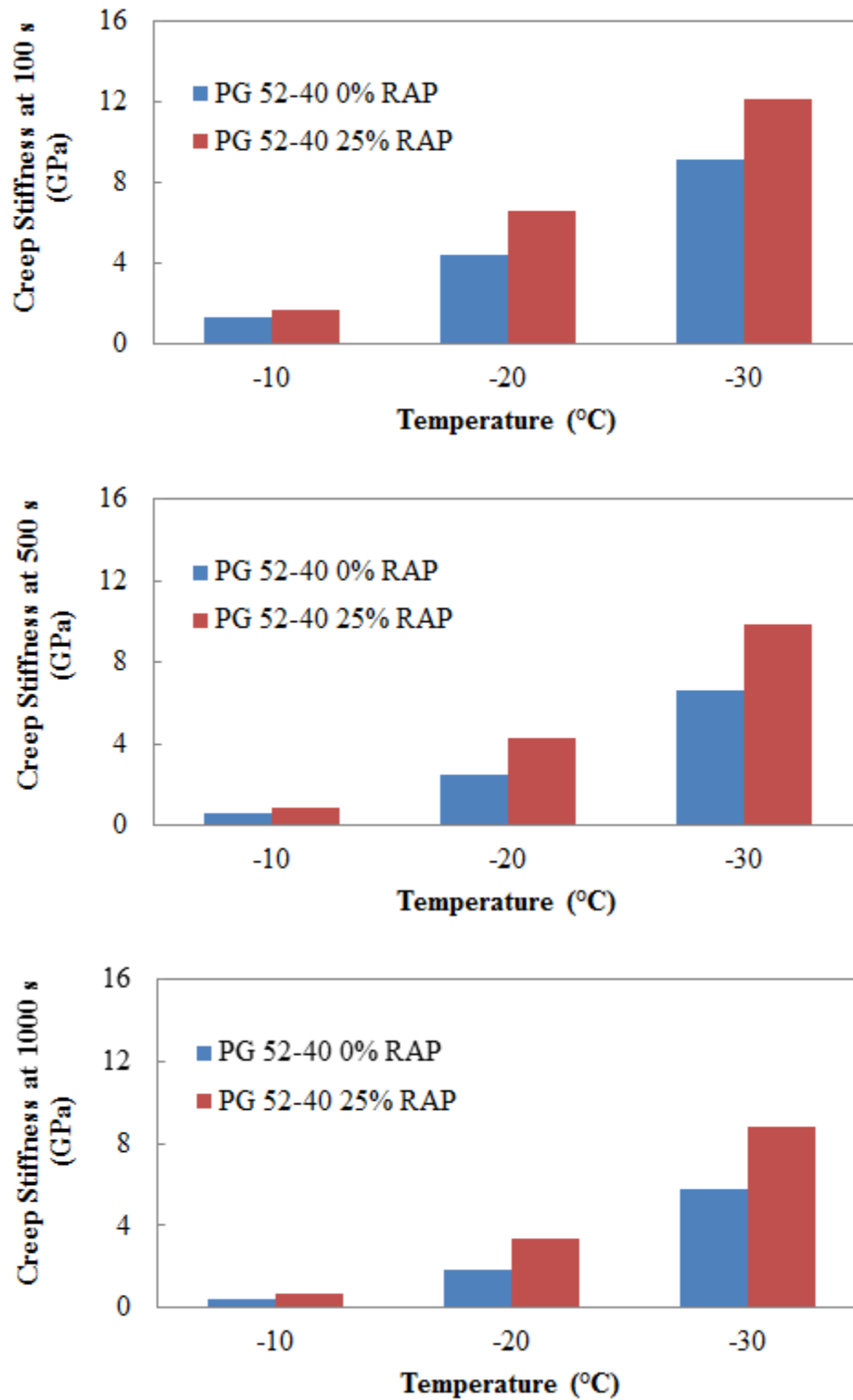


Figure 4.32 Creep stiffness of asphalt (PG 52-40) concrete at different temperature and RAP contents (Northern region)

4.3.2 IDT strength

The temperature-controlled IDT strength test results for mixes from the Northern region tested at -10°C, -20°C, and -30°C are summarized in Table 4.7. The mean strength is the average strength of three replicated specimens tested at the same temperature. The standard deviation and coefficient of variation of results from three replicated specimens are presented in Table 4.7. The strength test results are plotted in Figure 4.33 for mixes prepared using the binders PG 52-28 and PG 52-40.

Table 4.7 IDT strength test results for materials from the Northern region

Mix type	T (°C)	Mean strength (kPa)	STDEVA. (kPa)	CV (%)
PG 52-28 0% RAP Laboratory mixing	-10	2385	393	16.5
	-20	2354	215	9.1
	-30	2963	279	9.4
PG 52-28 25% RAP Laboratory mixing	-10	2642	405	15.3
	-20	3027	319	9.4
	-30	2556	108	4.9
PG 52-28 35% RAP Laboratory mixing	-10	3004	203	6.8
	-20	3344	302	9.0
	-30	2860	196	6.0
PG 52-40 0% RAP Laboratory mixing	-10	1899	120	6.3
	-20	2521	145	5.7
	-30	2911	441	15.2
PG 52-40 25% RAP Laboratory mixing	-10	2068	104	5.0
	-20	2719	477	17.5
	-30	3480	510	14.7

* STDEVA. represents the standard deviation, and CV represents coefficient of variation

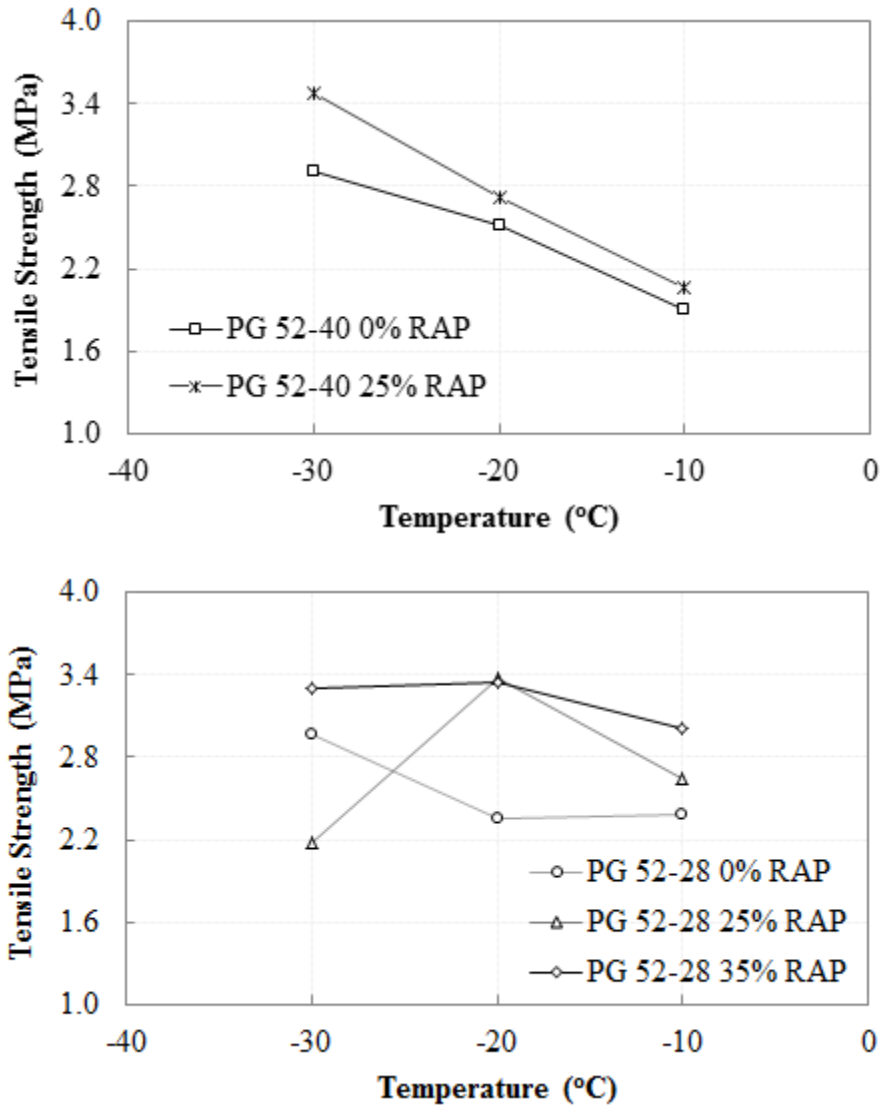


Figure 4.33 Tensile strengths of mixes at different temperatures (Northern region)

As shown in Figure 4.33, the tensile strength of mixes prepared using PG 52-40 from and materials from the Northern region with 0 and 25% RAP content increases with decreasing temperature, and the strength versus temperature relationship is nearly linear within the temperature range from -30°C to -10°C. In addition, the tensile strength increases with an increase of RAP content. For the mixes prepared using PG 52-28, the linear relationship between

strength and temperature no longer exists especially for the materials with RAP content of 25%, as shown in Figure 4.33. Instead, the maximum strength was found to be the material tested at the temperature of -20°C.

Table 4.8 IDT strength test results for materials from the Central region

Mix type	T (°C)	Mean strength (kPa)	STDEVA. (kPa)	CV (%)
PG 52-28 0% RAP Field mixing Type II-B	-10	3340	316	9.4
	-20	3982	359	12.4
	-30	3729	137	3.7
PG 58-34 0% RAP, Laboratory mixing Type II-B	-10	3668	290	7.9
	-20	4466	126	2.8
	-30	5073	387	7.6
PG 58-34 0% RAP Field mixing Type II-A	-10	3144	220	7.0
	-20	4154	167	4.0
	-30	3922	415	10.6
PG 58-34 25% RAP Field mixing Type II-A	-10	3114	500	16.1
	-20	4283	439	10.3
	-30	4113	364	8.8
PG 58-34 25% RAP Field mixing Type II-B	-10	3843	188	4.9
	-20	4785	341	7.1
	-30	5091	45	0.9
PG 52-28 35% RAP Field mixing Type II-B	-10	2901	452	15.6
	-20	3990	730	18.3
	-30	3881	405	10.4

* STDEVA. represents the standard deviation, and CV represents coefficient of variation.

The temperature-controlled IDT strength test results for mixes from the Central region tested at temperatures of -10°C, -20°C, and -30°C are summarized in Table 4.8. In addition, these strength test results are plotted in Figure 4.34 for mixes prepared using the binders PG 52-28 and PG 58-34.

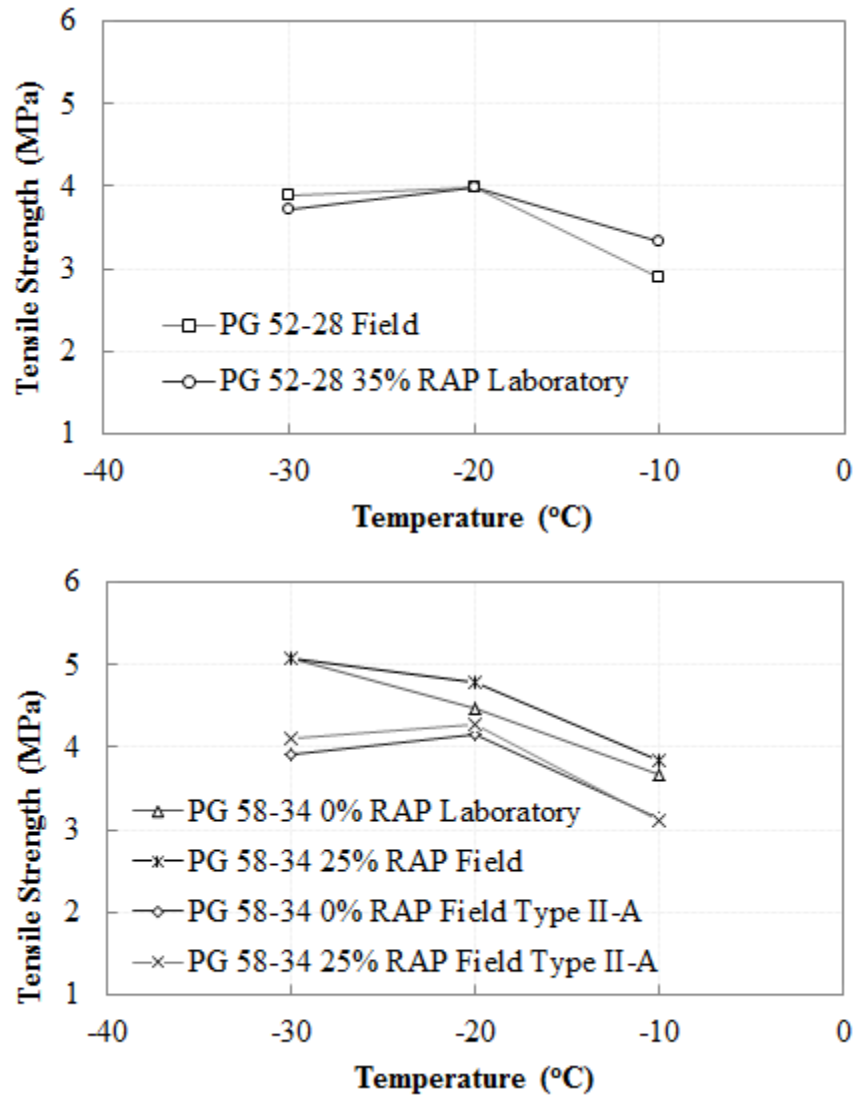


Figure 4.34 Tensile strengths of mixes at different temperatures (Central region)

Figure 4.34 shows that the tensile strength of mixes prepared using PG 52-28 and materials from the Central region with 0 and 35% RAP content increase with a decrease of temperature when temperatures range from -20°C to -10°C. The maximum tensile strength of mixes is found at -20°C, with temperatures ranging from -30°C to -10°C. In other words, tensile strength does not increase with decreasing temperature, as shown in Figure 4.34. Similar test results were found for the mixtures collected from the field using PG 58-34 binder with a RAP content of 0 and 25% and the Type II-A compaction method, as shown in Figure 4.34. However, for the mixes prepared using the same PG 58-34 binder, with 0 and 25% RAP content and the Type II-B compaction method, the strength versus temperature relationship was nearly linear within the temperature range from -30°C to -10°C. In addition, the overall strength of the mixes prepared using Type II-B are slightly higher than the strength of the mixes prepared using Type II-A, as shown in Figure 4.34.

4.3.3 Mixture Cracking Temperature

Indirect tension (IDT) creep stiffness data can be used to generate the stress curve of each mixture, as shown in Figure 4.35. An LTStress template (2012 version) (Christensen 1998, which is commonly used for analyzing data from IDT creep and strength tests, was used to process the data, as performed according to the Superpave protocol. The template develops a

master curve of creep compliance (stiffness) versus time, and determines the slope of the log-shift factor versus temperature function with the input of lab-obtained IDT creep stiffness data.

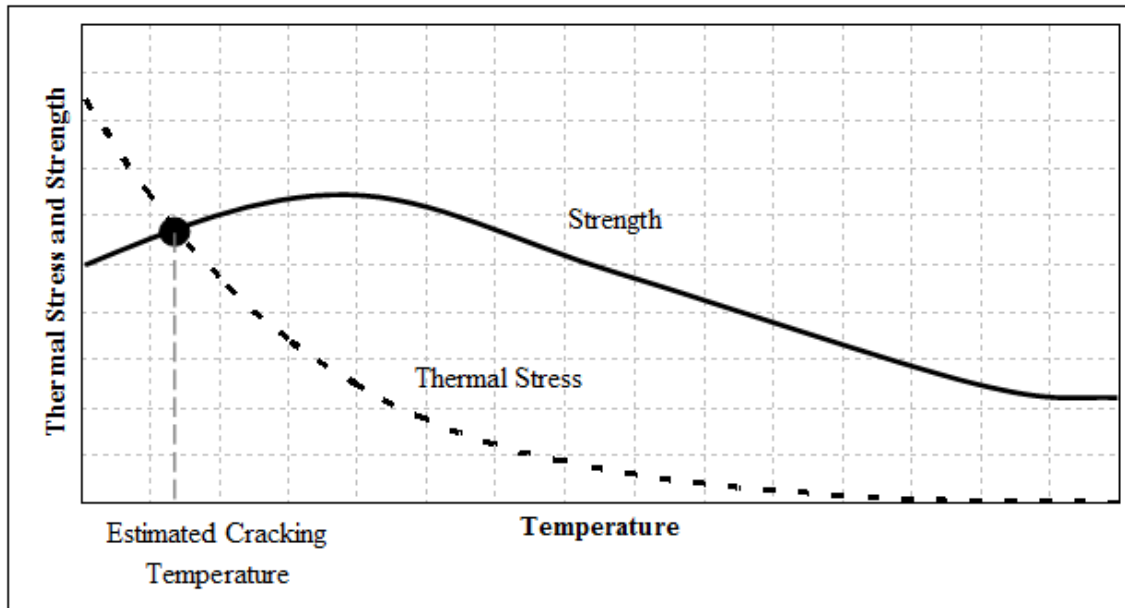


Figure 4.35 Example of determination of mixture cracking temperature

Figures 4.36 to 4.46 present the process of mixture cracking temperature determination for each mix.

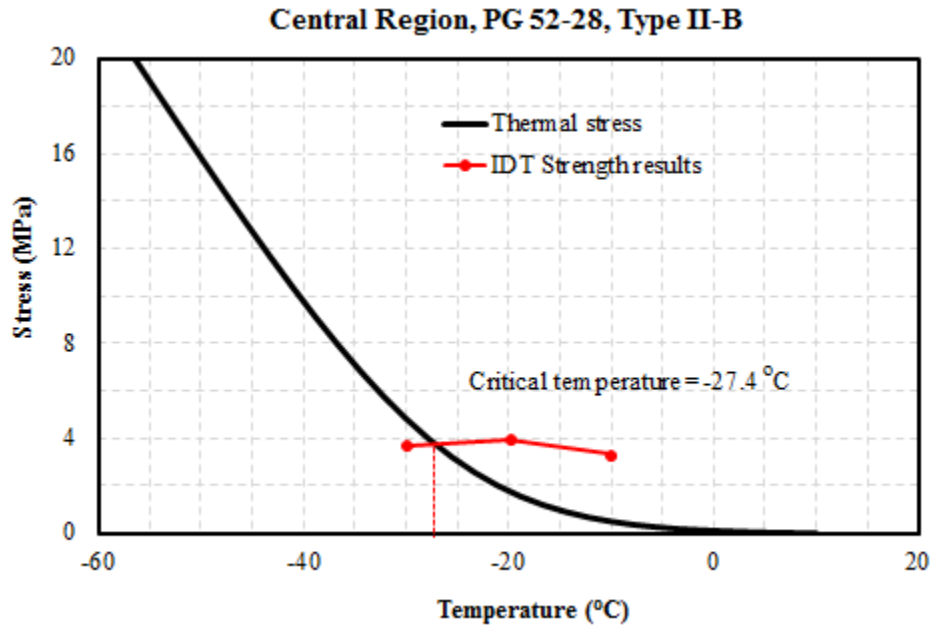


Figure 4.36 Determining mixture cracking temperature for Mix 1 in Table 3.1

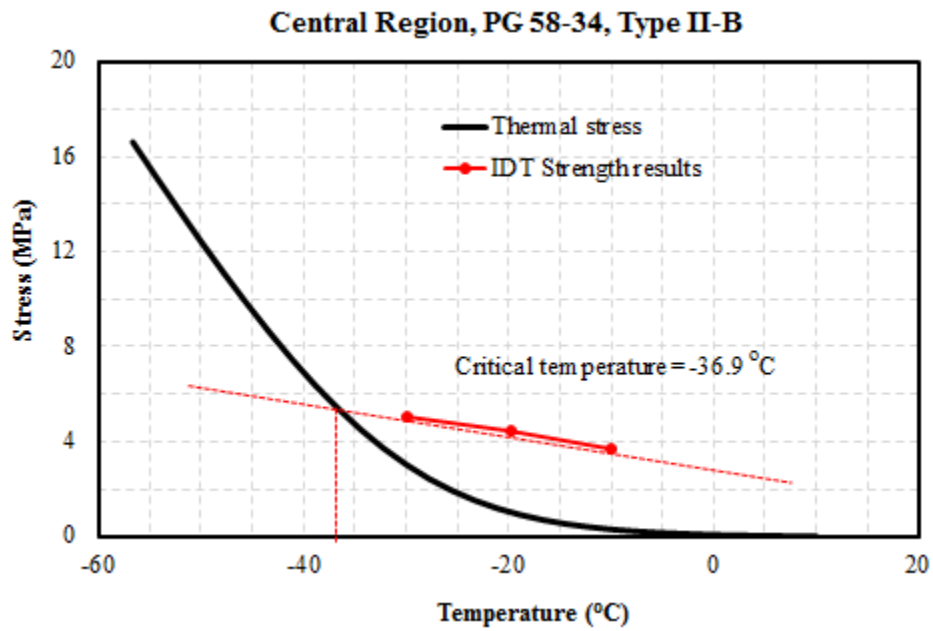


Figure 4.37 Determining mixture cracking temperature for Mix 2 in Table 3.1

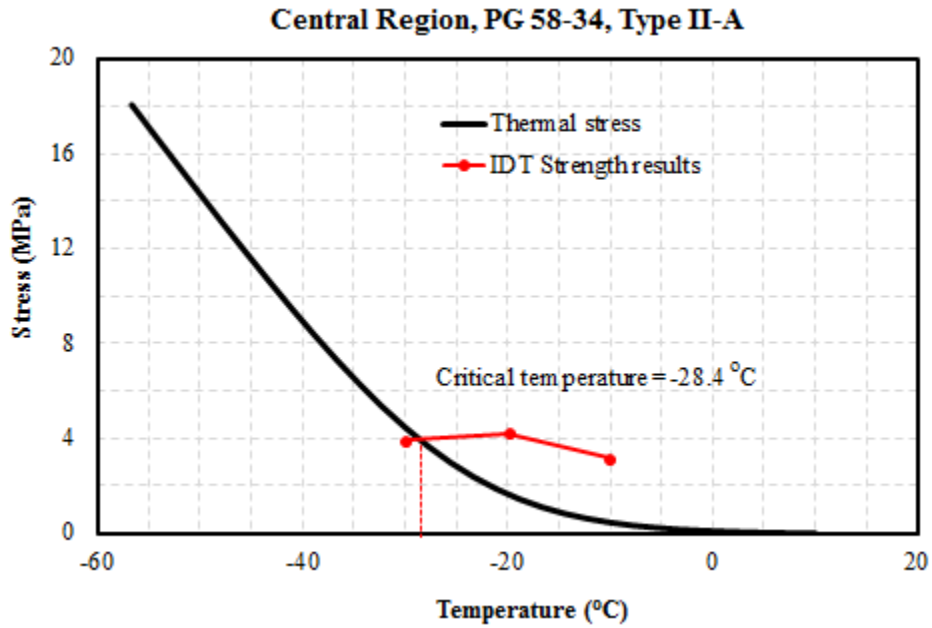


Figure 4.38 Determining mixture cracking temperature for Mix 3 in Table 3.1

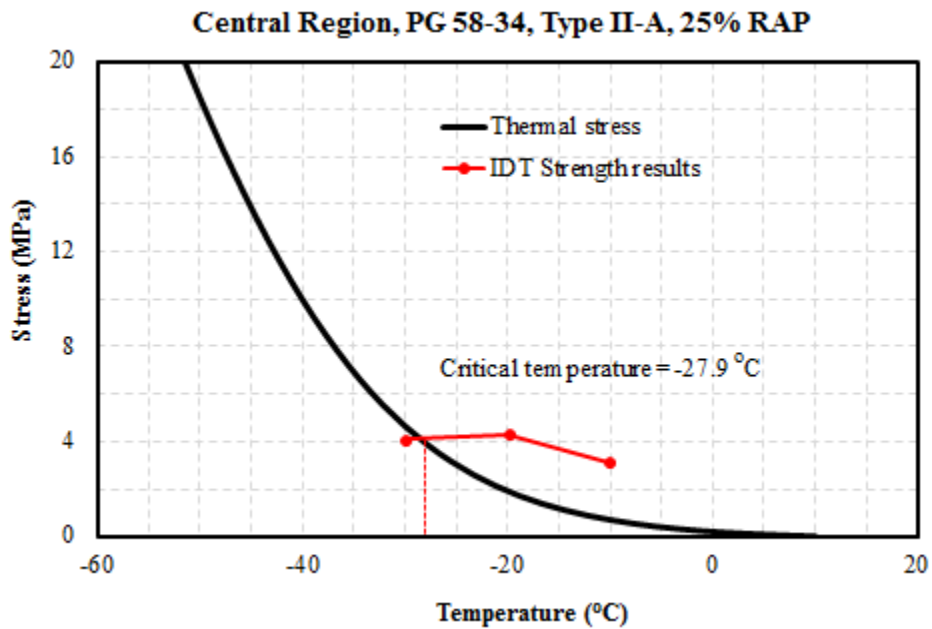


Figure 4.39 Determining mixture cracking temperature for Mix 4 in Table 3.1

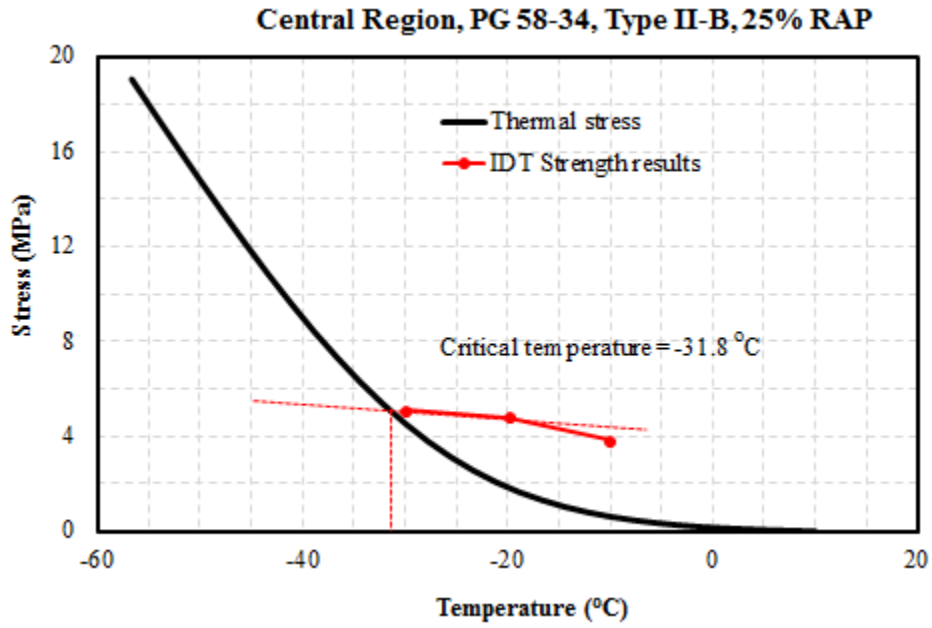


Figure 4.40 Determining mixture cracking temperature for Mix 5 in Table 3.1

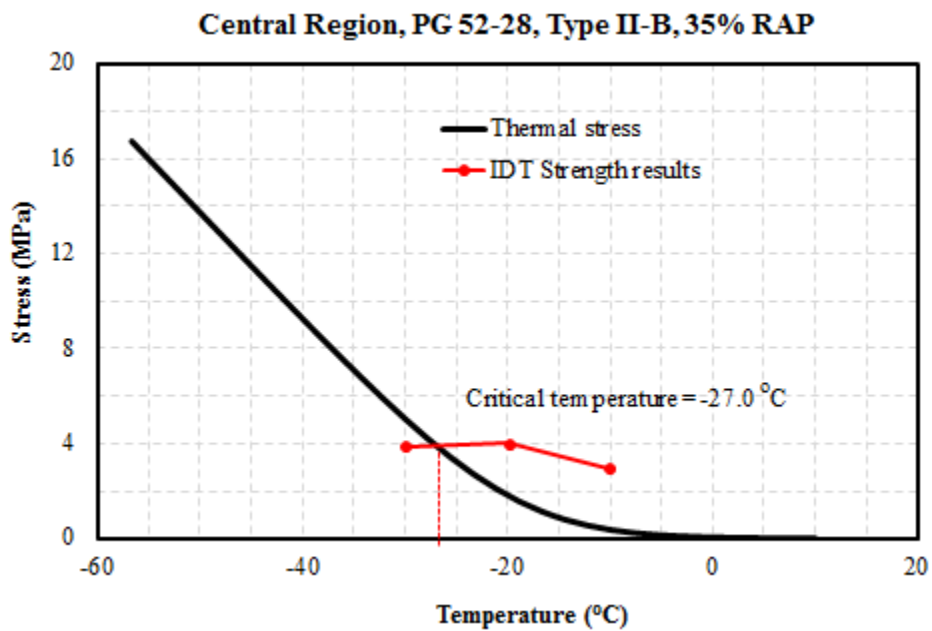


Figure 4.41 Determining mixture cracking temperature for Mix 6 in Table 3.1

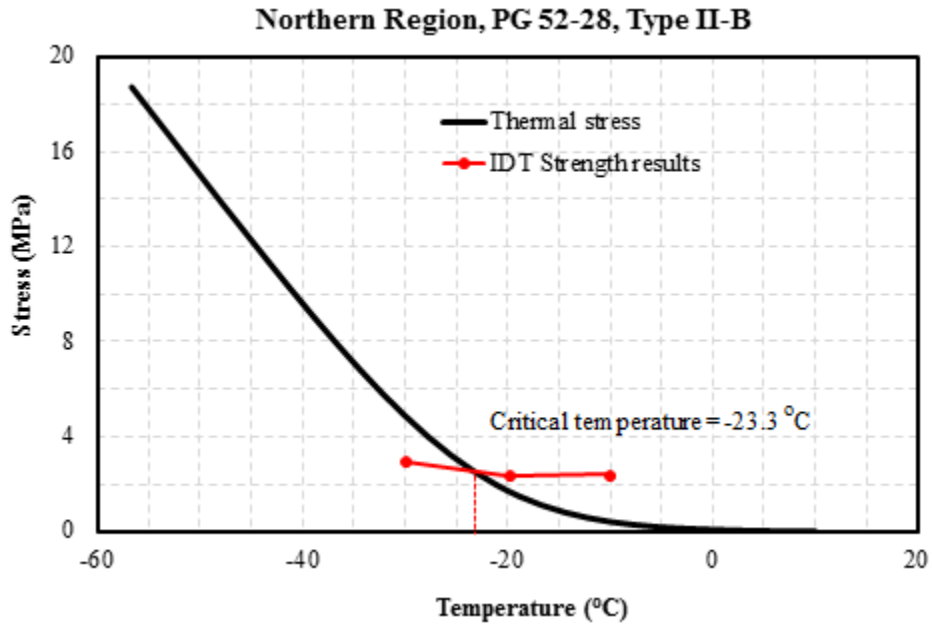


Figure 4.42 Determining mixture cracking temperature for Mix 7 in Table 3.1

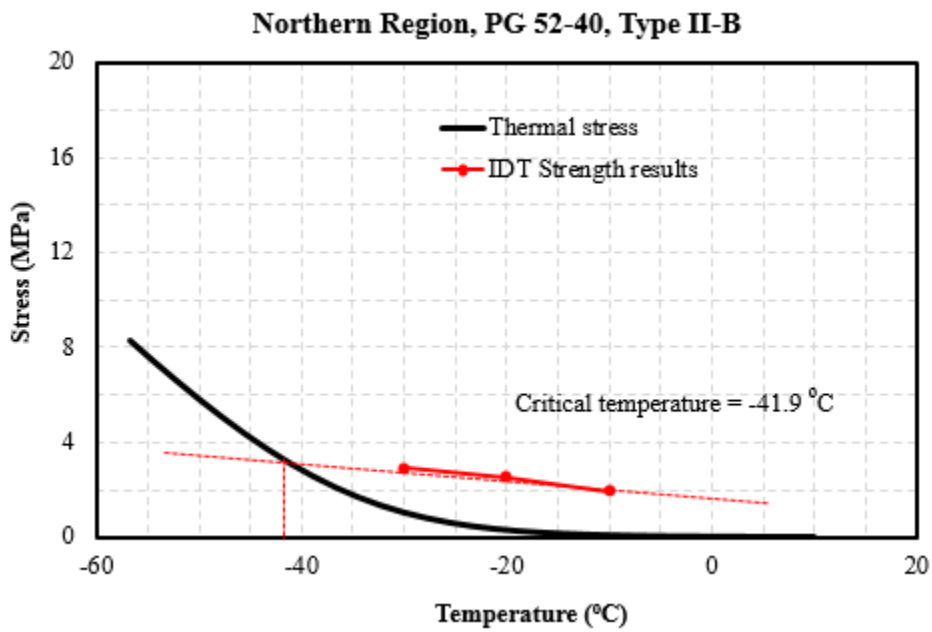


Figure 4.43 Determining mixture cracking temperature for Mix 8 in Table 3.1

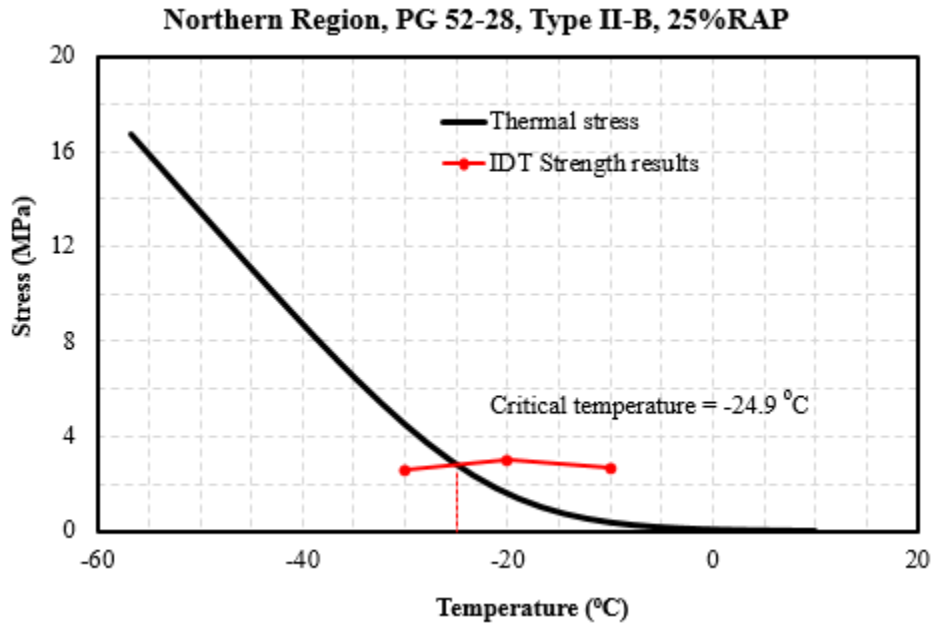


Figure 4.44 Determining mixture cracking temperature for Mix 9 in Table 3.1

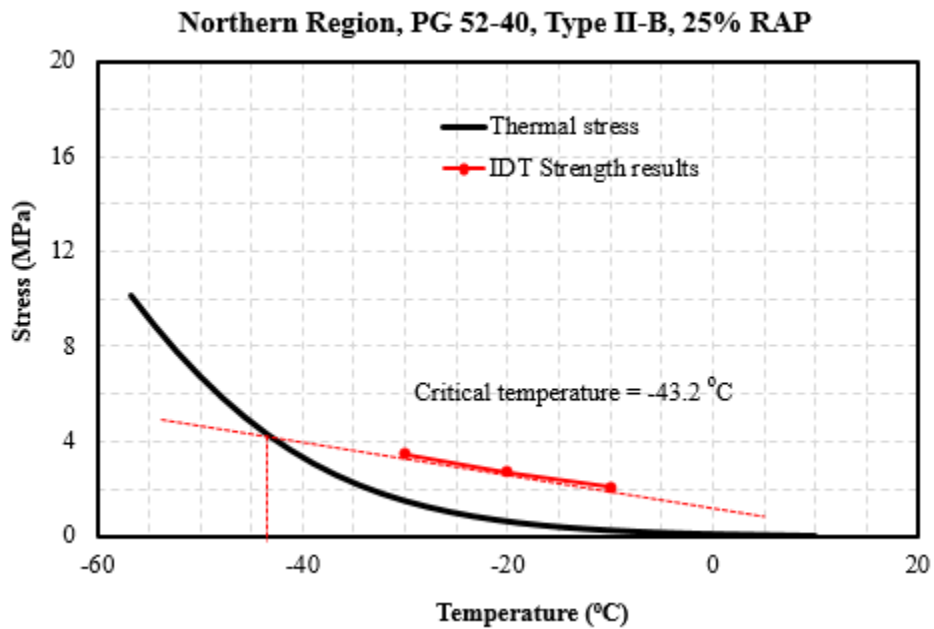


Figure 4.45 Determining mixture cracking temperature for Mix 10 in Table 3.1

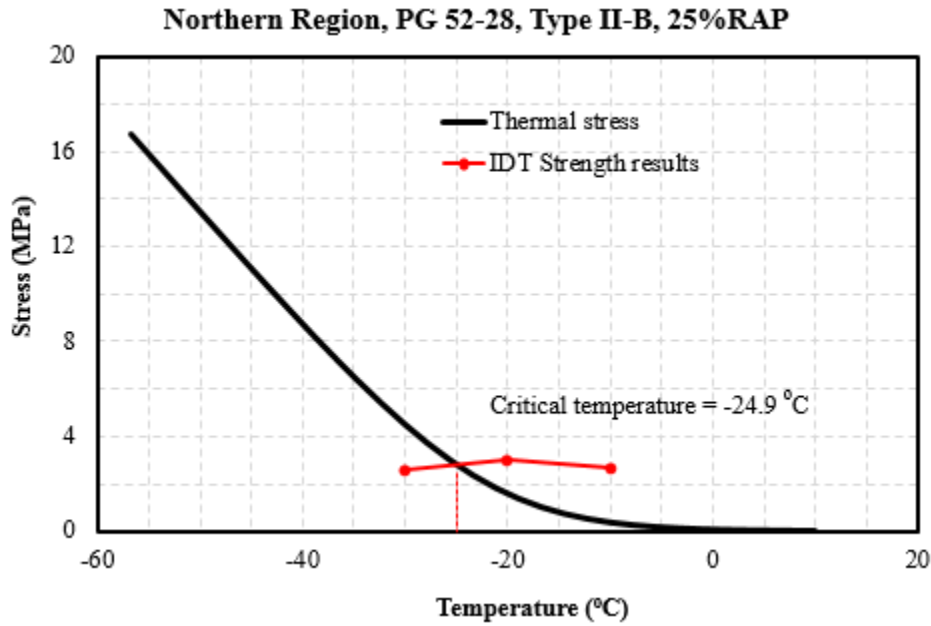


Figure 4.46 Determining mixture cracking temperature for Mix 11 in Table 3.1

Table 4.9 summarizes the cracking temperature results of all 11 mixes tested. For the Central region mixes, it can be seen that the cracking temperatures of PG 52-28 and PG 58-34 Type II-B control mixes were closer to their low-temperature grades, while the PG 58-34 binder Type II-A control mix showed a higher mixture cracking temperature than its low PG. This indicates that binder cracking may not dominate the cracking of the Type II-A mix. When RAP is added, the PG 52-28 Type II-B (35% RAP) and PG 58-34 Type II-A mixes (25% RAP) show comparable mixture cracking temperatures with their control mixes. The PG 58-34 Type II-B mix with 25% RAP showed a higher mixture cracking temperature than its control mix. These observations indicate that adding certain amounts of RAP may not affect the low-temperature performance of some mixes, while it may increase the low-temperature cracking temperature of some mixes.

Table 4.9 also shows the cracking temperature results of the Northern region mixes. For PG 52-28 mixes, the addition of 25% or 35% RAP did not affect the mixture's cracking temperature. The same phenomenon was observed on PG 52-40 mixes. These observations were consistent with those of the Central region mixes. It may contradict common sense that RAP addition generally impairs the mixture's low-temperature performance due to stiffer binder. More testing or data analyses on more mixtures should be conducted to verify these observations.

Table 4.9 Cracking temperature results of all 11 mixes

Mix #	Region	Mix type	Mix name	RAP (%)	Binder	Critical T (°C)
1	Central	Control	Type II -B	0	PG 52-28	-27.4
2		Control	Type II -B	0	PG 58-34	-36.9
3		Control	Type II -A	0	PG 58-34	-28.4
4		RAP 25	Type II -A	25	PG 58-34	-27.9
5		RAP 25	Type II -B	25	PG 58-34	-31.8
6		RAP 35	Type II -B	35	PG 52-28	-27.0
7	North	Control	Type II -B	0	PG 52-28	-23.3
8		Control	Type II -B	0	PG 52-40	-41.9
9		RAP 25	Type II -B	25	PG 52-28	-24.9
10		RAP 25	Type II -B	25	PG 52-40	-43.2
11		RAP 35	Type II -B	35	PG 52-28	-22.8

4.4 Cost Analysis

Due to a lack of necessary information, such as maintenance and environmental data, to calculate the cost of the entire life cycle of HMA containing RAP in Alaska, the cost analysis of RAP use focus was on preliminary comparison of cost in materials only. Through many phone calls and

personal communication with ADOT&PF staff and local contractors, the following assumptions were made (Table 4.10).

Table 4.10 Assumptions for the cost analysis

Items	Assumptions
Aggregate price	\$15/ton
Asphalt binder price	\$603/ton
Aggregate hauling	\$3/ton
Asphalt binder hauling	\$18/ton
RAP fractionation	\$2/ton
Markup	15%
RAP binder content	5%
Optimum binder content	6%

This cost analysis was to investigate the potential savings of using a 25% RAP mix compared with using a control mix without any RAP. Table 4.11 shows the composition of a control mix without any RAP and a 25% RAP mix. Table 4.12 organizes the calculation process. Note that RAP was considered free of charge, as typically in Alaska all contractors would use RAP collected from their old projects. It can be seen that a total savings of \$13.3/ton could be reached for a job with 25% RAP.

Table 4.11 The composition of a control mix without any RAP and with 25% RAP mix

Mix	Virgin Aggregate	Virgin Binder	RAP Aggregate	RAP Binder
Control Mix 0% RAP	94%	6%	-	-
25% RAP Mix	70.25	4.75%	23.75	1.25%

Table 4.12 Calculations

Items	Calculation	Results
Aggregate \$/ton (delivered to plant)	$(\$15+\$3)*(1+15\%)$	\$20.7/ton
Binder \$/ton (delivered to plant)	$(\$603+\$18)*(1+15\%)$	\$714.1/ton
RAP processing fee for 25% RAP mix \$/ton	$25\%*2$	\$0.5/ton
Aggregate saving for 25% RAP mix	$(94\%-70.25%)*20.7$	\$4.9/ton
Binder saving for 25% RAP mix	$(6\%-4.75%)*714.1$	\$8.9/ton
Total savings of 25% mix	$\$8.9+\$4.9-\$0.5$	\$13.3

CHAPTER 5 SUMMARIES AND CONCLUSIONS

The aim of this study was to evaluate the properties of three asphalt binders typically used in Alaska for HMA containing RAP to properly characterize the materials. The asphalt binders included one virgin binder (PG 52-28) and two modified binders (PG 52-40 and PG 58-34). Eleven HMA mixtures were either produced in the lab or collected from paving projects for laboratory performance evaluation. These materials covered two ADOT&PF regions, two mix types, RAP content up to 35%, and the three aforementioned binders. The binder tests included DSR tests for verification of binder grading, evaluation of viscoelastic behavior, master curves, MSCR tests associated with DSR setup, and BBR and DTT tests for low-temperature performance evaluation. Binder cracking temperature was determined using TSAR software and BBR and DTT data. The mixture performance tests included AMPT tests for dynamic modulus and flow number, and IDT tests for creep stiffness and low-temperature strengths. Mixture cracking temperature was determined with the IDT data. A cost analysis of a 25% RAP mix was conducted assuming Alaskan typical conditions. Based on the testing results and analyses, the following conclusions were made:

- The high-temperature grades of the three Alaskan binders were verified. The true grades of PG 52-28 binder without aging and after RTFO aging were 56.6°C and 56.9°C; the true grades of PG 52-40 binder without aging and after RTFO aging were 60.6°C and

56.4°C; the true grades of PG 58-34 binder without aging and after RTFO aging were 64.3°C and 61.4°C.

- The viscoelastic behavior of the three binders was characterized in terms of complex modulus ($|G^*|$) and phase angle (δ) data as well as their master curves. These data can be used to develop the Alaskan material library and further used in various software or models for binder or mixture characterization.
- According to the MSCR test results, all of the selected binders satisfied the nonrecoverable creep compliance (J_{nr}) standard for all traffic levels at corresponding high PG grades specified in AASHTO MP 19. The two modified binders, PG 52-40 and PG 58-34, showed significantly higher MSCR recovery rates than the unmodified PG 52-28 binder, indicating potentially higher rutting resistance under various traffic levels for modified asphalt as compared with unmodified binder with the same high PG grade.
- According to BBR results, the stiffness and m -value criteria showed similar critical low temperatures for each binder, both close to the binder's low PG grade. No noticeable difference in low critical temperature was found in short-term aged and long-term aged PG 52-40, indicating that this highly modified binder's low-temperature property may not be affected by long-term aging.
- The critical temperature determined by limiting the DTT failure strain showed questionable results. For PG 52-40, the critical low temperature could not even be determined based on DTT failure strain criteria. Note that the temperature limit of DTT

was reached, and for highly modified binder such as PG 52-40, lower testing temperature than the machine's limit should have been required. Testing on more binders should be done to evaluate DTT's ability to determine the binder's critical temperature.

- According to TSAR analyses, the binder cracking temperatures were -38.1°C , -38°C , and -35.4°C for RTFO-aged PG 52-28, PG 52-40, and PG 58-34 binders, respectively, and the binder cracking temperatures for RTFO plus PAV-aged binders were -28°C , -37°C , and -26°C . The PAV-aged cracking temperatures were found to be close to their PG low grades for PG 52-28 and PG 52-40, but an 8°C difference was found between cracking temperature and PG low grade for PG 58-34 binder. This indicates that the new TSAR method is evaluating a different property of the binder from the previous PG specification, which may be better correlated with binder cracking resistance.
- The incorporation of RAP into Alaskan HMA increased the dynamic modulus and flow number of the mixtures, which indicates that the addition of RAP may increase the rut resistance of HMA in Alaska. Typically, the higher the RAP content, the higher the increase. Only one exception was found in flow number results from one pair of mixes; the control mix and RAP mix were produced in the field and plant, respectively. The difference in production method affects the mixture's performance noticeably and contributes to the inconsistent flow number trend compared with other pairs.
- The IDT stiffness results of the Northern region mixes followed a trend, which showed that adding RAP increased the IDT creep stiffness of the mixture regardless of testing

temperature. This could potentially result in lower resistance to low-temperature cracking.

The higher the RAP content, the higher the creep stiffness. However, the three pairs of Central region mixes were interesting, in that they produced comparable results, higher stiffness in RAP mix, and higher stiffness in control mix. Note that the Central region mixes were produced with varying production parameters, such as production method and JMF, even for the same pair of mixes, which may cause unpredictable comparison.

That said, the observations based on the Northern region testing results are more reliable.

- The RAP mix and control mix in most pairs showed similar IDT strengths at low temperatures, with the exception of PG 52-28 mixes from the Northern region. In addition, the IDT strength results did not follow a general trend when temperature varied. These IDT strength data can be stored in the material library as engineering properties of all the mixes tested.
- The mixture cracking temperature was found to be close to the binder's low PG grade on some mixes, while with other mixes, the mixture cracking temperature was a little higher. This indicates that binder cracking may contribute significantly to mixture low-temperature cracking, while with some mixes, the binder may not fail before the mixture fails.
- Adding certain amounts of RAP may not affect the low-temperature performance of some mixes, but may increase the low-temperature cracking temperature of some mixes. This indicates that RAP may not impair the low-temperature performance of some Alaskan

mixes. However, RAP mixes are still questionable, as not all grouped mixes showed comparable cracking temperatures. In addition, the parameters in RAP mix production and construction that significantly contribute to low-temperature cracking are still unknown.

- According to a typical cost analysis that considered Alaskan conditions, a rough estimate of \$13.3/ton savings can be reached if 25% RAP is used in an HMA paving job in Alaska.

According to the conclusions just listed, the following recommendations are made:

- The cracking temperature of highly modified asphalt binder such as PG 52-40 was barely affected by the long-term aging process. It is recommended that the highly modified binder be further used in RAP mix for better cracking resistance.
- Recently updated binder testing methods such as MSCR and cracking temperature determination would provide more meaningful understanding about modified binder performance. Further use of these methods for binder evaluation in Alaska is recommended.
- The binder test results obtained were generally used to develop the material library in Alaska for binders that can be used in RAP mixes. It is recommended that binders of RAP mixes be extracted to compare their properties with control binders for performance evaluation.

- Mixes containing RAP will perform adequately in terms of rutting resistance according to this study. RAP mix's rutting resistance should not be concerned in Alaska.
- For Alaskan RAP mixes, low-temperature performance may not be impaired with the addition of RAP. However, low-temperature cracking concerns of RAP mixes still exist. It is recommended that more binders and mixtures be tested for a more complete evaluation of Alaskan RAP mixes in terms of the material collection and production method.
- The way virgin binder and RAP binder affect a mixture's performance (especially the low-temperature cracking performance) is still unknown. It is recommended that further research be conducted to address this issue.
- Testing efforts on more Alaskan RAP mixes are recommended to verify the conclusions drawn from this preliminary study.
- Trial sections with RAP mix and control mix included should be developed to correlate the laboratory testing results and actual field performance of RAP mixes.

REFERENCES

- Alaska Flexible Pavement Design Manual (2004). Alaska Department of Transportation and Public Facilities.
- Al-Qadi, I. L., Elseifi, M., and Carpenter, S. H. (2007). “Reclaimed Asphalt Pavement—A Literature Review.” Report No. FHWA-ICT-07-001.
- Al-Qadi, I. L., Aurangzeb, Q., Carpenter, S. H., Pine, W. J., and Trepanier, J. (2012). “Impact of High RAP Contents on Structural and Performance Properties of Asphalt Mixtures.” Report No. FHWA-ICT-12-002.
- Apeageyi, A., Diefenderfer, B., and Diefenderfer, S. (2011). “Rutting resistance of asphalt concrete mixtures that contain recycled asphalt pavement.” Transportation Research Record: Journal of the Transportation Research Board, 2208, 9–16.
- Appea, A. K., Rorrer, T., and Clark, T. (2009). “Case studies on processes involved in the production and placement of high RAP asphalt concrete mixes in 2007 on selected routes in Virginia”, In Transportation Research Board 88th Annual Meeting (No. 09-3659).
- Aurangzeb, Q., and Al-Qadi, I. (2014). “Asphalt pavements with high reclaimed asphalt pavement content: Economic and environmental perspectives.” Transportation Research Record: Journal of the Transportation Research Board, 2456, 161–169.

- Behnia, B., Ahmed, S., Dave, E., and Buttlar, W. (2010). "Fracture characterization of asphalt mixtures with reclaimed asphalt pavement." *International Journal of Pavement Research and Technology*, 3(2), 72–78.
- Bonaquist, R. (2007). "Can I Run More RAP?" *Hot Mix Asphalt Technology*, 12(5), 11–12.
- Botella, R., Perez-Jimenez, F., Miro, R., Guisado-Mateo, F., and Rodriguez, A. R. (2016). "Charaterization of Half-Warm-Mix Asphalt with High Rates of Reclaimed Asphalt Pavement." In *Transportation Research Board 95th Annual Meeting (No. 16-2599)*, Washington D.C.
- Brock, J. D., and Richmond, J. L. (2007). "Milling and Recycling." Chattanooga, TN: ASTEC, Technical Paper T-127.
- Christensen (1998). "Analysis of Creep Data from Indirect Tension Test on Asphalt Concrete." *Journal of the Association of Asphalt Paving Technologists*, 67, 485-492.
- Colbert, B., and You, Z. (2012). "The determination of mechanical performance of laboratory produced hot mix asphalt mixtures using controlled RAP and virgin aggregate size fractions." *Construction and Building Materials*, 26(1), 655–662.
- Connor, B., and Li, P. (2009). "Evaluation of the Addition of 15% Recycled Asphalt Pavement." Research Report, Alaska Transportation Research Center, AK.
- Copeland, A. (2011). "Reclaimed Asphalt Pavement in Asphalt Mixtures: State of the Practice." McLean, VA: Turner-Fairbank Highway Research Center, U.S. Department of Transportation Federal Highway Administration Report Number FHWA-HRT-11-021.

- Daniel, J., and Lachance, A. (2005). "Mechanistic and volumetric properties of asphalt mixtures with recycled asphalt pavement." *Transportation Research Record: Journal of the Transportation Research Board*, 1929, 28–36.
- FHWA. (1993). "Study of the Use of Recycled Paving Materials: A Report to Congress." FHWARD-93-417, Federal Highway Administration (FHWA), Washington, DC.
- Franke, R., and Ksaibati, K. (2014). "A methodology for cost-benefit analysis of recycled asphalt pavement (RAP) in various highway applications." *International Journal of Pavement Engineering* 16(7), 660–666.
- Hajj, E. Y., Sebaaly, P. E., and Kandiah, P. (2008). "Use of Reclaimed Asphalt Pavements (RAP) in Airfields HMA Pavements." Final Report AAPTTP Project (05-06).
- Hansen, K. R., and Newcomb, D. E. (2011). "Asphalt Pavement Mix Production Survey on Reclaimed Asphalt Pavement, Reclaimed Asphalt Shingles, and Warm-mix Asphalt Usage: 2009-2010." *Information Series*, 138, 21.
- Hansen, K. R., and Copeland, A. (2015). "Asphalt Pavement Industry Survey on Recycled Materials and Warm-Mix Asphalt Usage." *Information Series* 138.
- Hellriegel, E. J. (1980). "Bituminous Concrete Pavement Recycling." Interim Report Number FHWA/NJ-81/002 Arlington, VA: New Jersey Department of Transportation.
- Horvath, A. (2003). "Life-Cycle Environmental and Economical Assessment of Using Recycled Materials for Asphalt Pavements." Technical Report: University of California Transportation Center (UCTC), Berkeley, California.

- Howard, I. L., Cooley, L. A., and Doyle, J. D. (2009). "Laboratory Testing and Economic Analysis of High RAP Warm Mixed Asphalt." Report No. FHWA/MS-DOT-RD-09-200, James Worth Bagley College of Engineering, Mississippi State University, Civil & Environmental Engineering.
- Huang, B., Zhang, Z., and King, W. (2004). "Fatigue Crack Characteristics of HMA Mixtures Containing RAP." Proceedings, 5th International RILEM Conference on Cracking in Pavements, Limoges, France.
- Huang, B., Li, G., Vukosavljevic, D., Shu, X., and Egan, B. K. (2005). "Laboratory investigation of mixing hot-mix asphalt with reclaimed asphalt pavement." Transportation Research Record 1929, 37–45.
- Huang, B., Shu, X., and Vukosavljevic, D. (2011). "Laboratory investigation of cracking resistance of hot-mix asphalt field mixtures containing screened reclaimed asphalt pavement." Journal of Materials in Civil Engineering, 23, 1535–1543.
- Kandhal, P., and Mallick, R. B. (1997). "Pavement Recycling Guidelines for State and Local Governments—Participant's Reference Book." Report No. FHWA-SA-98-042, Federal Highway Administration, Washington, DC.
- Kandhal, P. S., Rao, S. S., Watson, D. E., and Young, B. (1995). "Performance of Recycled Hot-Mix Asphalt Mixtures in the State of Georgia." National Center for Asphalt Technology, NCAT Report 95-01, Auburn, AL.

- Kennedy, T. W., Tam, W. O., and Solaimanian, M. (1998). "Optimizing use of reclaimed asphalt pavement with the SuperPave system." *Journal of the Association of Asphalt Paving Technologists*, 67, 311–333.
- Kristjánisdóttir, Ó., Muench, S. T., Michael, L., and Burke, G. (2007). "Assessing potential for warm-mix asphalt technology adoption." *Transportation Research Record*, 2040(1), 91–99.
- Li, X., Marasteanu, M., Williams, R., and Clyne, T. (2008). "Effect of reclaimed asphalt pavement (proportion and type) and binder grade on asphalt mixtures." *Transportation Research Record: Journal of the Transportation Research Board*, 2051, 90–97.
- Maupin, G. W., Jr., Diefenderfer, S. D., and Gillespie, J. S. (2009), "Virginia's higher specification for reclaimed asphalt pavement: Performance and economic evaluation." *Transportation Research Record: Journal of the Transportation Research Board, National Academies, Washington, D.C., No. 2126*, pp. 142–149.
- McDaniel, R., and Anderson, R. M. (2001). "Recommended Use of Reclaimed Asphalt Pavement in the Superpave Mix Design Method: Technician's Manual", NCHRP Report No. 452, Transportation Research Board, Washington, D.C.
- McDaniel, R., Soleymani, H., and Shah, A. (2002). "Use of Reclaimed Asphalt Pavement (RAP) under Superpave Specification." A Regional Pooled Fund Study, West Lafayette, IN: Purdue University, Joint Transportation Research Program, Report Number FHWA/IN/JTRP-2002/6.

McDaniel, R. S., Soleymani, H., Anderson, R. M., Turner, P., and Peterson, R. (2000).

“Recommended Use of Reclaimed Asphalt Pavement in the Superpave Mix Design Method.”

NCHRP Web document, 30.

McDaniel, R. S., Shah, A., Huber, G. A., and Copeland, A. (2012). “Effects of reclaimed asphalt pavement content and virgin binder grade on properties of plant produced mixes.” *Journal of the Association of Asphalt Paving Technologists*, 81.

Mogawer, W., Bennert, T., Daniel, J. S., Bonaquist, R., Austerman, A., and Booshehrian, A.

(2012). “Performance characteristics of plant produced high RAP mixtures.” *Road Material and Pavement Design*, 13(S1), 183–207.

Morian, D., and Ramirez, L. (2016). “Economic Consideration for Asphalt Pavement Recycling Techniques.” Submitted to the 95th Annual Meeting of the Transportation Research Board, Washington D.C.

Nahar, S. N., Mohajeri, M., Schmets, A. J. M., Scarpas, A., van de Ven, M. F. C., and Schitter, G.

(2013). “First observation of the blending zone morphology at the interface of reclaimed asphalt binder and virgin bitumen.” *Transportation Research Record: Journal of the Transportation Research Board*, 2370(1), 1–9.

NAPA. (1996). “Recycling Hot Mix Asphalt Pavements, Information Series 123.” National Asphalt Pavement Association.

- Newcomb, D., Brown, E., and Epps, J. (2007). "Designing HMA Mixtures with High RAP Content: A Practical Guide, Quality Improvement Series 124." National Asphalt Pavement Association.
- Page, G. C., and Murphy, K. H. (1987). "Hot-mix recycling saves Florida DOT \$38 million." *Asphalt*, 1(1).
- Paul, H. (1996). "Evaluation of recycled projects for performance." *Asphalt Paving Technology*, 65, 231–254.
- Read, J., and Whiteoak, D. (2003). *The Shell Bitumen Handbook*. 5th ed. London: Thomas Telford.
- Saboundjian, S., and Teclemariam, S. (2010). "Performance Grade of asphalt containing RAP." Research Report, ADOT&PF, AK.
- Shah, A., McDaniel, R., Huber, G., and Gallivan, V. (2007). "Investigation of properties of plant-produced reclaimed asphalt pavement mixtures." *Transportation Research Record: Journal of the Transportation Research Board*, 1998, 103–111.
- Shirodkar, P., Mehta, Y., Nolan, A., Sonpal, K., Norton, A., Tomlinson, C., Dubois, E., Sullivan, P., and Sauber, R. (2011). "A study to determine the degree of partial blending of reclaimed asphalt pavement (RAP) binder for high RAP hot mix asphalt." *Construction and Building Materials*, 25(1), 150–155.

- Shu, X., Huang, B., and Vukosavljevic, D. (2008). "Laboratory evaluation of fatigue characteristics of recycled asphalt mixture." *Construction and Building Materials*, 22(7), 1323–1330.
- Soleymani, H. R., Anderson, M., McDaniel, R. and Abdelrahman, M. (2000). "Investigation of the black rock issue for recycled asphalt mixtures." *Journal of the Association of Asphalt Paving Technologists*, 69, 366–390.
- Stroup-Gardiner, M., and Wagner, C. (1999). "Use of reclaimed asphalt pavement in Superpave hot-mix asphalt applications." *Transportation Research Record: Journal of the Transportation Research Board*, 1681, 1–9.
- Sullivan, J. (1996). "Pavement Recycling Executive Summary and Report." Report No. FHWA-SA-95-060, Federal Highway Administration, Washington, DC.
- Tam, K. K., Joseph, P., and Lynch, D. F. (1992). "Five-year experience of low-temperature performance of recycled hot mix." *Transportation Research Record*, 1362, 56–65.
- West, R. (2009). "LTPP data shows RAP mixes perform as well as virgin mixes. *Asphalt Technology News*, 21(2).
- West, R. (2010). "Reclaimed Asphalt Pavement Management: Best Practices." Auburn, AL: National Center for Asphalt Technology, NCAT Draft Report.
- West, R. C., Rada, G. R., Willis, J. R., and Marasteanu, M. O. (2013). "Improved Mix Design, Evaluation, and Materials Management Practices for Hot Mix Asphalt with High Reclaimed Asphalt Pavement Content." *Transportation Research Board*.

- Willis, J., Turner, P., de Goes Padula, F., Tran, N., and Julian, G. (2013). "Effects of changing virgin binder grade and content on high reclaimed asphalt pavement mixture properties." *Transportation Research Record: Journal of the Transportation Research Board*, 2371, 66–73.
- Willis, J. R., Turner, P., Julian, G., Taylor, A. J., Tran, N., and Padula, F. (2012). "Effects of Changing Virgin Binder Grade and Content on RAP Mixture Properties." Auburn, AL: National Center for Asphalt Technology, Report Number NCAT, 12-03.
- Willis, R. (2015). "Effect of Recycled Materials on Pavement Life-Cycle Assessment: A Case Study." Submitted to the 94th Annual Meeting of the Transportation Research Board, Washington D.C.
- Xiao, F., and Amirghani, S. N. (2009). "Laboratory investigation of moisture damage in rubberised asphalt mixtures containing reclaimed asphalt pavement." *International Journal of Pavement Engineering*, 10(5), 319–328.
- Zaghloul, S., Holland, T. J., and El Halim, A. A. (2007) "Evaluation of the Performance of Recycled Asphalt Sections in California Environmental Zones." In *Transportation Research Board 86th Annual Meeting Compendium of Papers CDROM*.
- Zaumanis, M., and Mallick, R. B. (2014). "Review of very high-content reclaimed asphalt use in plant-produced pavements: State of the art." *International Journal of Pavement Engineering*, 16(1), 39–55.

Zhao, S., Huang, B., Shu, X., and Woods, M. E. (2015). “Quantitative characterization of binder blending: How much recycled binder is mobilized during mixing?” *Transportation Research Record: Journal of the Transportation Research Board*, (2506), 72–80.

Zhao, S., Huang, B., Shu, X., and Woods, M. E. (2016). “Quantitative evaluation of blending and diffusion in high RAP and RAS mixtures.” *Materials and Design*, 89, 1161–1170.

APPENDIX A JOB MIX FORMULAE



State of Alaska
 Department of Transportation & Public Facilities
 Central Materials Lab
 5750 East Tudor Road
 Anchorage, AK 99507
 Phone (907) 269-6200 FAX (907) 269-6201

Laboratory Report

Quality

Name: **AMATS: Ast Resurfacing: Northern Lts. To 9th Ave** Project No.: **56000 / 0527023**
 Sample: **HMA Type IIB** Item/Spec No.: **401(1B)** Field No.: **Q-ATBIIB-MD-2**
 Sampled From: **Manufacturer's Stock** Date Sampled: **07/27/2014**
 Source: **MP 78 Parks Pit (KASH)/ Cst QAP** Quantity Represented: **Source** Date Received: **07/30/2014**
 Location: **Anchorage** Submitted By: **QAP** Date Completed: **08/06/2014**
 Examined For: **Bituminous Mix Design** Date Reported: **08/06/2014**

AGGREGATE		
Blend Ratio	27:50: :13:10: :	
	CA:IA:Nf:CF:BS:MF:RP	
Blend Specific Gravity	Bulk	2.685
	Effective	2.734
Sieve	% Pass	Specs
1"		100
3/4"	100	100
1/2"	87	81-93
3/8"	76	70-82
#4	57	51-63
#8	41	35-47
#16	30	25-35
#30	22	18-26
#50	14	10-18
#100	9	6-12
#200	6.2	4.2-8.2
FA FM	2.96	
FA Angularity		
CA Absorption	0.7	2.0 max
% Fracture		
Single Face	100	80 min
% Flat / Elongated		
@ 1:3	18	
@ 1:5	2	8 max
Plastic Index	NP	4 max

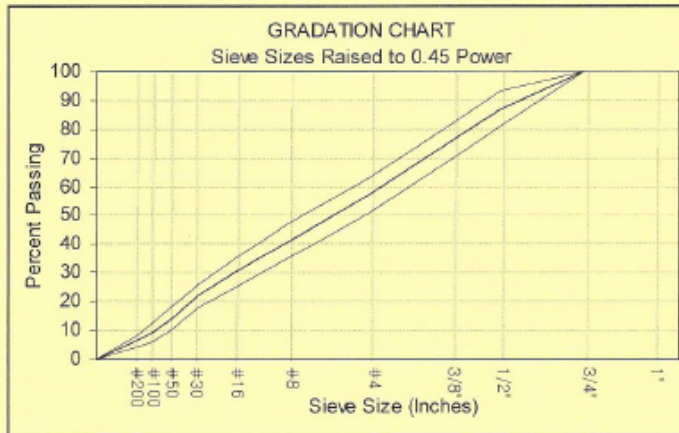
ASPHALT	
Brand & Typ	Tesoro PG 52-28
Specific Gravity	1.011
Mixing Temp. Range	277-287°F
Comp. Temp. Range	254-264°F

ANTI-STRIP ADDITIVE	
Brand & Type	Adhere 6500
Minimum Required	0.25%

ATM 417
50 Blow

Related Tests
2014A-1762
2014A-0554

ASPHALT CONTENT, %	
@ 4.0% Voids Total Mix	5.2
Approved Optimum	5.4
Specifications	5.0-5.8
PROPERTIES @ OPTIMUM	
Max. SpG (AASHTO T209)	2.504
Max. SpG Unit Wt., pcf	155.9
Voids	
Filled	78
Total Mix	3.2
In Mineral Aggregate	14.6
In Coarse Aggregate	
Stability, lbs	2330
Flow, 0.01 inches	10
Unit Weight, pcf	150.9
Dust/Asphalt Ratio	1.3
Rut Index	0.6-1.4



Remarks:

D1 The Material as Submitted Conforms to Specifications
 Yes No NA
 THE TEST RESULTS ARE ONLY REPRESENTATIVE OF THE MATERIAL AS SUBMITTED

Signature: *Newton Bingham*
 Newton J. Bingham, PE
 Regional Materials Engineer



State of Alaska
 Department of Transportation & Public Facilities
 Central Materials Lab
 5750 East Tudor Road
 Anchorage, AK 99507
 Phone (907) 269-6200 FAX (907) 269-6201

Laboratory Report

Quality

Laboratory No.: 2014A-0904

Name: W. Dowling Phase II Project No.: 51030 / 0532(008)
 Sample: ATB Type IIB Mix with 25% RAP Item/Spec No.: 306(1) Field No.: Q-ATBIIB-MD-2
 Sampled From: Manufacturer's Stock Date Sampled: 05/13/2014
 Source MP 39 Glenn Highway / AS&G Quantity Represented: Source Date Received: 05/17/2014
 Location: 11195 Lang St. / Anchorage Submitted By: Granite Const. Date Completed: 06/12/2014
 Examined For: Bituminous Mix Design Date Reported: 06/12/2014

AGGREGATE
 Blend Ratio 18:15: :42: : :25
 CA:IA:NF:CF:BS:MF:RP
 Blend Specific Gravity Bulk 2.688
 Effective 2.759

Sieve	% Pass	Specs
1"		
3/4"	100	100
1/2"	89	83-95
3/8"	78	72-84
#4	58	52-64
#8	40	34-46
#16	28	23-33
#30	20	16-24
#50	13	9-17
#100	9	6-12
#200	6.0	4.0-8.0

FA FM 3.10
 FA Angularity
 CA Absorption 0.9 2.0 max
 % Fracture
 Single Face 99 80 min
 % Flat / Elongated
 @ 1:3
 @ 1:5 4 8 max
 Plastic Index NP 4 max

ASPHALT
 Brand & Typ Denali PG 58-34
 Specific Gravity 1.007
 Mixing Temp. Range 325-335°F

ANTI-STRIP ADDITIVE
 Brand & Type Morlife 5000
 Minimum Required 0.25%

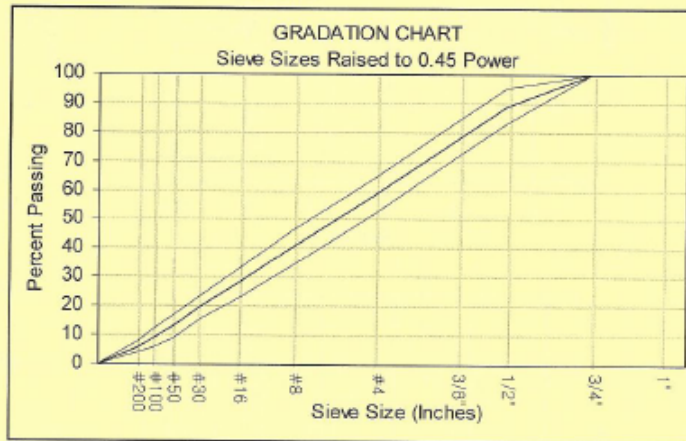
**ATM 417
 50 Blow**

Related Tests
 2014A-0826
 2014A-1163

ASPHALT CONTENT, %
 @ 4.0% Voids Total Mix 5.0
 Approved Optimum 5.3
 Specifications 4.9-5.7

PROPERTIES @ OPTIMUM Specs

Max. SpG (AASHTO T209)	2.526	
Max. SpG Unit Wt., pcf	157.2	
Voids		
Filled	78	65-78
Total Mix	3.1	3-5
In Mineral Aggregate	13.8	12.0+
In Coarse Aggregate		
Stability, lbs	3480	1200+
Flow, 0.01 inches	12	8-16
Unit Weight, pcf	152.5	
Dust/Asphalt Ratio	1.4	0.6-1.4
Rut Index		



Remarks:

D1 The Material as Submitted Conforms to Specifications
 Yes No [] NA []

THE TEST RESULTS ARE ONLY REPRESENTATIVE OF THE MATERIAL AS SUBMITTED

Signature: *Newton J. Bingham*
 Newton J. Bingham, PE
 Regional Materials Engineer

Appendix A2. JMF for PG 58-34 Type II-B Mixes in the Central Region (No. 2 and 5 in Table 3.1)



State of Alaska
Department of Transportation & Public Facilities
Central Materials Lab
 5750 East Tudor Road
 Anchorage, AK 99507
 Phone (907) 269-6200 FAX (907) 269-6201

Laboratory Report

Quality

Laboratory No.: **2015A-1242**

Name: **Lake Hood A&B Parking Rehabilitation**

Project No.: **54465 / 3-02-0013-XXX-2014**

Sample: **HMA Type IIA**

Item/Spec No.: **P-401a**

Field No.: **Q-HMAIIA-MD-1**

Sampled From: **Manufacturer's Stock**

Date Sampled: **05/26/2015**

Source: **MP 39 Glenn Highway / AS&G**

Quantity Represented: **Source**

Date Received: **05/30/2015**

Location: **Anchorage**

Submitted By: **Granite Const.**

Date Completed: **06/29/2015**

Examined For: **Bituminous Mix Design**

Date Reported: **06/29/2015**

AGGREGATE

Blend Ratio **24:26: :50: : : :**
 CA: IA: NF: CF: BS: MF: RP

Blend Specific Gravity Bulk **2.709**
 Effective **2.761**

Sieve	% Pass	Specs
1"		
3/4"	100	100
1/2"	85	79-91
3/8"	71	65-77
#4	49	43-55
#8	34	28-40
#16	22	17-27
#30	15	11-19
#50	10	6-14
#100	7	4-10
#200	5.0	3.0-7.0

FA FM **3.20**
 FA Angularity
 CA Absorption **0.7** 2.0 max
 % Fracture
 Double Face **99** 90 min
 % Flat / Elongated
 @ 1:3 **16**
 @ 1:5 **2** 8 max
 Plastic Index **NP** 6 max

ASPHALT

Brand & Typ **Denall PG 58-34**
 Specific Gravity **1.007**
 Mixing Temp. Range **325-335°F**
 Comp. Temp. Range **305-315°F**

ANTI-STRIP ADDITIVE

Brand & Type **Morelife 5000**
 Minimum Required **0.25%**

ATM 417
75 Blow

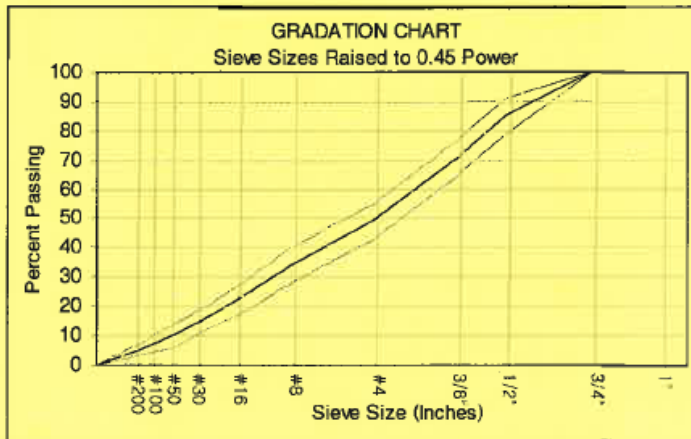
Related Tests
2015A-1243
2015A-1195

ASPHALT CONTENT, %

@ 4.0% Voids Total Mix **5.2**
 Approved Optimum **5.3**
 Specifications **4.9-5.7**

PROPERTIES @ OPTIMUM

Property	Value	Specs
Max. SpG (AASHTO T209)	2.528	
Max. SpG Unit Wt., pcf	157.4	
Voids		
Filled	75	
Total Mix	3.8	2.8-4.2
In Mineral Aggregate	15.0	13.0+
In Coarse Aggregate		
Stability, lbs	3210	2150+
Flow, 0.01 inches	12	10-14
Unit Weight, pcf	151.4	
Dust/Asphalt Ratio	1.1	
Rut Index		



Remarks:

D9 The Material as Submitted Conforms to Specifications
 Yes No [] NA []

THE TEST RESULTS ARE ONLY REPRESENTATIVE OF THE MATERIAL AS SUBMITTED

Signature: *Newton Bingham*
 Newton J. Bingham, PE
 Regional Materials Engineer



State of Alaska
Department of Transportation & Public Facilities
Central Materials Lab
 5750 East Tudor Road
 Anchorage, AK 99507
 Phone (907) 269-6200 FAX (907) 269-6201

Laboratory Report

Quality

Name: **AIA 7L/25R Runway Rehabilitation**
 Sample: **HMA Type IIA Mix Design**
 Sampled From: **Manufacturer's Stock**
 Source: **MP 39 Glenn Highway / AS&G**
 Location: **Anchorage**
 Examined For: **Bituminous Mix Design**

Project No.: **53598 / AIP 3-02-0018-171-2014**
 Item/Spec No.: **P-401a(2).n1**
 Field No.: **Q-HMAIIA-MD-1**
 Quantity Represented: **Source**
 Submitted By: **Granite Const.**

Laboratory No.: **2014A-1207**
 Date Sampled: **06/17/2014**
 Date Received: **06/25/2014**
 Date Completed: **07/09/2014**
 Date Reported: **07/10/2014**

AGGREGATE
 Blend Ratio **18:15: :42: : :25**
 CA:IA:NF:CF:BS:MF:RP
 Blend Specific Gravity Bulk **2.707**
 Effective **2.755**

Sieve	% Pass	Specs
1"		
3/4"	100	100
1/2"	89	83-95
3/8"	78	72-84
#4	58	52-64
#8	40	34-46
#16	28	23-33
#30	20	16-24
#50	13	9-17
#100	9	6-12
#200	6.0	4.0-8.0
FA FM	3.10	
FA Angularity		
CA Absorption	0.8	2.0 max
% Fracture Double Face	100	90 min
% Flat / Elongated @ 1.3	20	
@ 1.5	1	8 max
Plastic Index	NP	6 max

ASPHALT
 Brand & Typ **Denali PG 58-34**
 Specific Gravity **1.007**
 Mixing Temp. Range **325-335°F**
 Comp Temp Range **305-315°F**

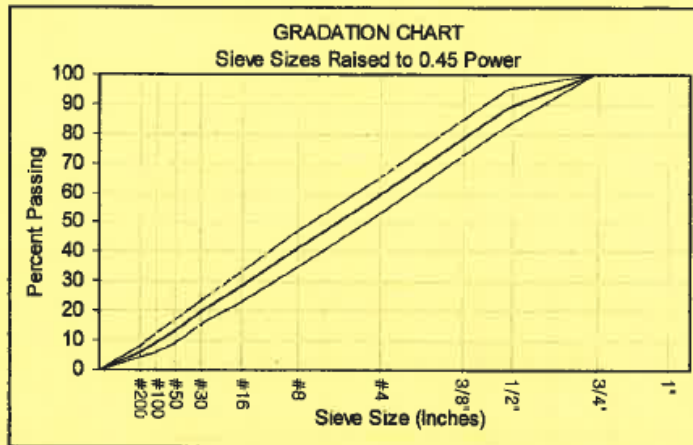
ANTI-STRIP ADDITIVE
 Brand & Type **Morlife 5000**
 Minimum Required **0.25%**

**ATM 417
75 Blow**

Related Tests
2014A-1294
2014A-1163

ASPHALT CONTENT, %
 @ 4.0% Voids Total Mix **4.7**
 Approved Optimum **5.0**
 Specifications **4.6-5.4**

PROPERTIES @ OPTIMUM	Specs
Max. SpG (AASHTO T209)	2.535
Max. SpG Unit Wt., pcf	157.8
Voids Filled	77
Total Mix	3.1 2.8-4.2
In Mineral Aggregate	13.8 13.0+
In Coarse Aggregate	
Stability, lbs	3920 2150+
Flow, 0.01 inches	11 10-14
Unit Weight, pcf	152.9
Dust/Asphalt Ratio	1.4 0.6-1.4
Rut Index	



Remarks

Not for transfer.

D9 The Material as Submitted Conforms to Specifications
 Yes No NA

THE TEST RESULTS ARE ONLY REPRESENTATIVE OF THE MATERIAL AS SUBMITTED

Signature: *Newton J. Bingham*
 Newton J. Bingham, PE
 Regional Materials Engineer

Appendix A4. JMF for PG 58-34 Type II-A Mix with 25% RAP in the Central Region (No. 4 in Table 3.1)

STATE OF ALASKA - NORTHERN REGION
 DEPARTMENT OF TRANSPORTATION AND PUBLIC FACILITIES
 BITUMINOUS MIX DESIGN MARSHALL METHOD RECEIVED:
 2301 PEGER ROAD
 FAIRBANKS, AK 99709

PROJECT NAME: North Pole Homestead Rd/NPHS
 PROJECT NUMBER: HPP-STP-HPRM-0002(193)63025
 GENERAL CONTRACTOR: **Exclusive**

REGIONAL LAB #: 09-340
 FIELD #: HMA-MD-1
 TYPE/CLASS: II B

AGGREGATE SOURCE: Twin Rich Pit
 AGGREGATE QUALITY#: 06-142
 BLEND RATIO: **16:14:70 CA:INT:FA**
 BLENDED BULK SPG: 2.679
 EFFECTIVE SPG: 2.719

BINDER SOURCE: Emulsion Products
 BINDER GRADE: **52-28**
 BINDER SPG: 1.0087
 ANTISTRIP: .25% Morlife

MIX DESIGN PARAMETERS	
STABILITY	1200
FLOW	8-16
VOIDS TOTAL MIX	3-5
COMPACTION, BLOWS	50
VOIDS FILLED	65-78
VMA	12
DUST ASPHALT RATIO	.6-1.4

MIXING TEMP (DEG F) 281-290
 COMPACTING TEMP (DEG F) 264-271

MARSHALL RESULTS	
% ASPHALT @ MAX UNIT WT	6
% ASPHALT @ MAX STABILITY	5.5
% ASPHALT @ 4% VOIDS	5.1
OPTIMUM OIL CONTENT = 5.2 %	
STABILITY	2200
FLOW	9
VOIDS TOTAL MIX	3.6
VOIDS FILLED	76
VMA	14.7
MTD/RICE	2.499
UNIT WEIGHT	150.3
DUST ASPHALT RATIO	1.3

APPROVED:



AGGREGATE DESIGN PARAMETERS			
		Reg Lab	Spec
FLAT & ELONGATED		1.3	8max
LIQUID LIMIT		NV	
PLASTIC INDEX		NP	
FINENESS MODULUS			
UNCOMP. VOID -T304			
SAND EQUIVALENT			
FRACTURE:	Single Face	98	
	Double Face	94	90min
SIEVE SIZE	PROPOSED GRADATION	MIX DESIGN SPEC BAND	
		LSL	HSL
1"		---	---
3/4"		100	---
1/2"	90	84	96
3/8"	79	73	85
#4	52	46	58
#8	36	30	42
#10		---	---
#16	26	21	31
#20		---	---
#30	19	15	23
#40		---	---
#50	15	11	19
#60		---	---
#80		---	---
#100	9	6	12
#200	6.2	4.2	8.2

REMARKS:

Approved for 63025

Appendix A5. JMF for PG 52-28 Mixes in the Northern Region (No. 7, 9 and 11 in Table 3.1)

STATE OF ALASKA - NORTHERN REGION
DEPARTMENT OF TRANSPORTATION AND PUBLIC FACILITIES
BITUMINOUS MIX DESIGN MARSHALL METHOD
2301 PEGER ROAD
FAIRBANKS, AK 99709

PROJECT NAME: Nordale Rd Pavement Rehabilitation REGIONAL LAB #: 10-241
PROJECT NUMBER: STP-0653(6) / 63158 FIELD #: NR-HMA-MD-1
GENERAL CONTRACTOR: **Exclusive** TYPE/CLASS: II/B
RECEIVED: 7/19/2010

AGGREGATE SOURCE: Coarse, Fines: Van Horn Pit; Intermed.: Delta Sand & Gravel
AGGREGATE QUALITY#: Van Horn Pit: 08-047; Delta Sand & Gravel: 10-071
BLEND RATIO: 18:15:67 / Coarse:Intermed:Fines
BLENDED BULK SPG: 2.674
EFFECTIVE SPG: 2.728

= Tanana Valley alluvial agg

BINDER SOURCE: Emulsion Products Company
BINDER GRADE: **PG 52-40**
BINDER SPG: 0.990
ANTISTRIP: More Life 5000 at 0.25%

MIX DESIGN PARAMETERS	
STABILITY	1200 min
FLOW	8-16
VOIDS TOTAL MIX	3-5
COMPACTION, BLOWS	50
VOIDS FILLED	65-78
VMA	12 min
DUST ASPHALT RATIO	0.6-1.4

MIX DESIGN TEMPERATURES:
MIXING TEMP (°F) 336
COMPACTING TEMP (°F) 311

MARSHALL RESULTS	
% ASPHALT @ MAX UNIT WT	5.7
% ASPHALT @ MAX STABILITY	5.5
% ASPHALT @ 4% VOIDS	5.0
OPTIMUM OIL CONTENT = 5.0 %	
STABILITY	3240
FLOW	11
VOIDS TOTAL MIX	3.9
VOIDS FILLED	73
VMA	14.4
MTD/RICE	2.508
UNIT WEIGHT	150.4
DUST ASPHALT RATIO	1.4

AGGREGATE DESIGN PARAMETERS			
		Reg Lab	Spec
FLAT & ELONGATED		0	0-8
LIQUID LIMIT		NV	
PLASTIC INDEX		NP	
FINENESS MODULUS			
UNCOMP. VOID -T304		0	
SAND EQUIVALENT		0	
FRACTURE: Single Face		93	
Double Face		89	90-100
SIEVE SIZE	PROPOSED GRADATION	MIX DESIGN SPEC BAND	
		LSL	HSL
1"		---	---
3/4"	100	100	---
1/2"	89	83	95
3/8"	79	73	85
#4	55	49	61
#8	37	31	43
#10		---	---
#16	24	19	29
#20		---	---
#30	18	14	22
#40		---	---
#50	12	8	16
#60		---	---
#80		---	---
#100	9	6	12
#200	6.0	4	8

REMARKS: Approved for 63159
* APPROVE NO COST
cc: if prop. FWD'S
is needed
.. may need to work
Buy house times if
mix too firm

APPROVED: 
Northern Region Materials Engineer 8-9-10

Appendix A6. JMF for PG 52-40 Mixes in the Northern Region (No. 8 and 10 in Table 3.1)

APPENDIX B AIR VOIDS OF SPECIMENS

Appendix B1. G_{mm} of all the mixes

Mix #	Field or Lab	Sample #	Dry Weight (g)	Bucket in water (g)	Bucket & sample in water (g)	G_{mm}	Ave.	Std.
1	Field	-	-	-	-	2.504	2.504	-
2	Lab	A	1514.5	1473.2	2379.1	2.488	2.492	0.0052
		B	1511.3	1473.2	2377.3	2.489		
		C	1538.3	1473.2	2395.6	2.498		
3	Field	-	-	-	-	2.528	2.528	-
4	Field	-	-	-	-	2.535	2.535	-
5	Field	-	-	-	-	2.526	2.526	-
6	Lab	A	1506.1	1473.2	2378.9	2.508	2.504	0.0050
		B	1500.7	1473.2	2374.5	2.504		
		C	1507.6	1473.2	2377.4	2.499		
7	Lab	A	1500.3	1484.8	2370.8	2.442	2.453	0.0097
		B	1500.5	1484.8	2375.6	2.461		
		C	1511.2	1484.8	2380.6	2.456		
8	Lab	A	1502.7	1484.8	2374.2	2.450	2.450	0.0044
		B	1500.4	1484.8	2374.8	2.458		
		C	1510.6	1484.8	2377	2.443		
9	Lab	A	1500.2	1484.8	2372	2.447	2.452	0.0052
		B	1500.1	1484.8	2374	2.456		
		C	1504.2	1484.8	2376.1	2.454		
10	Lab	A	1507.1	1484.8	2374.5	2.441	2.445	0.0077
		B	1506.4	1484.8	2374.9	2.444		
		C	1509.6	1484.8	2378	2.449		
11	Lab	A	1500.9	1484.8	2377.2	2.467	2.461	0.0040
		B	1501.9	1484.8	2376	2.459		
		C	1504.8	1484.8	2377	2.456		

Appendix B2. Air voids of the AMPT samples for Central Region Mixes

Mix #	Sample #	Dry Weight (g)	Weight in water (g)	Saturated Surface Dry (SSD) Weight (g)	G_{mb}	G_{mm}	Air Voids
1	A	2838.5	1629.6	2848	2.330	2.504	6.96%
	B	2789.7	1596.8	2793.5	2.331	2.504	6.90%
	C	2811.1	1613	2815.4	2.338	2.504	6.63%
2	A	2788.5	1592.3	2791.5	2.325	2.492	6.68%
	B	2828.9	1619	2834.2	2.328	2.492	6.57%
	C	2813.6	1610.8	2819.8	2.327	2.492	6.60%
3	A	2828.1	1633.7	2833.1	2.358	2.528	6.73%
	B	2816.9	1623.6	2819.8	2.355	2.528	6.85%
	C	2850.7	1652.8	2860.4	2.361	2.528	6.62%
4	A	2845	1645.1	2847.6	2.366	2.535	6.67%
	B	2812.1	1615.8	2814.8	2.345	2.535	7.48%
	C	2861.7	1645.3	2863.9	2.348	2.535	7.36%
5	A	2821	1617.7	2823.1	2.340	2.526	7.35%
	B	2827	1623.6	2829.2	2.345	2.526	7.17%
	C	2882.8	1662.4	2884	2.360	2.526	6.58%
6	A	2826.9	1610.7	2828.9	2.321	2.504	7.33%
	B	2769	1583.4	2772.8	2.328	2.504	7.03%
	C	2797.4	1602.3	2800.7	2.334	2.504	6.78%

Appendix B3. Air voids of the AMPT samples for Northern Region Mixes

Mix #	Sample #	Dry Weight (g)	Weight in water (g)	Saturated Surface Dry (SSD) Weight (g)	G_{mb}	G_{mm}	Air Voids
7	A	2747.4	1554.5	2765.5	2.269	2.453	7.49%
	B	2756	1558.9	2772.1	2.272	2.453	7.37%
	C	2731.4	1542.9	2743.9	2.274	2.453	7.27%
8	A	2715.1	1534.6	2732.7	2.266	2.450	7.52%
	B	2707.5	1529.2	2722.1	2.270	2.450	7.37%
	C	2732.7	1549.1	2748.7	2.278	2.450	7.03%
9	A	2752.4	1559.6	2770.6	2.273	2.452	7.32%
	B	2751	1562.6	2770.3	2.278	2.452	7.11%
	C	2752.6	1558	2770.8	2.270	2.452	7.45%
10	A	2743.3	1552.5	2764.1	2.264	2.445	7.39%
	B	2820	1597.1	2830.5	2.286	2.445	6.48%
	C	2743.2	1557.5	2765.6	2.271	2.445	7.12%
11	A	2772.7	1582.9	2796.9	2.284	2.461	7.19%
	B	2761.3	1566.4	2777.3	2.280	2.461	7.33%
	C	2788.8	1586	2798.8	2.299	2.461	6.55%

Appendix B4. Air voids of the IDT samples for Central Region Mixes

Mix #	Sample #	Dry Weight (g)	Weight in water (g)	Saturated Surface Dry (SSD) Weight (g)	G _{mb}	G _{mm}	Air Voids	Creep Test	IDT Strength Test Temperature (°C)
1	A	2038	1178.5	2052.8	2.331	2.504	6.91%	Yes	-10 °C
1	B	2057.7	1183.1	2069.9	2.320	2.504	7.33%	-	-10 °C
1	C	2030.7	1169	2045.6	2.317	2.504	7.49%	-	-10 °C
1	D	1979.8	1132.2	1985	2.322	2.504	7.29%	-	-20 °C
1	E	2019.1	1164.6	2034.7	2.321	2.504	7.33%	Yes	-20 °C
1	F	2043.2	1175.8	2057.8	2.317	2.504	7.49%	-	-20 °C
1	G	2140.1	1231.5	2153.4	2.321	2.504	7.29%	Yes	-30 °C
1	H	2080	1195.2	2092.8	2.317	2.504	7.46%	Yes	-30 °C
1	I	2028.6	1169.2	2044.7	2.317	2.504	7.47%	-	-30 °C
2	A	2069.9	1190.2	2079.1	2.329	2.492	6.55%	-	-10 °C
2	B	1994.6	1144.1	2001.5	2.326	2.492	6.64%	Yes	-10 °C
2	C	2087.2	1191.5	2096.3	2.307	2.492	7.42%	-	-10 °C
2	D	2072.6	1194.3	2084.8	2.327	2.492	6.59%	-	-20 °C
2	E	2015.9	1160.1	2026.6	2.326	2.492	6.63%	-	-20 °C
2	F	2030.2	1171.5	2049.6	2.312	2.492	7.21%	Yes	-20 °C
2	G	2140.1	1236.7	2155.9	2.328	2.492	6.56%	-	-30 °C
2	H	2050.8	1184	2066.5	2.324	2.492	6.74%	Yes	-30 °C
2	I	2028.5	1169.1	2042.3	2.323	2.492	6.77%	Yes	-30 °C
3	A	2104.9	1226.1	2118	2.360	2.528	6.64%	-	-10 °C
3	B	2067.4	1194.2	2076.9	2.342	2.528	7.35%	Yes	-10 °C
3	C	2071.3	1198.1	2083.7	2.339	2.528	7.48%	-	-10 °C
3	D	2098.8	1216.5	2108.4	2.353	2.528	6.92%	Yes	-20 °C
3	E	2106.7	1217.1	2116.4	2.343	2.528	7.33%	Yes	-20 °C
3	F	2042.6	1178.7	2051.9	2.339	2.528	7.47%	-	-20 °C
3	G	2016.3	1174.6	2030.4	2.356	2.528	6.80%	-	-30 °C
3	H	2074.8	1200.8	2086.7	2.342	2.528	7.36%	Yes	-30 °C
3	I	2074.7	1203.6	2089.9	2.341	2.528	7.40%	-	-30 °C
4	A	2073.7	1207.2	2082.5	2.369	2.535	6.54%	-	-10 °C
4	B	2069.2	1202	2083.1	2.348	2.535	7.36%	Yes	-10 °C
4	C	2069.3	1195.5	2078.1	2.345	2.535	7.51%	-	-10 °C
4	D	2060.2	1194.6	2070	2.353	2.535	7.16%	-	-20 °C
4	E	2044.3	1183.8	2053.8	2.350	2.535	7.31%	Yes	-20 °C
4	F	2049.5	1183.8	2057.1	2.347	2.535	7.42%	-	-20 °C
4	G	2101.9	1219.4	2109.2	2.362	2.535	6.82%	Yes	-30 °C
4	H	2027.7	1172.8	2036.4	2.348	2.535	7.38%	Yes	-30 °C
4	I	2099.2	1223.2	2117.5	2.347	2.535	7.40%	-	-30 °C
5	A	2129.3	1233.8	2136.4	2.359	2.526	6.61%	-	-10 °C
5	B	2053.3	1182.1	2059.6	2.340	2.526	7.37%	Yes	-10 °C
5	C	2075	1194.7	2082.6	2.337	2.526	7.48%	-	-10 °C
5	D	2081.3	1207.4	2093	2.350	2.526	6.96%	-	-20 °C
5	E	2022.9	1166.7	2028.4	2.348	2.526	7.06%	Yes	-20 °C
5	F	2052.1	1180.5	2058.3	2.338	2.526	7.45%	-	-20 °C
5	G	2126	1233.9	2135.7	2.358	2.526	6.67%	Yes	-30 °C
5	H	2127.3	1223.7	2133	2.339	2.526	7.38%	Yes	-30 °C
5	I	2121.9	1218.2	2125.5	2.339	2.526	7.41%	-	-30 °C
6	A	2036.9	1169.3	2040.4	2.338	2.504	6.60%	-	-10 °C
6	B	2069.2	1192.5	2079.6	2.333	2.504	6.83%	Yes	-10 °C
6	C	2009	1149.8	2016.6	2.318	2.504	7.42%	-	-10 °C
6	D	2077.2	1192.8	2082.9	2.334	2.504	6.79%	-	-20 °C
6	E	2040.5	1173.6	2048.2	2.333	2.504	6.81%	-	-20 °C
6	F	2116.8	1211	2124.3	2.318	2.504	7.42%	Yes	-20 °C
6	G	2123.4	1221.6	2131.5	2.334	2.504	6.79%	Yes	-30 °C
6	H	2056.3	1182.7	2066.5	2.327	2.504	7.07%	Yes	-30 °C
6	I	2080.7	1191.2	2088.1	2.320	2.504	7.34%	-	-30 °C

Appendix B5. Air voids of the IDT samples for Northern Region Mixes

Mix #	Sample #	Dry Weight (g)	Weight in water (g)	Saturated Surface Dry (SSD) Weight (g)	G _{mb}	G _{mm}	Air Voids	Creep Test	IDT Strength Test Temperature (°C)
7	A	1994.1	1138.1	2009.1	2.289	2.453	6.65%	Yes	-10 °C
7	B	2027.8	1153.8	2044.4	2.277	2.453	7.16%	-	-10 °C
7	C	1983.8	1121.9	1996.5	2.268	2.453	7.51%	-	-10 °C
7	D	2048.9	1164.1	2061.1	2.284	2.453	6.86%	Yes	-20 °C
7	E	1968.5	1120.0	1982.7	2.282	2.453	6.96%	Yes	-20 °C
7	F	2078.5	1184.9	2100.4	2.270	2.453	7.43%	-	-20 °C
7	G	2126.6	1213.4	2143.3	2.287	2.453	6.75%	Yes	-30 °C
7	H	2072.1	1177.7	2089.7	2.272	2.453	7.36%	-	-30 °C
7	I	2032.2	1153.6	2049.1	2.269	2.453	7.47%	-	-30 °C
8	A	2046.7	1174.3	2068.8	2.288	2.450	6.62%	Yes	-10 °C
8	B	2080.9	1181.3	2097.9	2.270	2.450	7.35%	-	-10 °C
8	C	2147.7	1222.6	2168.2	2.271	2.450	7.31%	-	-10 °C
8	D	2043.7	1170.8	2065.4	2.284	2.450	6.77%	Yes	-20 °C
8	E	1983.3	1130.6	2001.7	2.277	2.450	7.08%	Yes	-20 °C
8	F	1926.3	1096.7	1943.5	2.275	2.450	7.16%	-	-20 °C
8	G	2000.4	1141.2	2016.0	2.287	2.450	6.68%	Yes	-30 °C
8	H	2020.0	1152.3	2040.7	2.274	2.450	7.21%	-	-30 °C
8	I	2068.1	1179.1	2090.2	2.270	2.450	7.36%	-	-30 °C
9	A	2094.4	1194.6	2112.7	2.281	2.452	6.98%	-	-10 °C
9	B	2230.9	1272.1	2254.3	2.271	2.452	7.38%	Yes	-10 °C
9	C	1970.6	1120.0	1988.3	2.269	2.452	7.46%	-	-10 °C
9	D	2075.2	1183.6	2094.7	2.278	2.452	7.12%	Yes	-20 °C
9	E	1853.6	1059.5	1874.3	2.275	2.452	7.24%	Yes	-20 °C
9	F	1957.0	1111.4	1973.4	2.270	2.452	7.42%	-	-20 °C
9	G	2103.6	1200.6	2123.8	2.279	2.452	7.09%	Yes	-30 °C
9	H	2068.5	1181.6	2092.4	2.271	2.452	7.39%	-	-30 °C
9	I	2000.5	1141.7	2022.8	2.270	2.452	7.42%	-	-30 °C
10	A	1893.7	1086.2	1917.0	2.279	2.445	6.77%	Yes	-10 °C
10	B	1960.1	1118.6	1983.4	2.267	2.445	7.29%	-	-10 °C
10	C	2022.4	1149.2	2043.8	2.261	2.445	7.53%	-	-10 °C
10	D	2103.4	1197.2	2124.4	2.269	2.445	7.21%	Yes	-20 °C
10	E	1931.3	1106.7	1959.5	2.265	2.445	7.37%	Yes	-20 °C
10	F	2006.7	1138.9	2026.2	2.262	2.445	7.49%	-	-20 °C
10	G	1998.8	1139.4	2019.9	2.270	2.445	7.15%	Yes	-30 °C
10	H	2040.3	1160.0	2060.8	2.265	2.445	7.35%	-	-30 °C
10	I	1951.4	1105.4	1968.0	2.262	2.445	7.47%	-	-30 °C
11	A	2052.3	1173.8	2068.6	2.294	2.461	6.79%	Yes	-10 °C
11	B	2027.2	1157.8	2045.5	2.284	2.461	7.20%	-	-10 °C
11	C	2014.4	1152.6	2036.8	2.278	2.461	7.42%	-	-10 °C
11	D	1921.3	1096.1	1934.7	2.291	2.461	6.90%	Yes	-20 °C
11	E	2070.9	1183.3	2089.7	2.285	2.461	7.15%	-	-20 °C
11	F	2099.5	1194.4	2115.7	2.279	2.461	7.39%	-	-20 °C
11	G	2030.6	1159.9	2045.4	2.293	2.461	6.81%	Yes	-30 °C
11	H	2082.1	1186.8	2099.0	2.283	2.461	7.24%	-	-30 °C
11	I	2059.4	1176.7	2080.2	2.279	2.461	7.37%	Yes	-30 °C

APPENDIX C BINDER TESTING RESULTS

Appendix C1. High continuous grading temperature for PG 52-28

Condition	Test Method	Specification Criteria	Test Results at T ₁		Test Results at T ₂		T _c (°C)	Mean (°C)
			T1 (°C)	P1 (kPa)	T2 (°C)	P2 (kPa)		
Original 1	D7175	G* /sinδ, kPa, ≥1.00	52	2.00335655	58	0.8166889	56.6459897	56.5796451
Original 2				9		5	8	
Original 3				1.91302789		0.8104266	56.5316174	
RTFOT 1		1		7		56.5613283		
RTFOT 2		1.92324691		0.8136049		56.5613283		
RTFOT 3		7		1		3		
RTFOT 1	G* /sinδ, kPa, ≥2.20	52	58	4.30748808	1.8461065	56.7580540	56.8991693	
RTFOT 2				4	2	2		
RTFOT 3				4.36887465	1.9053689	56.9604010		
	4			5	5			
	4.53747317			1.8965190	56.9790528			
	1			5	5			

Appendix C2. High continuous grading temperature for PG 52-40

Condition	Test Method	Specification Criteria	Test Results at T ₁		Test Results at T ₂		T _c (°C)	Mean (°C)
			T1 (°C)	P1 (kPa)	T2 (°C)	P2 (kPa)		
Original 1	D7175	G* /sinδ, kPa, ≥1.00	52	1.96687973	58	1.25328709	61.0057308	60.6180508
Original 2				3		7	60.0456673	
Original 3				1.81484227		1.16362113	60.0456673	
RTFOT 1		8		1.23215575		60.8027543		
RTFOT 2		1.9264517		1		7		
RTFOT 3		3.23282700		1.98765664		56.7479335		
RTFOT 1	G* /sinδ, kPa, ≥2.20	52	58	3.04726457	1.91961438	56.2299008	56.3917195	
RTFOT 2				4	8	9		
RTFOT 3				3.03466063	1.91614963	56.1973243		
	3			5	2			

Appendix C3. High continuous grading temperature for PG 58-34

Condition	Test Method	Specification Criteria	Test Results at T ₁		Test Results at T ₂		T _c (°C)	Mean (°C)
			T1 (°C)	P1 (kPa)	T2 (°C)	P2 (kPa)		
Original 1	D7175	G* /sinδ, kPa, ≥1.00	58	1.82218953	64	1.11864060	65.3786	64.2973443
Original 2				2		1	7	
Original 3				1.35002888		0.81204518	61.5425	
RTFOT 1		4		6		3		
RTFOT 2		1.79540250		1.15569463		65.9708		
RTFOT 3		6		7		4		
RTFOT 1	G* /sinδ, kPa, ≥2.20	58	64	2.85573854	1.72950288	61.1211	61.4040502	
RTFOT 2				1	1	4		
RTFOT 3				2.99608526	1.80258430	61.6472		
	2			1	1			
	2.94550424			1.77153932	61.4438			
	4			3				

Appendix C4. Dynamic shear modulus and phase angle at 10 rad/s for PG 52-28

T (°C)	Sample	G* (kPa)	δ(rad)
46	1	10.364	1.459606
	2	10.57064	1.455125
	3	10.66998	1.456206
	mean	10.53487	1.456979
52	1	4.293722	1.490827
	2	4.354413	1.48941
	3	4.523716	1.492905
	mean	4.390617	1.491047
58	1	1.843051	1.513251
	2	1.902683	1.517688
	3	1.893257	1.512134
	mean	1.879663	1.514358

Appendix C5. Dynamic shear modulus and phase angle at 10 rad/s for PG 52-40

T (°C)	Sample	G* (kPa)	δ(rad)
46	1	4.3809131	1.0499515
	2	4.3585892	1.0496582
	3	4.3289722	1.0430544
	mean	4.3561582	1.0475547
52	1	2.7679957	1.0278985
	2	2.6067988	1.0264295
	3	2.5897104	1.02243
	mean	2.654835	1.025586
58	1	1.6859267	1.0125743
	2	1.6334822	1.0177777
	3	1.6202237	1.0076174
	mean	1.6465442	1.0126565

Appendix C6. Dynamic shear modulus and phase angle at 10 rad/s for PG 58-34

T (°C)	Sample	G* (kPa)	δ(rad)
52	1	4.571312722	1.088478688
	2	4.284390272	1.101075918
	3	4.655802831	1.094854255
	mean	4.503835275	1.094802954
58	1	2.505992817	1.070684202
	2	2.648244702	1.084140227
	3	2.603536057	1.084140227
	mean	2.585924525	1.079654885
64	1	1.509863901	1.061329281
	2	1.571559735	1.058940484
	3	1.552611027	1.068375057
	mean	1.544678221	1.062881607

Appendix C7. Master curve test data of RTFO Aged PG 52-28

Meas. Pts.	Angular Frequency	Storage Modulus	Loss Modulus	Damping Factor	Complex Viscosity	Dynamic Modulus	Phase Angle
	[rad/s]	[Pa]	[Pa]	[1]	[Pa-s]	[Pa]	[Degree]
1	0.000644	1.61E-01	2.51E+01	156	3.90E+04	2.51E+01	89.63249
2	0.00139	5.37E-01	5.26E+01	97.9	3.79E+04	5.26E+01	89.41508
3	0.00299	2.00E+00	1.10E+02	55.1	3.69E+04	1.10E+02	88.95837
4	0.00449	4.07E+00	1.63E+02	40	3.64E+04	1.63E+02	88.56966
5	0.00644	7.47E+00	2.31E+02	30.9	3.59E+04	2.31E+02	88.14783
6	0.00966	1.42E+01	3.41E+02	24.1	3.53E+04	3.41E+02	87.61545
7	0.0139	2.41E+01	4.82E+02	20	3.48E+04	4.83E+02	87.13759
8	0.0208	4.26E+01	7.11E+02	16.7	3.42E+04	7.12E+02	86.57119
9	0.0299	6.91E+01	1.00E+03	14.5	3.36E+04	1.00E+03	86.04715
10	0.0442	1.15E+02	1.46E+03	12.6	3.30E+04	1.46E+03	85.49628
11	0.0449	1.17E+02	1.47E+03	12.6	3.30E+04	1.47E+03	85.44932
12	0.0644	1.86E+02	2.07E+03	11.1	3.23E+04	2.08E+03	84.86547
13	0.0953	3.06E+02	3.00E+03	9.8	3.16E+04	3.02E+03	84.17597
14	0.0966	3.11E+02	3.04E+03	9.76	3.16E+04	3.06E+03	84.15881
15	0.139	4.90E+02	4.25E+03	8.68	3.09E+04	4.28E+03	83.42317
16	0.205	8.07E+02	6.12E+03	7.59	3.01E+04	6.17E+03	82.48816
17	0.208	8.21E+02	6.20E+03	7.55	3.00E+04	6.25E+03	82.45682
18	0.299	1.29E+03	8.64E+03	6.68	2.93E+04	8.74E+03	81.50815
19	0.442	2.08E+03	1.24E+04	5.96	2.84E+04	1.26E+04	80.47774
20	0.449	2.11E+03	1.25E+04	5.93	2.83E+04	1.27E+04	80.41879
21	0.6	2.96E+03	1.63E+04	5.5	2.76E+04	1.66E+04	79.70753
22	0.644	3.20E+03	1.74E+04	5.42	2.74E+04	1.77E+04	79.57929
23	0.953	4.77E+03	2.47E+04	5.17	2.64E+04	2.52E+04	79.06974
24	0.966	4.83E+03	2.50E+04	5.17	2.63E+04	2.55E+04	79.06518
25	1.29	6.45E+03	3.23E+04	5.01	2.55E+04	3.29E+04	78.70712
26	2.05	1.03E+04	4.84E+04	4.69	2.41E+04	4.95E+04	77.98611
27	2.08	1.05E+04	4.90E+04	4.68	2.41E+04	5.01E+04	77.90524
28	2.79	1.42E+04	6.30E+04	4.44	2.32E+04	6.46E+04	77.29798
29	4.42	2.29E+04	9.34E+04	4.08	2.17E+04	9.62E+04	76.22386
30	4.49	2.32E+04	9.45E+04	4.07	2.17E+04	9.73E+04	76.20653
31	6	3.12E+04	1.21E+05	3.87	2.08E+04	1.25E+05	75.54116
32	9.53	4.94E+04	1.77E+05	3.58	1.93E+04	1.84E+05	74.40579
33	12.9	6.67E+04	2.28E+05	3.41	1.83E+04	2.38E+05	73.69349
34	20.5	1.04E+05	3.31E+05	3.18	1.69E+04	3.47E+05	72.55731
35	27.9	1.39E+05	4.23E+05	3.05	1.60E+04	4.45E+05	71.80921
36	44.2	2.13E+05	6.10E+05	2.86	1.46E+04	6.46E+05	70.7518
37	60	2.82E+05	7.76E+05	2.75	1.38E+04	8.26E+05	70.02875
38	129	5.60E+05	1.41E+06	2.52	1.17E+04	1.52E+06	68.33885
39	279	1.08E+06	2.56E+06	2.38	9.96E+03	2.78E+06	67.12633
40	600	2.02E+06	4.62E+06	2.28	8.40E+03	5.04E+06	66.38364

Appendix C8. Master curve test data of RTFO Aged PG 52-40

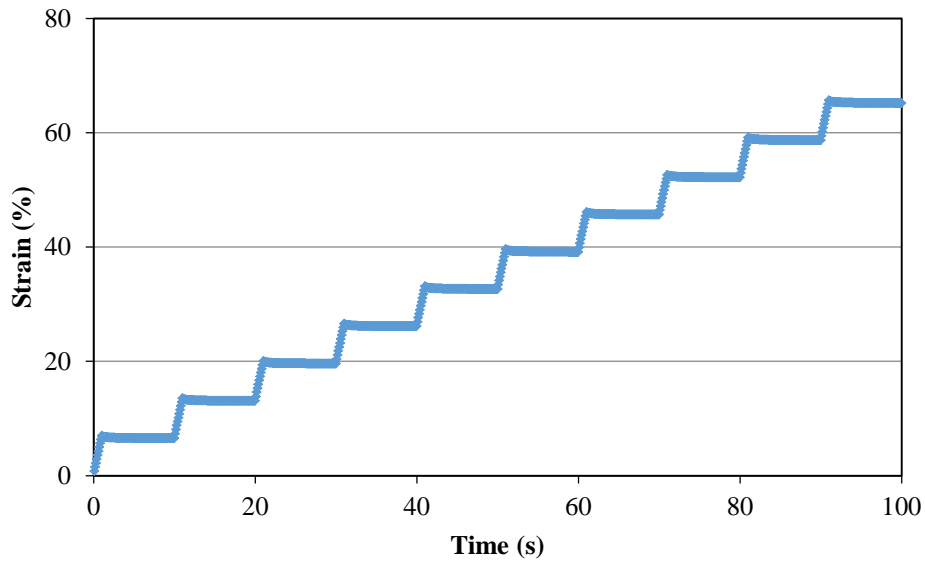
Meas. Pts.	Angular Frequency	Storage Modulus	Loss Modulus	Damping Factor	Complex Viscosity	Dynamic Modulus	Phase Angle
	[rad/s]	[Pa]	[Pa]	[1]	[Pa-s]	[Pa]	[Degree]
1	0.054	6.79E+02	6.85E+02	1.01	1.79E+04	9.65E+02	45.25203
2	0.0781	8.11E+02	8.79E+02	1.08	1.53E+04	1.20E+03	47.30415
3	0.116	9.84E+02	1.15E+03	1.17	1.30E+04	1.51E+03	49.44798
4	0.168	1.18E+03	1.48E+03	1.25	1.12E+04	1.89E+03	51.43474
5	0.189	1.25E+03	1.60E+03	1.28	1.07E+04	2.03E+03	52.00127
6	0.251	1.45E+03	1.94E+03	1.34	9.64E+03	2.42E+03	53.22473
7	0.363	1.76E+03	2.49E+03	1.41	8.40E+03	3.05E+03	54.74629
8	0.408	1.87E+03	2.70E+03	1.44	8.04E+03	3.28E+03	55.29381
9	0.54	2.18E+03	3.26E+03	1.49	7.27E+03	3.92E+03	56.22889
10	0.6	2.32E+03	3.50E+03	1.51	7.00E+03	4.20E+03	56.46131
11	0.781	2.69E+03	4.20E+03	1.56	6.38E+03	4.99E+03	57.36141
12	0.879	2.87E+03	4.55E+03	1.58	6.12E+03	5.38E+03	57.75753
13	1.16	3.38E+03	5.51E+03	1.63	5.56E+03	6.46E+03	58.47379
14	1.29	3.60E+03	5.93E+03	1.65	5.36E+03	6.94E+03	58.73879
15	1.68	4.21E+03	7.11E+03	1.69	4.91E+03	8.26E+03	59.36922
16	1.89	4.52E+03	7.72E+03	1.71	4.72E+03	8.95E+03	59.65136
17	2.51	5.36E+03	9.38E+03	1.75	4.31E+03	1.08E+04	60.25512
18	2.79	5.72E+03	1.01E+04	1.77	4.16E+03	1.16E+04	60.47553
19	3.63	6.74E+03	1.21E+04	1.8	3.83E+03	1.39E+04	60.88111
20	4.08	7.26E+03	1.32E+04	1.82	3.69E+03	1.51E+04	61.18921
21	5.4	8.68E+03	1.61E+04	1.86	3.39E+03	1.83E+04	61.66954
22	6	9.28E+03	1.74E+04	1.87	3.28E+03	1.97E+04	61.92751
23	7.81	1.10E+04	2.10E+04	1.9	3.03E+03	2.37E+04	62.35402
24	8.79	1.19E+04	2.28E+04	1.92	2.93E+03	2.57E+04	62.4386
25	11.6	1.43E+04	2.80E+04	1.95	2.70E+03	3.14E+04	62.94595
26	12.9	1.54E+04	3.02E+04	1.97	2.62E+03	3.39E+04	62.98143
27	16.8	1.83E+04	3.66E+04	2	2.43E+03	4.09E+04	63.43495
28	18.9	1.99E+04	3.99E+04	2.01	2.35E+03	4.46E+04	63.49242
29	25.1	2.40E+04	4.91E+04	2.05	2.18E+03	5.47E+04	63.95069
30	27.9	2.58E+04	5.32E+04	2.06	2.12E+03	5.91E+04	64.12836
31	36.3	3.09E+04	6.47E+04	2.09	1.98E+03	7.17E+04	64.47138
32	40.8	3.35E+04	7.07E+04	2.11	1.92E+03	7.82E+04	64.64686
33	54	4.07E+04	8.74E+04	2.15	1.78E+03	9.64E+04	65.02978
34	60	4.38E+04	9.46E+04	2.16	1.74E+03	1.04E+05	65.15576
35	78.1	5.25E+04	1.16E+05	2.2	1.62E+03	1.27E+05	65.64915
36	87.9	5.69E+04	1.26E+05	2.22	1.58E+03	1.38E+05	65.69667
37	129	7.43E+04	1.70E+05	2.28	1.43E+03	1.86E+05	66.39184
38	189	9.68E+04	2.27E+05	2.35	1.30E+03	2.47E+05	66.90506
39	279	1.26E+05	3.06E+05	2.42	1.19E+03	3.31E+05	67.61986
40	600	2.15E+05	5.51E+05	2.56	9.85E+02	5.91E+05	68.68429

Appendix C9. Master curve test data of RTFO Aged PG 58-34

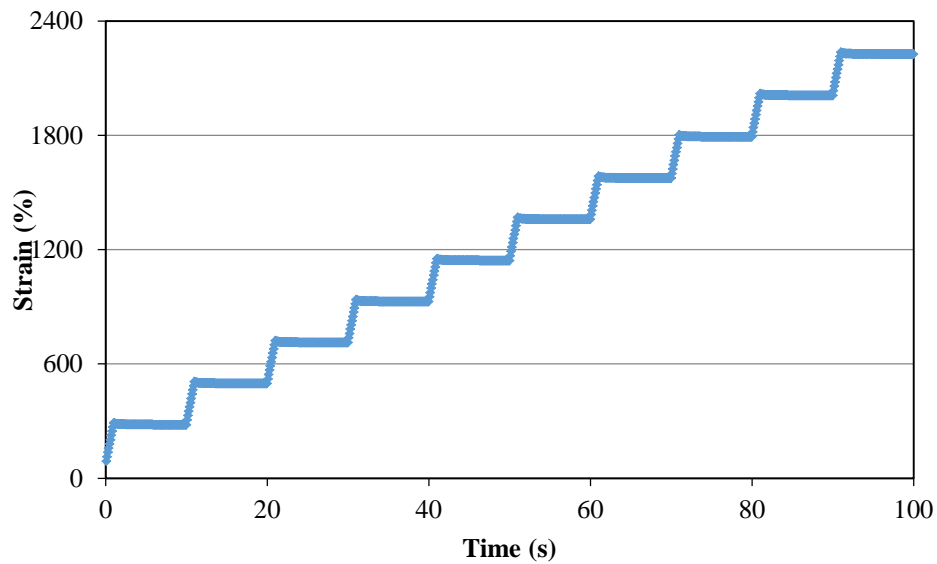
Meas. Pts.	Angular Frequency	Storage Modulus	Loss Modulus	Damping Factor	Complex Viscosity	Dynamic Modulus	Phase Angle
	[rad/s]	[Pa]	[Pa]	[1]	[Pa·s]	[Pa]	[Degree]
1	0.042	9.88E+02	1.42E+03	1.44	4.12E+04	1.73E+03	55.17078
2	0.0906	1.50E+03	2.43E+03	1.62	3.15E+04	2.86E+03	58.31363
3	0.11	1.67E+03	2.78E+03	1.67	2.96E+04	3.24E+03	59.00594
4	0.195	2.35E+03	4.17E+03	1.78	2.45E+04	4.79E+03	60.5966
5	0.236	2.64E+03	4.78E+03	1.81	2.31E+04	5.46E+03	61.08807
6	0.42	3.80E+03	7.19E+03	1.89	1.94E+04	8.13E+03	62.14302
7	0.509	4.30E+03	8.25E+03	1.92	1.83E+04	9.30E+03	62.47093
8	0.6	4.78E+03	9.28E+03	1.94	1.74E+04	1.04E+04	62.74763
9	0.906	6.25E+03	1.25E+04	2	1.54E+04	1.40E+04	63.43495
10	1.1	7.09E+03	1.44E+04	2.03	1.46E+04	1.61E+04	63.78616
11	1.29	7.89E+03	1.62E+04	2.05	1.39E+04	1.80E+04	64.0322
12	1.56	8.93E+03	1.86E+04	2.08	1.32E+04	2.06E+04	64.35399
13	1.95	1.03E+04	2.19E+04	2.12	1.24E+04	2.42E+04	64.81148
14	2.36	1.17E+04	2.52E+04	2.15	1.18E+04	2.78E+04	65.09523
15	2.79	1.31E+04	2.85E+04	2.18	1.13E+04	3.14E+04	65.31416
16	3.36	1.48E+04	3.28E+04	2.22	1.07E+04	3.60E+04	65.71417
17	4.2	1.71E+04	3.88E+04	2.26	1.01E+04	4.24E+04	66.21587
18	5.09	1.95E+04	4.48E+04	2.3	9.58E+03	4.89E+04	66.47806
19	6	2.18E+04	5.07E+04	2.33	9.19E+03	5.52E+04	66.73325
20	7.24	2.47E+04	5.84E+04	2.36	8.75E+03	6.34E+04	67.0743
21	9.06	2.87E+04	6.92E+04	2.41	8.27E+03	7.49E+04	67.47427
22	11	3.28E+04	8.00E+04	2.44	7.88E+03	8.65E+04	67.70637
23	12.9	3.67E+04	9.06E+04	2.47	7.56E+03	9.78E+04	67.94825
24	15.6	4.19E+04	1.05E+05	2.5	7.22E+03	1.13E+05	68.24565
25	19.5	4.90E+04	1.24E+05	2.53	6.83E+03	1.33E+05	68.43799
26	23.6	5.62E+04	1.43E+05	2.55	6.51E+03	1.54E+05	68.54483
27	27.9	6.34E+04	1.62E+05	2.56	6.26E+03	1.74E+05	68.62671
28	33.6	7.28E+04	1.87E+05	2.57	5.98E+03	2.01E+05	68.7288
29	42	8.61E+04	2.22E+05	2.57	5.66E+03	2.38E+05	68.80182
30	50.9	9.99E+04	2.56E+05	2.56	5.40E+03	2.75E+05	68.68256
31	60	1.14E+05	2.90E+05	2.54	5.18E+03	3.12E+05	68.54004
32	72.4	1.32E+05	3.33E+05	2.52	4.95E+03	3.58E+05	68.3768
33	110	1.85E+05	4.53E+05	2.45	4.46E+03	4.89E+05	67.78546
34	129	2.11E+05	5.11E+05	2.42	4.28E+03	5.53E+05	67.56349
35	156	2.46E+05	5.87E+05	2.39	4.08E+03	6.36E+05	67.26241
36	279	3.93E+05	8.95E+05	2.28	3.51E+03	9.77E+05	66.29343
37	336	4.56E+05	1.02E+06	2.25	3.34E+03	1.12E+06	65.91255
38	600	7.22E+05	1.56E+06	2.15	2.86E+03	1.72E+06	65.16433
39	724	8.37E+05	1.78E+06	2.13	2.71E+03	1.97E+06	64.81593
40	1,560	1.52E+06	3.08E+06	2.03	2.20E+03	3.43E+06	63.73336

Appendix C10. MSCR results for RTFO aged PG 52-28 binder

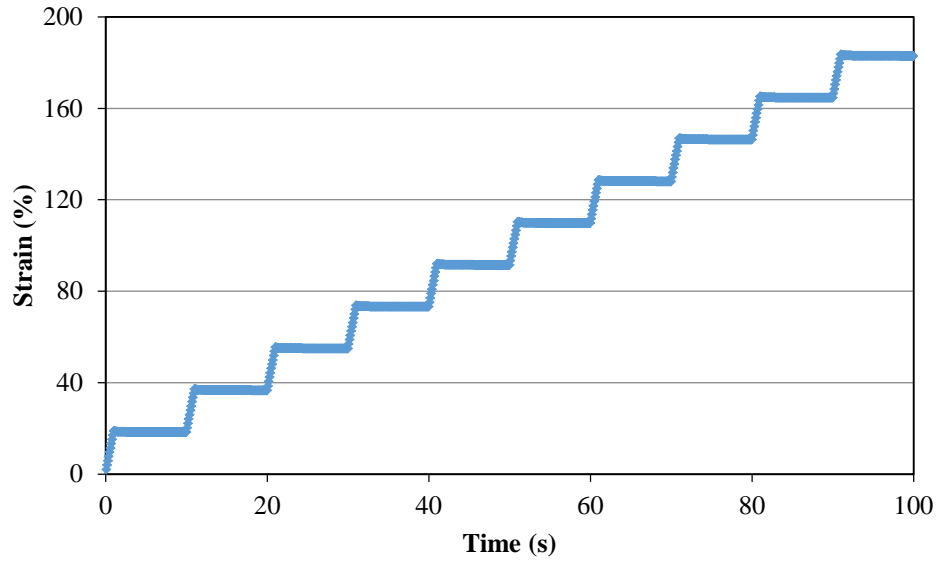
T (°C)	Specimen	R_{100} (%)	R_{3200} (%)	R_{diff} (%)	J_{nr100} (1/kPa)	J_{nr3200} (1/kPa)	$J_{nr-diff}$ (%)
46	1	6.7	4.4	34.1	0.652	0.696	6.7
	2	6.7	4.4	34.2	0.639	0.686	7.2
	3	7.4	4.9	34.7	0.615	0.660	7.3
52	1	3.1	0.8	74.6	1.83	2.01	10.1
	2	3.1	0.7	76.3	1.82	2.00	10.0
	3	3.5	1.0	71.9	1.76	1.94	10.7



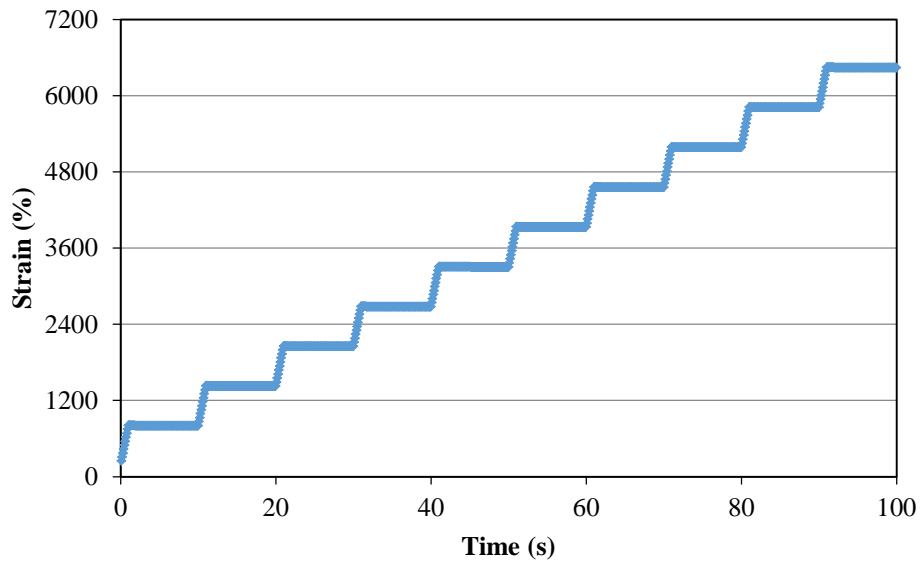
Appendix C11. Strain curve of RTFO aged PG 52-28 binder at 0.1 kPa, 46°C



Appendix C12. Strain curve of RTFO aged PG 52-28 binder at 3.2 kPa, 46°C



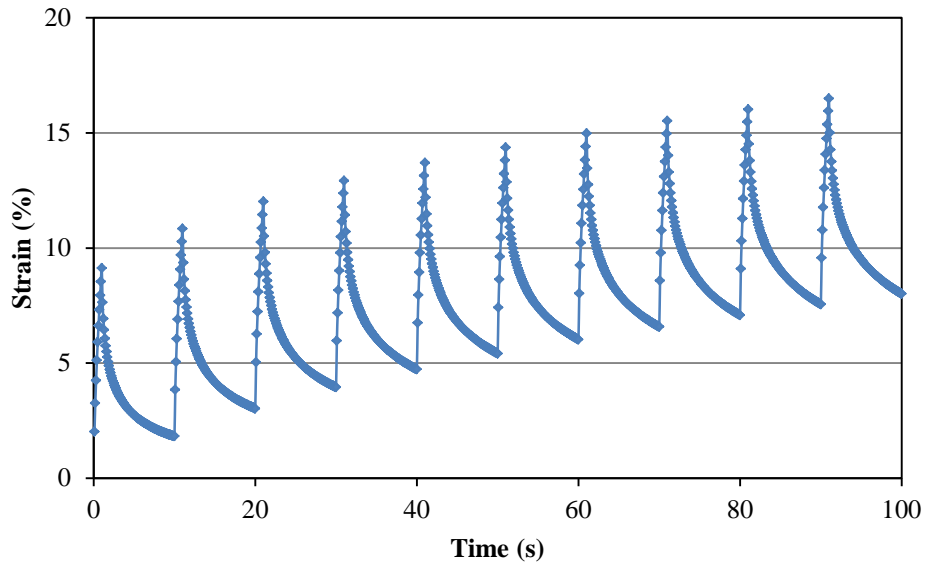
Appendix C13. Strain curve of RTFO aged PG 52-28 binder at 0.1 kPa, 52°C



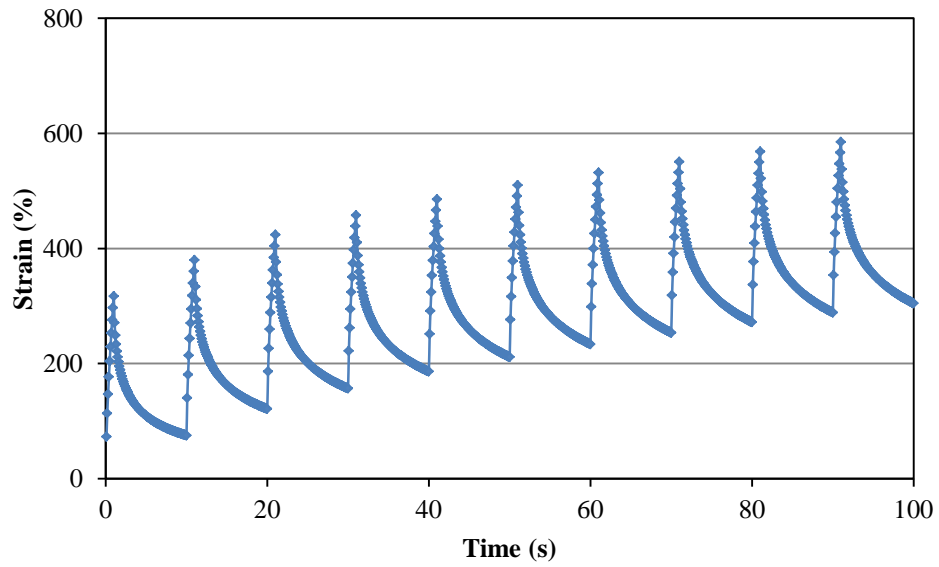
Appendix C14. Strain curve of RTFO aged PG 52-28 binder at 3.2 kPa, 52°C

Appendix C15. MSCR results for RTFO aged PG 52-40 binder

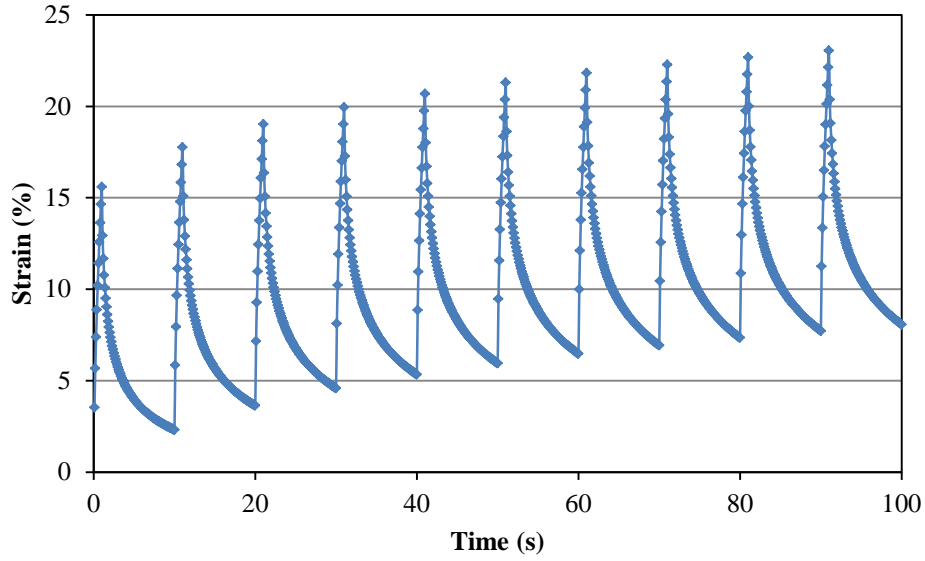
T (°C)	Specimen	R_{100} (%)	R_{3200} (%)	R_{diff} (%)	$J_{nr,100}$ (1/kPa)	$J_{nr,3200}$ (1/kPa)	$J_{nr-diff}$ (%)
46	1	91.1	90.0	1.2	0.0801	0.0953	18.9
	2	91.5	90.2	1.4	0.0685	0.0833	21.5
	3	91.5	91.0	0.5	0.0728	0.0813	11.6
52	1	94.8	92.7	2.2	0.0807	0.118	46.1
	2	94.9	92.9	2.1	0.0709	0.103	45.8
	3	95.2	93.6	1.7	0.0697	0.0978	40.4



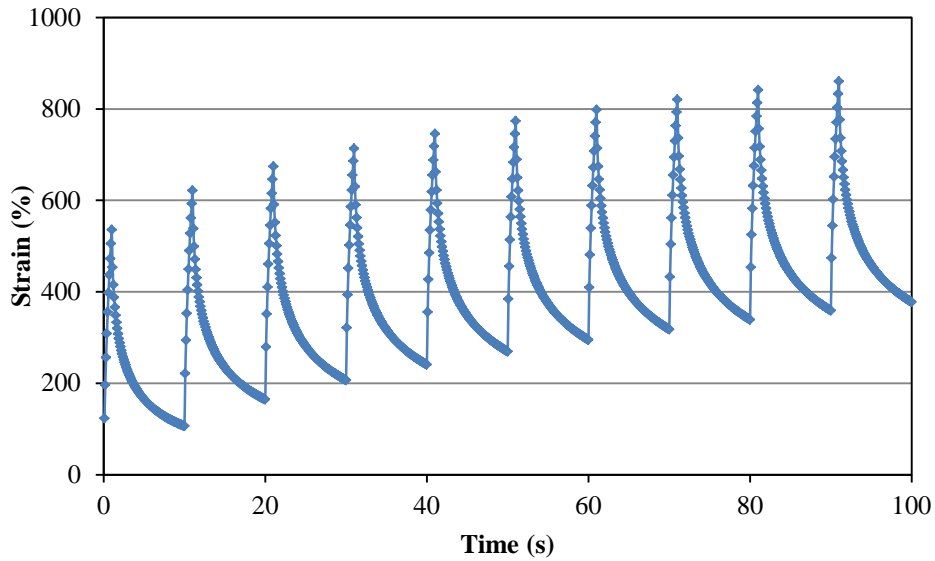
Appendix C16. Strain curve of RTFO aged PG 52-40 binder at 0.1 kPa, 46°C



Appendix C17. Strain curve of RTFO aged PG 52-40 binder at 3.2 kPa, 46°C



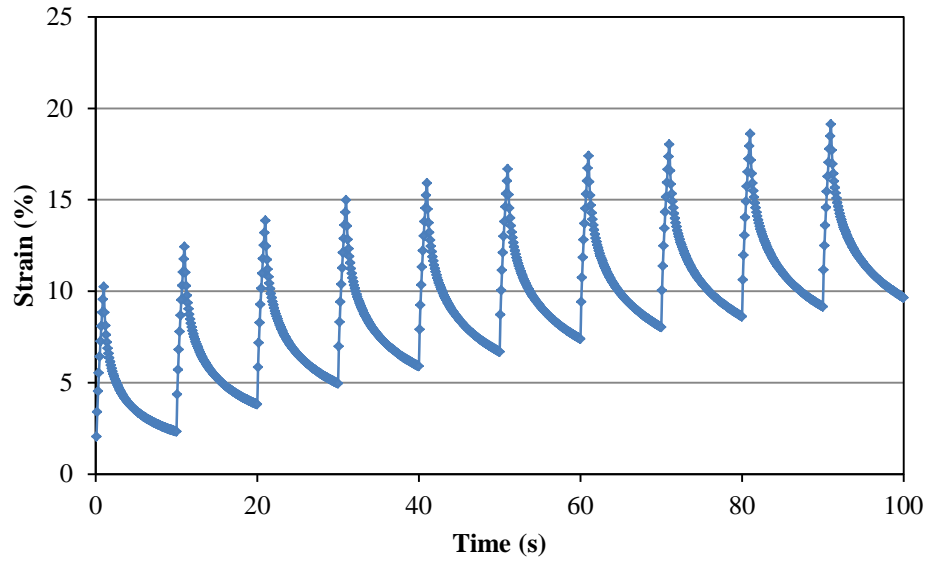
Appendix C18. Strain curve of RTFO aged PG 52-40 binder at 0.1 kPa, 52°C



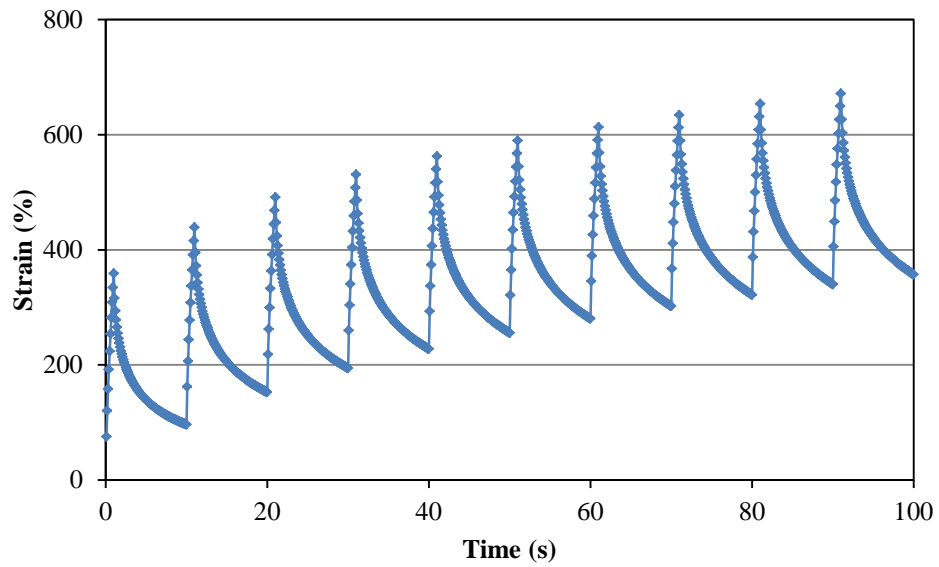
Appendix C19. Strain curve of RTFO aged PG 52-40 binder at 3.2 kPa, 52°C

Appendix C20. MSCR results for RTFO aged PG 58-34 binder

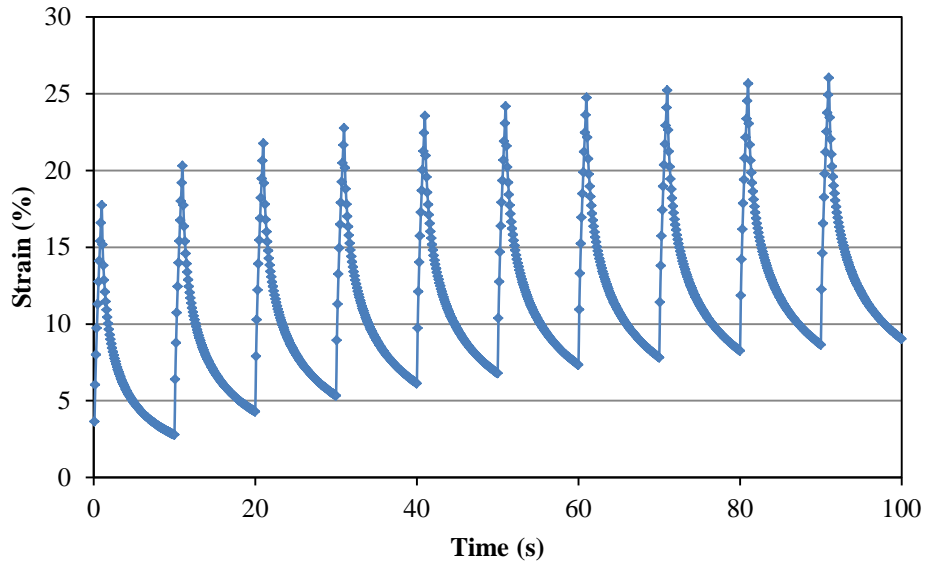
T (°C)	Specimen	R_{100} (%)	R_{3200} (%)	R_{diff} (%)	J_{nr100} (1/kPa)	J_{nr3200} (1/kPa)	$J_{nr-diff}$ (%)
52	1	90.4	89.6	1.0	0.0965	0.112	15.7
	2	90.9	90.4	0.5	0.0921	0.103	11.8
	3	91.3	91.5	-0.3	0.0841	0.0866	3.0
58	1	94.9	93.7	1.3	0.0902	0.115	27.8
	2	95.2	94.2	1.0	0.0843	0.105	24.7
	3	95.1	94.4	0.8	0.0832	0.0973	17.0



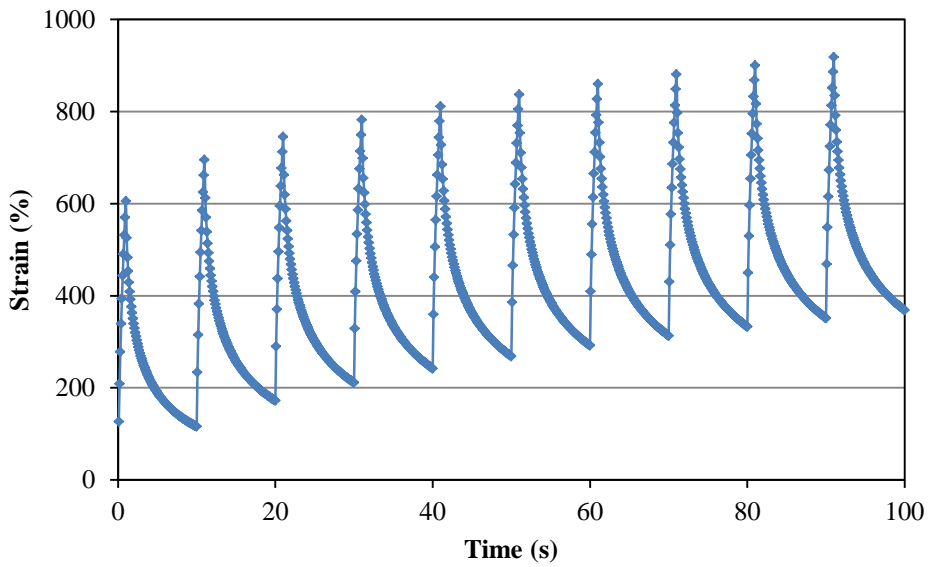
Appendix C21. Strain curve of RTFO aged PG 58-34 binder at 0.1 kPa, 52°C



Appendix C22. Strain curve of RTFO aged PG 58-34 binder at 3.2 kPa, 52°C



Appendix C23. Strain curve of RTFO aged PG 58-34 binder at 0.1 kPa, 58°C



Appendix C23. Strain curve of RTFO aged PG 58-34 binder at 3.2 kPa, 58°C

Appendix C24 . PG 52-28 BBR results for respective low temperatures and aging method

PG 52-28			Sample 1		Sample 2		Sample 3	
Testing T (°C)	Aging Method	Time (s)	S (MPa)	m-value	S (MPa)	m-value	S (MPa)	m-value
-18	RTFO	8	208.0	0.330	189.0	0.338	207.0	0.309
		15	168.0	0.353	153.0	0.352	169.0	0.333
		30	130.0	0.379	119.0	0.367	132.0	0.359
		60	99.4	0.404	91.2	0.382	103.0	0.386
		120	74.6	0.430	70.3	0.397	77.8	0.413
		240	54.7	0.455	52.9	0.412	57.8	0.439
-24	RTFO	8	435.0	0.241	481.0	0.262	480.0	0.254
		15	372.0	0.257	406.0	0.287	406.0	0.275
		30	309.0	0.276	330.0	0.314	333.0	0.298
		60	254.0	0.294	262.0	0.341	269.0	0.320
		120	206.0	0.313	205.0	0.368	214.0	0.343
		240	165.0	0.331	158.0	0.395	167.0	0.366
-30	RTFO	8	737.0	0.200	720.0	0.190	726.0	0.188
		15	639.0	0.222	637.0	0.216	630.0	0.205
		30	556.0	0.247	545.0	0.243	548.0	0.223
		60	453.0	0.271	451.0	0.271	471.0	0.242
		120	375.0	0.296	370.0	0.299	395.0	0.260
		240	304.0	0.321	300.0	0.327	325.0	0.279
-18	RTFO +PAV	8	442.0	0.259	439.0	0.281	439.0	0.265
		15	371.0	0.285	365.0	0.307	368.0	0.292
		30	302.0	0.314	293.0	0.336	298.0	0.322
		60	241.0	0.343	230.0	0.365	235.0	0.352
		120	188.0	0.373	176.0	0.393	183.0	0.382
		240	143.0	0.402	133.0	0.422	139.0	0.412
-24	RTFO +PAV	8	859.0	0.174	835.0	0.171	877.0	0.174
		15	760.0	0.195	741.0	0.199	781.0	0.198
		30	664.0	0.218	640.0	0.229	675.0	0.224
		60	564.0	0.242	540.0	0.260	571.0	0.250
		120	473.0	0.265	448.0	0.291	477.0	0.277
		240	390.0	0.289	360.0	0.321	390.0	0.303

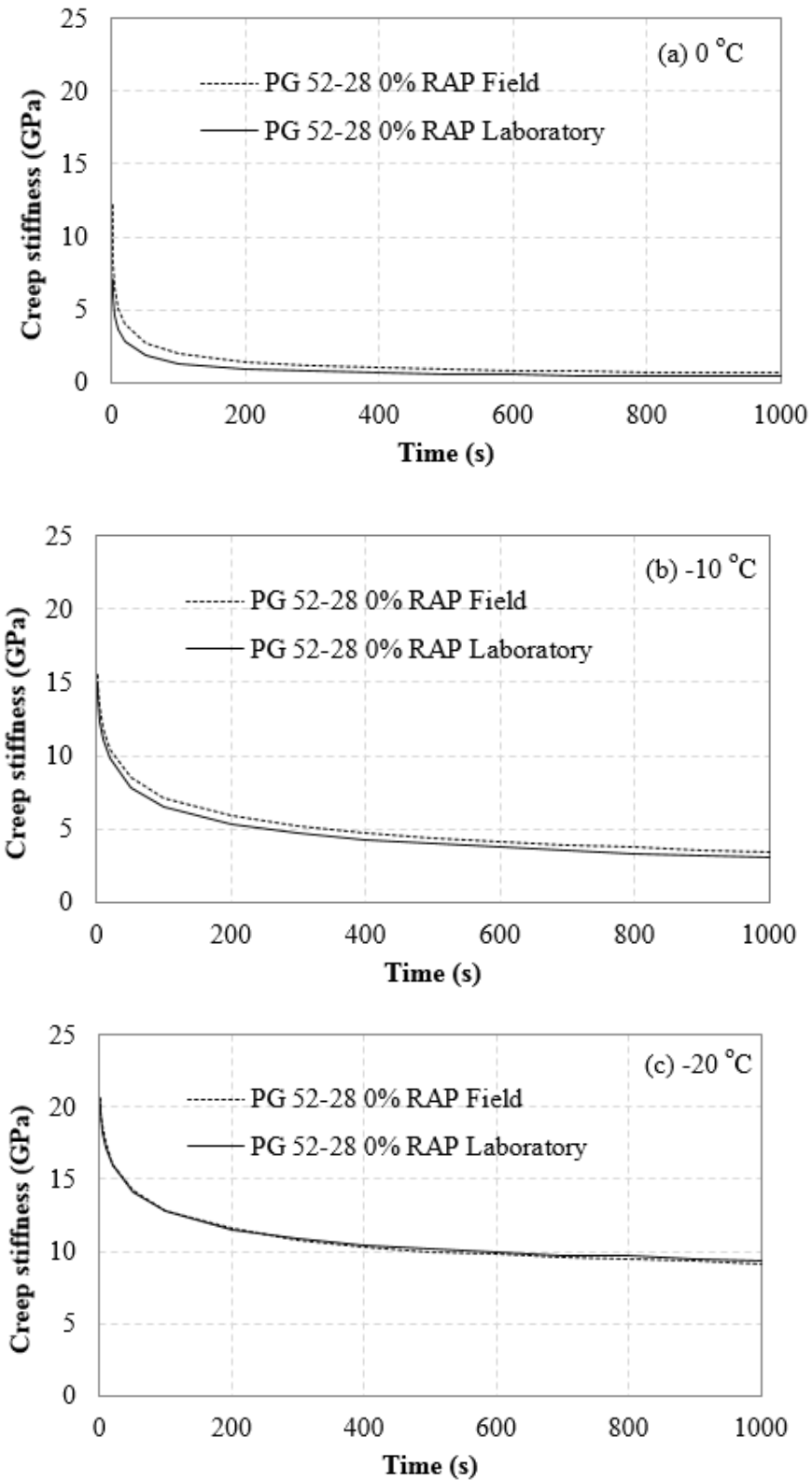
Appendix C25. PG 52-40 BBR results for respective low temperatures and aging method

PG 52-40			Sample 1		Sample 2		Sample 3	
Testing T (°C)	Aging Method	Time (s)	S (MPa)	m-value	S (MPa)	m-value	S (MPa)	m-value
-30	RTFO	8	366.0	0.278	358.0	0.300	361.0	0.302
		15	305.0	0.301	295.0	0.325	298.0	0.325
		30	246.0	0.327	233.0	0.353	236.0	0.349
		60	194.0	0.353	180.0	0.381	183.0	0.373
		120	150.0	0.378	137.0	0.409	140.0	0.398
		240	115.0	0.404	102.0	0.437	106.0	0.422
-34	RTFO	8	554.0	0.211	544.0	0.219	575.0	0.237
		15	486.0	0.232	470.0	0.242	496.0	0.257
		30	407.0	0.256	396.0	0.268	411.0	0.279
		60	339.0	0.279	325.0	0.293	335.0	0.301
		120	277.0	0.303	262.0	0.319	269.0	0.322
		240	223.0	0.327	209.0	0.345	215.0	0.344
-30	RTFO +PAV	8	388.0	0.249	395.0	0.264	400.0	0.270
		15	329.0	0.273	332.0	0.287	335.0	0.291
		30	271.0	0.300	270.0	0.314	272.0	0.314
		60	217.0	0.326	215.0	0.340	217.0	0.338
		120	171.0	0.353	168.0	0.367	170.0	0.361
		240	134.0	0.380	129.0	0.393	131.0	0.384
-34	RTFO +PAV	8	1030.0	0.137	1010.0	0.151	1050.0	0.135
		15	939.0	0.152	916.0	0.170	955.0	0.157
		30	854.0	0.167	810.0	0.192	850.0	0.180
		60	738.0	0.183	705.0	0.214	742.0	0.204
		120	651.0	0.199	599.0	0.235	643.0	0.227
		240	569.0	0.214	508.0	0.257	542.0	0.251

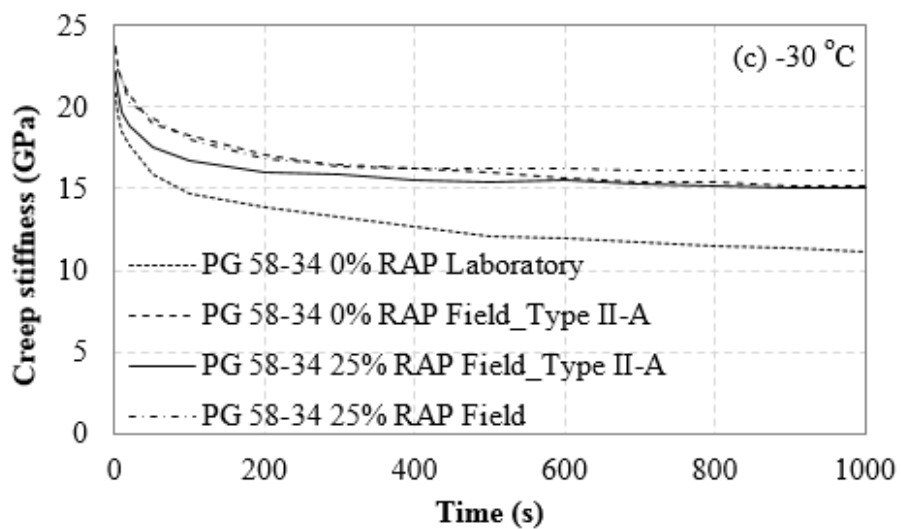
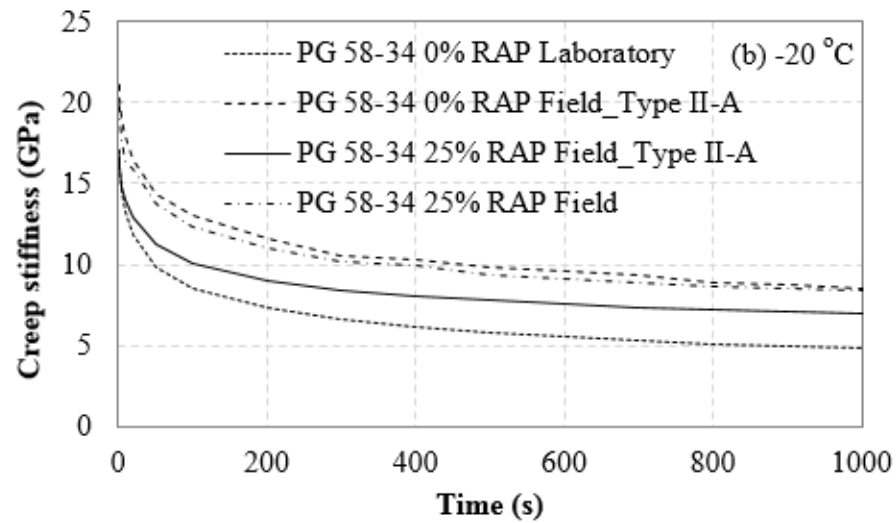
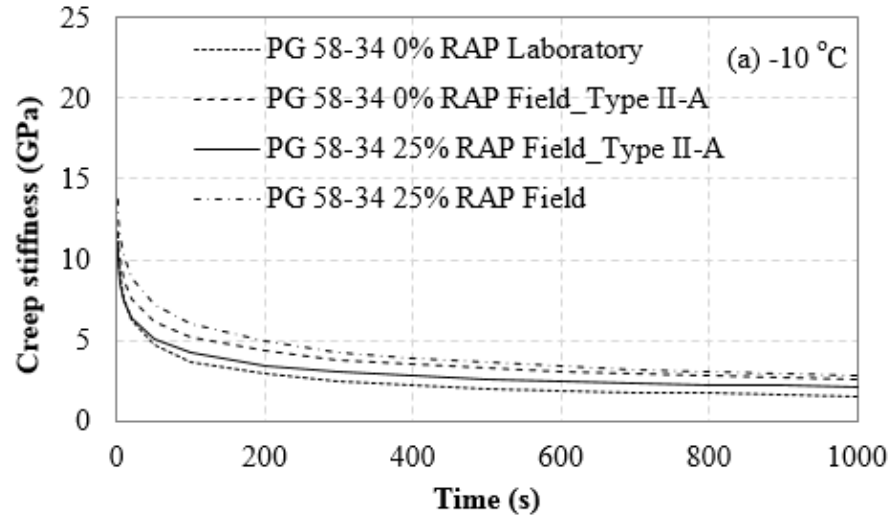
Appendix C26. PG 58-34 BBR results for respective low temperatures and aging method

PG 52-34			Sample 1		Sample 2		Sample 3	
Testing T (°C)	Aging Method	Time (s)	S (MPa)	m-value	S (MPa)	m-value	S (MPa)	m-value
-24	RTFO	8	469.0	0.272	442.0	0.291	352.0	0.299
		15	392.0	0.295	368.0	0.315	302.0	0.251
		30	317.0	0.320	293.0	0.342	251.0	0.276
		60	252.0	0.344	228.0	0.369	206.0	0.300
		120	197.0	0.369	175.0	0.395	166.0	0.325
		240	151.0	0.394	132.0	0.422	131.0	0.349
-30	RTFO	8	870.0	0.180	826.0	0.179	864.0	0.186
		15	768.0	0.200	741.0	0.200	772.0	0.208
		30	667.0	0.221	634.0	0.222	657.0	0.232
		60	567.0	0.242	539.0	0.245	557.0	0.256
		120	478.0	0.264	452.0	0.267	459.0	0.280
		240	393.0	0.285	373.0	0.290	378.0	0.304
-18	RTFO +PAV	8	180.0	0.334	175.0	0.369	175.0	0.360
		15	144.0	0.360	138.0	0.388	139.0	0.381
		30	111.0	0.390	105.0	0.408	106.0	0.405
		60	84.2	0.419	78.3	0.428	79.4	0.428
		120	62.3	0.448	57.8	0.449	58.4	0.451
		240	45.2	0.477	42.2	0.469	42.5	0.475
-24	RTFO +PAV	8	842.0	0.184	869.0	0.176	850.0	0.198
		15	739.0	0.209	768.0	0.201	744.0	0.228
		30	637.0	0.237	665.0	0.227	626.0	0.261
		60	533.0	0.265	564.0	0.254	519.0	0.294
		120	443.0	0.292	467.0	0.280	417.0	0.327
		240	356.0	0.320	381.0	0.307	329.0	0.360
-30	RTFO +PAV	8	913.0	0.184	855.0	0.185	892.0	0.184
		15	810.0	0.210	757.0	0.207	786.0	0.207
		30	691.0	0.238	646.0	0.233	679.0	0.232
		60	580.0	0.267	549.0	0.258	571.0	0.257
		120	478.0	0.296	454.0	0.283	475.0	0.282
		240	385.0	0.324	369.0	0.308	387.0	0.307

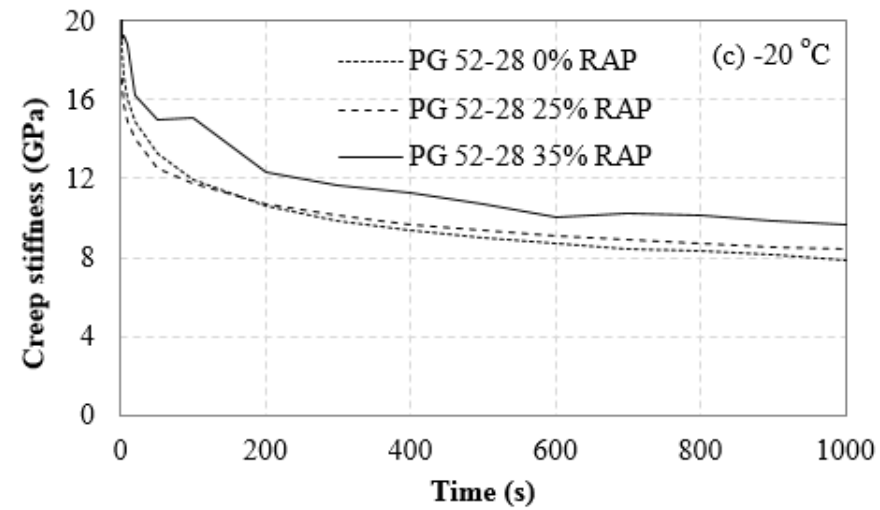
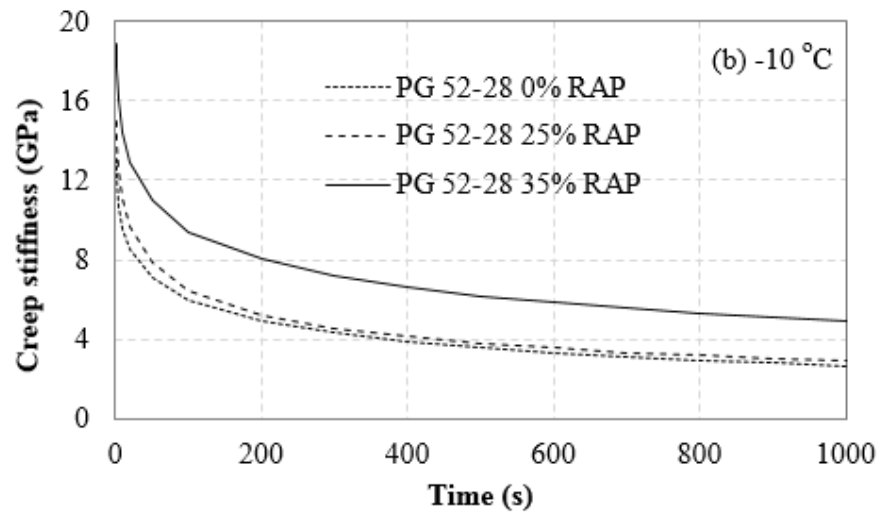
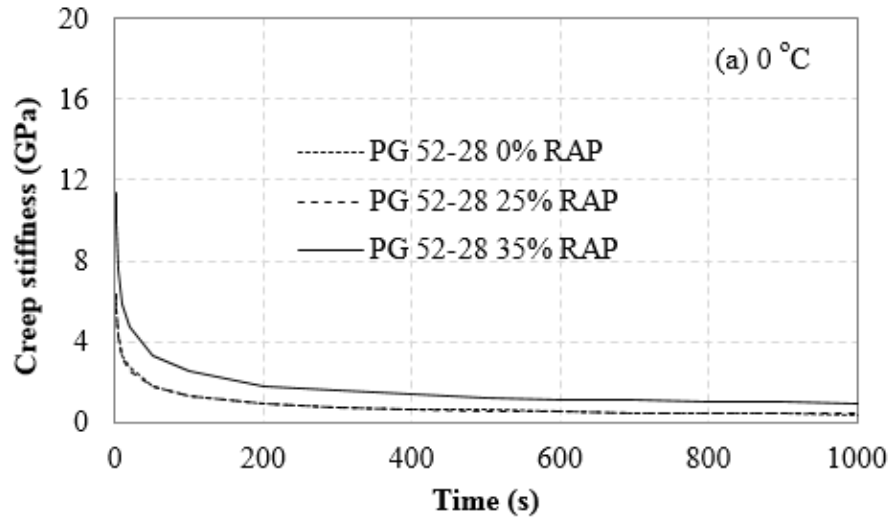
APPENDIX D MIXTURE TESTING RESULTS



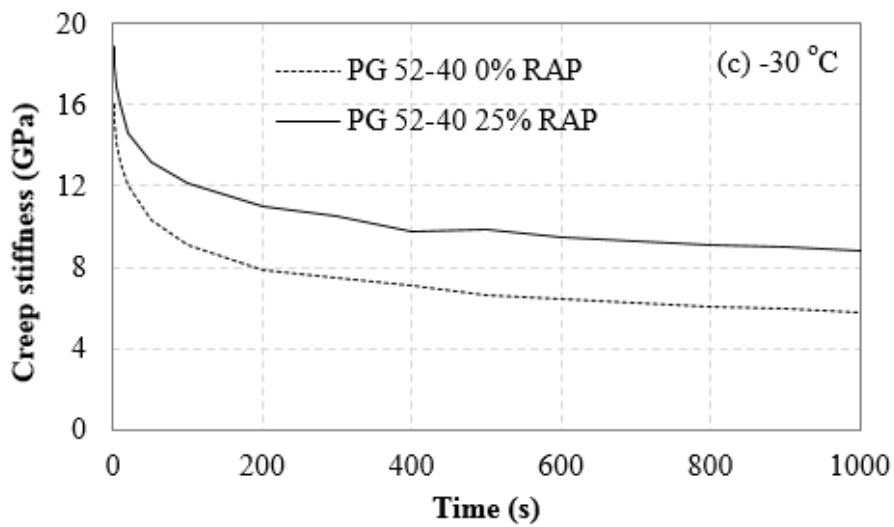
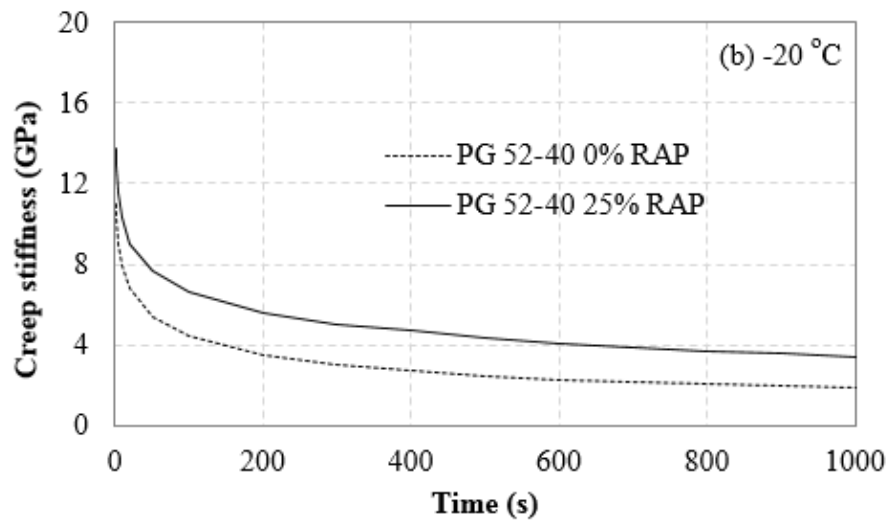
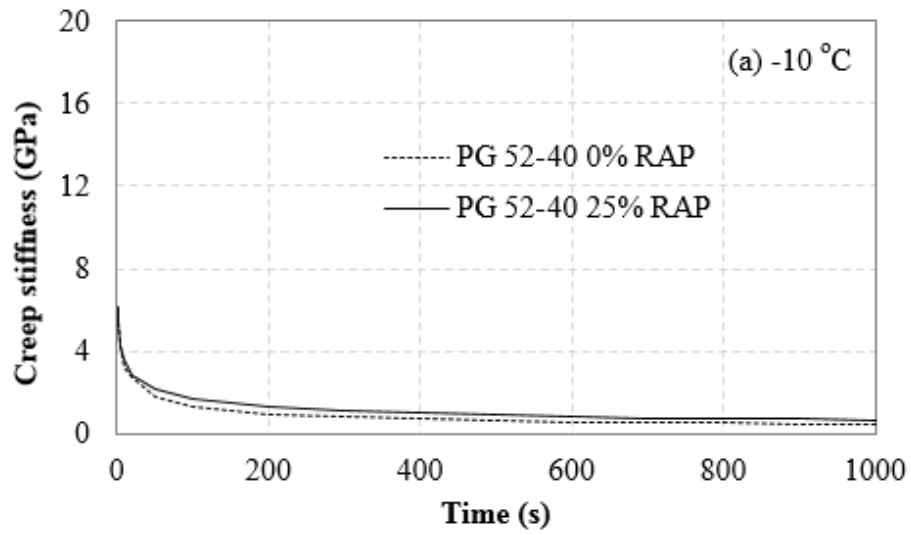
Appendix D1. Creep stiffness of PG 52-28 mixes for the Central Region



Appendix D2. Creep stiffness of PG 58-34 mixes for the Central Region



Appendix D3. Creep stiffness of PG 52-28 mixes for the Northern Region



Appendix D4. Creep stiffness of PG 52-40 mixes for the Northern Region